

# PACIFIC EARTHQUAKE ENGINEERING RESEARCH CENTER

## **Adjusting Ground-Motion Intensity Measures to a Reference Site for which $V_{s30} = 3000$ m/sec**

**David M. Boore**

U.S. Geological Survey  
Menlo Park, California

PEER Report No. 2015/06  
Pacific Earthquake Engineering Research Center  
Headquarters at the University of California, Berkeley

May 2015

#### Disclaimer

The opinions, findings, and conclusions or recommendations expressed in this publication are those of the author(s) and do not necessarily reflect the views of the study sponsor(s) or the Pacific Earthquake Engineering Research Center.

# **Adjusting Ground-Motion Intensity Measures to a Reference Site for which $V_{S30} = 3000$ m/sec**

**David M. Boore**

U.S. Geological Survey  
Menlo Park, California

PEER Report No. 2015/06  
Pacific Earthquake Engineering Research Center  
Headquarters at the University of California, Berkeley

May 2015



## ABSTRACT

Adjustment factors that can be used to convert ground-motion intensity measures at sites with  $V_{S30} = 760$  m/sec and  $V_{S30} = 2000$  m/sec to a reference rock site, defined as one with  $V_{S30} = 3000$  m/sec, are provided as tables: (1) for moment magnitudes from 2 to 8; (2) rupture distances from 2 km to 1200 km; (3) response spectra at periods from 0.01 sec to 10.0 sec; and (4) peak acceleration and peak velocity. Ten velocity models used in ground-motion studies in central and eastern North America with  $V_{S30}$  values very close to 760 m/sec were considered, and adjustment factors are provided for two of those models that effectively span the range of models; in addition, for the convenience of the user, adjustment factors are provided for an average of a representative set of models with  $V_{S30} = 760$  m/sec. For models with this velocity, adjustment factors are provided for four values of the diminution parameter  $\kappa$ , ranging from 0.005 sec to 0.030 sec. The adjustment factors are based on stochastic-method simulations of ground motion.



## **ACKNOWLEDGMENTS**

This report was prepared as an account of work sponsored by an agency of the U.S. Government. Neither the U.S. Government nor any agency thereof, nor any of their employees, makes any warranty, expressed or implied, or assumes any legal liability or responsibility for any third party's use, or the results of such use, of any information, apparatus, product, or process disclosed in this report, or represents that its use by such third party would not infringe privately owned rights. The views expressed in this paper are not necessarily those of the U.S. Nuclear Regulatory Commission. I thank Joseph Harmon, Youssef Hashash, and Walt Silva for providing velocity models, Christine Goulet for encouragement and numerous conversations, and Brad Aagaard, Rasool Anooshehpour, and Christine Goulet for their constructive reviews.





# CONTENTS

ABSTRACT.....	iii
ACKNOWLEDGMENTS .....	v
TABLE OF CONTENTS .....	vii
LIST OF TABLES .....	ix
LIST OF FIGURES .....	xi
1 INTRODUCTION.....	1
2 CRUSTAL AMPLIFICATIONS FOR SITES WITH $V_{S30} = 760$ M/SEC.....	5
2.1 Velocity Profiles for Sites with $V_{S30} = 760$ m/sec .....	5
2.2 Amplifications for Sites with $V_{S30} = 760$ m/sec .....	9
3 CRUSTAL AMPLIFICATIONS FOR SITES WITH $V_{S30} = 2000$ M/SEC AND $V_{S30} = 3000$ M/SEC .....	15
3.1 Velocity Profiles for Sites with $V_{S30} = 2000$ and $V_{S30} = 3000$ m/sec.....	15
3.2 Amplifications for sites with $V_{S30} = 3000$ m/sec.....	17
4 COMPARISON OF CRUSTAL AMPLIFICATIONS FOR SITES WITH $V_{S30} = 760$ M/SEC, $V_{S30} = 2000$ M/SEC, AND $V_{S30} = 3000$ M/SEC .....	19
5 COMPUTATION OF BC-TO-REFERENCE ROCK ADJUSTMENT FACTORS .....	21
5.1 Adjustments of GMIMs for sites with $V_{S30} = 2000$ m/sec to Those with $V_{S30} = 3000$ m/sec.....	21
5.2 Adjustments of GMIMs for sites with $V_{S30} = 760$ m/sec to Those with $V_{S30} = 3000$ m/sec.....	26
6 VARIABILITY OF THE <i>BC2RRAFS</i> .....	37
7 CONCLUSIONS .....	45
8 DATA AND RESOURCES .....	47
REFERENCES.....	49
APPENDIX A SMSIM PARAMETERS FILES USED IN THE SIMULATIONS .....	51
APPENDIX B TABLES OF PGV, PGA, AND PSA $V_{S30} = 760$ M/SEC TO $V_{S30} =$ 3000 M/SEC ADJUSTMENT FACTORS. ....	53



## LIST OF TABLES

Table 1	Crustal amplifications for three models with $V_{S30}$ close to 760 m/sec*.....	13
Table 2	Ratio of Fourier amplitude spectra (FAS). FAS for a site with $V_{S30} = 3000$ m/sec divided by the FAS of a site with $V_{S30} = 2000$ m/sec. $\kappa = 0.006$ sec for both sites.....	24
Table 3	Ratio of Fourier amplitude spectra (FAS): FAS for a site with $V_{S30} = 3000$ m/sec and $\kappa = 0.006$ sec divided by the FAS of a site with $V_{S30} = 760$ m/sec for the modified Frankel et al. [1996] (Fea) model and four values of $\kappa$ .....	27
Table 4	Ratio of Fourier amplitude spectra (FAS): FAS for a site with $V_{S30} = 3000$ m/sec and $\kappa = 0.006$ sec divided by the FAS of a site with $V_{S30} = 760$ m/sec for the Average BC model and four values of $\kappa$ .....	43
Table 5	Ratio of Fourier amplitude spectra (FAS): FAS for a site with $V_{S30} = 3000$ m/sec and $\kappa = 0.006$ sec divided by the FAS of a site with $V_{S30} = 760$ m/sec for the OTT model and four values of $\kappa$ .....	44



## LIST OF FIGURES

Figure 1	Histograms of $V_{S30}$ values in the NGA-East flatfile. The left graph includes all sites, whereas the right graph is the subset of sites east of St. Louis, Missouri, and north of New York City, New York (this is a rough way of choosing sites in northeastern U.S. and southeastern Canada).....2
Figure 2	Models with $V_{S30} = 760$ m/sec (Fea96=Frankel et al.; HH=Hashash and Harmon; S=Silva—see text for details). Some of the models extend below 32 m. The lowest depth of 32 m was chosen so that near-surface details can be seen. ....6
Figure 3	Models with $V_{S30} = 760$ m/sec; see caption to Figure 2 for explanation of model abbreviations. Some of the models extend below 100 m. The lowest depth of 100 m was chosen so that details deeper than the 32 m used in the previous figure can be seen.....7
Figure 4	Combined profiles; see caption to Figure 2 for explanation of model abbreviations. The maximum depth for the plot is 8500 m. The main purpose of this figure is to show the three profiles on to which the shallow profiles were merged.....8
Figure 5	Combined profiles; see caption to Figure 2 for explanation of model abbreviations. The maximum depth of 400 m was chosen to show model details between those shown in Figure 4 and Figure 3. ....9
Figure 6	Amplifications from the square-root-impedance method [Boore 2013] assuming an angle of incidence of 0 degrees; also shown are full-resonant amplifications (using the program <i>nrattle</i> ) for two of the Silva profiles (one gradient-like and one step-like), assuming <i>SH</i> waves with a 30 degree angle of incidence. The effect of applying a kappa operator with $\kappa = 0.02$ sec is also shown for two of the profiles. The Fea96 amplifications used a newer velocity-density relation than used to obtain the densities in Table A6 of Frankel et al. [1996] (Fea96), and therefore the amplifications shown in the figure are slightly different than those in Table A5 of Fea96. ....11
Figure 7	The subset of crustal amplifications shown in Figure 6 that are used in computing the adjustment factors to go from sites with $V_{S30} = 760$ m/sec to those with $V_{S30} = 3000$ m/sec.....12
Figure 8	The Boore and Joyner [1997] (BJ97) very hard rock (VHR) velocity profile and the modifications to that profile such that $V_{S30} = 2000$ m/sec and $V_{S30} = 3000$ m/sec. The modified profiles were used to compute the crustal amplifications used in the simulations in this report. ....16

Figure 9	(a) Velocity models for a modification of the Boore and Joyner [1997] very hard rock (VHR) site in eastern North America (ENA); see Boore and Thompson [2015] for an explanation of the models. The BJ97 model ended at 8 km, without the step shown in the left graph; the step is due to the velocity near the source being 3.7 km/sec, rather than 3.6 km/sec; and (b) amplifications for the two models, without and with the $\kappa$ attenuation operator for the modified BJ97 model. (Modified from Boore and Thompson [2015].) .....	17
Figure 10	Crustal amplifications for the three site conditions used in this report. The thin lines show the combined effect of the amplifications and kappa diminution operators [ $\exp(-\pi\kappa f)$ ]. .....	20
Figure 11	Ratios of PSA as a function of distance for $V_{S30} = 3000$ m/sec and $V_{S30} = 2000$ m/sec for the Atkinson [2004] (A04) and Boatwright and Seekins [2011] (BS11) attenuation models. Also shown are ratios of Fourier acceleration spectra (FAS) (no FAS ratio is shown for PGV). Each graph is for a single measure of ground motion (5%-damped PSA at the indicated periods and PGV) and a range of moment magnitudes (M). $\kappa = 0.006$ sec for all ratios. ....	23
Figure 12	Ratios of PSA for $V_{S30} = 3000$ m/sec and $V_{S30} = 2000$ m/sec as a function of period, for distances of 10 km and 100 km. The Boatwright and Seekins [2011] (BS11) attenuation model and a diminution operator with $\kappa = 0.006$ sec was used for the both site conditions. Also shown are ratios of Fourier acceleration spectra (FAS). .....	25
Figure 13	Ratios of PSA as a function of distance for $V_{S30} = 3000$ m/sec and $V_{S30} = 760$ m/sec for the Atkinson [2004] (A04) and Boatwright and Seekins [2011] (BS11) attenuation models. Also shown are ratios of Fourier acceleration spectra (FAS) (no FAS ratio is shown for PGV). Each graph is for a single measure of ground motion (5%-damped PSA at the indicated periods and PGV) and a range of moment magnitudes (M). $\kappa = 0.006$ sec for $V_{S30} = 3000$ m/sec and $\kappa = 0.005$ sec for $V_{S30} = 760$ m/sec. The modified Frankel et al. [1996] model was used for the $V_{S30} = 760$ m/sec crustal amplifications. ....	28
Figure 14	Ratios of PSA as a function of distance for $V_{S30} = 3000$ m/sec and $V_{S30} = 760$ m/sec for the Atkinson [2004] (A04) and Boatwright and Seekins [2011] (BS11) attenuation models. Also shown are ratios of Fourier acceleration spectra (FAS) (no FAS ratio is shown for PGV). Each graph is for a single measure of ground motion (5%-damped PSA at the indicated periods and PGV) and a range of moment magnitudes (M). $\kappa = 0.006$ sec for $V_{S30} = 3000$ m/sec and $\kappa = 0.010$ sec for $V_{S30} = 760$ m/sec. The modified Frankel et al. [1996] model was used for the $V_{S30} = 760$ m/sec crustal amplifications. ....	29

Figure 15	<p>Ratios of PSA as a function of distance for <math>V_{S30} = 3000</math> m/sec and <math>V_{S30} = 760</math> m/sec for the Atkinson [2004] (A04) and Boatwright and Seekins [2011] (BS11) attenuation models. Also shown are ratios of Fourier acceleration spectra (FAS) [no FAS ratio is shown for PGV, and it is off the top of the graph (33.9) for <math>T = 0.01</math> sec]. Each graph is for a single measure of ground motion (5%-damped PSA at the indicated periods and PGV) and a range of moment magnitudes (M). <math>\kappa = 0.006</math> sec for <math>V_{S30} = 3000</math> m/sec and <math>\kappa = 0.020</math> sec for <math>V_{S30} = 760</math> m/sec. The modified Frankel et al. [1996] model was used for the <math>V_{S30} = 760</math> m/sec crustal amplifications.....</p>	30
Figure 16	<p>Ratios of PSA as a function of distance for <math>V_{S30} = 3000</math> m/sec and <math>V_{S30} = 760</math> m/sec for the Atkinson [2004] (A04) and Boatwright and Seekins [2011] (BS11) attenuation models. Also shown are ratios of Fourier acceleration spectra (FAS) [no FAS ratio is shown for PGV, and it is off the top of the graph (784) for <math>T = 0.01</math> sec]. Each graph is for a single measure of ground motion (5%-damped PSA at the indicated periods and PGV) and a range of moment magnitudes (M). <math>\kappa = 0.006</math> sec for <math>V_{S30} = 3000</math> m/sec and <math>\kappa = 0.020</math> sec for <math>V_{S30} = 760</math> m/sec. The modified Frankel et al. [1996] model was used for the <math>V_{S30} = 760</math> m/sec crustal amplifications.....</p>	31
Figure 17	<p>Ratios of PSA as a function of distance for <math>V_{S30} = 3000</math> m/sec and <math>V_{S30} = 760</math> m/sec for the Atkinson [2004] (A04) and Boatwright and Seekins [2011] (BS11) attenuation model and the three values of <math>\kappa</math> (0.01 sec, 0.02 sec, and 0.03 sec) used for the <math>V_{S30} = 760</math> m/sec site condition. The modified Frankel et al. [1996] model was used for the <math>V_{S30} = 760</math> m/sec crustal amplifications. Also shown are ratios of Fourier acceleration spectra (FAS) [no FAS ratio is shown for PGV, and the ratios for <math>\kappa = 0.02</math> sec and 0.03 sec are off the top of the graph for <math>T = 0.01</math> sec]. Each graph is for a single measure of ground motion (5%-damped PSA at the indicated periods and PGV) and a range of moment magnitudes (M). <math>\kappa = 0.006</math> sec for <math>V_{S30} = 3000</math> m/sec . To make the period-dependent sensitivity of the ratios clear, all graphs have the same scale for the ordinate (sacrificing the ratios for <math>M = 2</math> and <math>T = 0.01</math> sec, which are off scale). .....</p>	32
Figure 18	<p>Ratios of PSA for <math>V_{S30} = 3000</math> m/sec and <math>V_{S30} = 760</math> m/sec as a function of period for distances of 10 km and 100 km. The Boatwright and Seekins [2011] (BS11) attenuation model and a diminution operation with <math>\kappa = 0.005</math> sec was used for the <math>V_{S30} = 760</math> m/sec site condition. The modified Frankel et al. [1996] model was used for the <math>V_{S30} = 760</math> m/sec crustal amplifications. Also shown are ratios of Fourier acceleration spectra (FAS). .....</p>	33

Figure 19	Ratios of PSA for $V_{S30} = 3000$ m/sec and $V_{S30} = 760$ m/sec as a function of period for distances of 10 km and 100 km. The Boatwright and Seekins [2011] (BS11) attenuation model and a diminution operation with $\kappa = 0.01$ sec was used for the $V_{S30} = 760$ m/sec site condition. The modified Frankel et al. [1996] model was used for the $V_{S30} = 760$ m/sec crustal amplifications. Also shown are ratios of Fourier acceleration spectra (FAS).....	34
Figure 20	Ratios of PSA for $V_{S30} = 3000$ m/sec and $V_{S30} = 760$ m/sec as a function of period for distances of 10 km and 100 km. The Boatwright and Seekins [2011] (BS11) attenuation model and a diminution operation with $\kappa = 0.02$ sec was used for the $V_{S30} = 760$ m/sec site condition. The modified Frankel et al. [1996] model was used for the $V_{S30} = 760$ m/sec crustal amplifications. Also shown are ratios of Fourier acceleration spectra (FAS).....	35
Figure 21	Ratios of PSA for $V_{S30} = 3000$ m/sec and $V_{S30} = 760$ m/sec as a function of period for distances of 10 km and 100 km. The Boatwright and Seekins [2011] (BS11) attenuation model and a diminution operation with $\kappa = 0.03$ sec was used for the $V_{S30} = 760$ m/sec site condition. The modified Frankel et al. [1996] model was used for the $V_{S30} = 760$ m/sec crustal amplifications. Also shown are ratios of Fourier acceleration spectra (FAS).....	36
Figure 22	Ratios of PSA for $V_{S30} = 3000$ m/sec and $V_{S30} = 760$ m/sec as a function of period for a distance of 10 km. The Boatwright and Seekins [2011] (BS11) attenuation model and a diminution operation with $\kappa = 0.02$ sec was used for the $V_{S30} = 760$ m/sec site condition. Three models were used for the $V_{S30} = 760$ m/sec crustal amplifications: Hashash and Harmon models HH1000 and HH3000, and the OTT model of Beresnev and Atkinson [1997]......	38
Figure 23	Ratios of PSA for $V_{S30} = 3000$ m/sec and $V_{S30} = 760$ m/sec as a function of period for a distance of 100 km. The Boatwright and Seekins [2011] (BS11) attenuation model and a diminution operation with $\kappa = 0.02$ sec was used for the $V_{S30} = 760$ m/sec site condition. Three models were used for the $V_{S30} = 760$ m/sec crustal amplifications: Hashash and Harmon models HH1000 and HH3000, and the OTT model of Beresnev and Atkinson [1997]......	39
Figure 24	Ratios of PSA for $V_{S30} = 3000$ m/sec and $V_{S30} = 760$ m/sec as a function of period for a distance of 10 km. The Boatwright and Seekins [2011] (BS11) attenuation model and a diminution operation with $\kappa = 0.02$ sec was used for the $V_{S30} = 760$ m/sec site condition. Three models were used for the $V_{S30} = 760$ m/sec crustal amplifications: Frankel et al. [1996] (Fca96), the average BC model derived in this report (Average BC), and the OTT model of Beresnev and Atkinson [1997]......	40



Figure 25	Ratios of PSA for $V_{S30} = 3000$ m/sec and $V_{S30} = 760$ m/sec as a function of period for a distance of 100 km. The Boatwright and Seekins [2011] (BS11) attenuation model and a diminution operation with $\kappa = 0.02$ sec was used for the $V_{S30} = 760$ m/sec site condition. Three models were used for the $V_{S30} = 760$ m/sec crustal amplifications: Frankel et al. [1996] (Fea96), the average BC model derived in this report (Average BC), and the OTT model of Beresnev and Atkinson [1997].....41
Figure 26	Ratios of PSA for $V_{S30} = 3000$ m/sec and $V_{S30} = 760$ m/sec as a function of period for distances of 10 km and 100 km. The Boatwright and Seekins [2011] (BS11) attenuation model and a diminution operation with $\kappa = 0.03$ sec was used for the $V_{S30} = 760$ m/sec site condition. The modified Frankel et al. [1996] model was used for the $V_{S30} = 760$ m/sec crustal amplifications. Also shown are ratios of Fourier acceleration spectra (FAS).....42



# 1 Introduction

The ground-motion intensity measures (GMIMs) used in the PEER NGA-East project were derived from recordings obtained from sites with a large range of  $V_{S30}$  values (the parameter used to characterize site amplification). The distribution of  $V_{S30}$  from the 18 November 2014 version of the NGA-East flatfile [Goulet et al. 2014] is shown in Figure 1. The figure is given in two parts: the left graph shows the distribution for all sites, and the right graph shows the distribution for sites somewhat subjectively defined as being in southeastern (SE) Canada and northeastern (NE) U.S. (north of New York City, New York, and east of St. Louis, Missouri). The latter graph was made because the fundamental interest in this report is to derive adjustment factors to modify the observed GMIMs to a reference rock site condition, defined by Hashash et al. [2014] as a hard rock site with  $V_{S30} = 3000$  m/sec. Hard rock sites are more likely to be found in glaciated regions such as SE Canada and NE U.S. than elsewhere. This is confirmed by Figure 1, in which it is clear that most of the sites in the NGA-East database correspond to stiff soil/soft rock conditions, whereas the distribution of  $V_{S30}$  in SE Canada and NE U.S. is quite different, with a number of sites corresponding to hard rock ( $V_{S30} = 2000$  m/sec). Although most, if not all, of the  $V_{S30} = 2000$  m/sec assignments are estimated from factors such as local site geology, topographic slopes, or type of terrain, and are not based on measurements, the value of  $V_{S30} = 2000$  m/sec serves as a proxy for sites that would be classified as being on hard rock.

It is of interest that no sites in the NGA-East database have  $V_{S30}$  values greater than 2000 m/sec. Therefore, the reference hard-rock condition is an idealization that does not exist or is rare in reality. The observations used by Hashash et al. [2014] to derive the reference-rock condition of 3000 m/sec were largely from measurements in boreholes at depths below the surface, where the velocities were not influenced by weathering layers and sedimentary overburden; thus they do not correspond to actual values of  $V_{S30}$  that would have been obtained from those sites. In spite of the absence of sites with  $V_{S30} = 3000$  m/sec, the simulations in the NGA-East project are for a site condition of  $V_{S30} = 3000$  m/sec. The choice of such a high value was motivated by not wanting site-specific amplifications to be significantly influenced by the material beneath any local sedimentary layers. In other words, input motions could be taken as those on the surface of the reference rock and then propagated through a site-specific velocity profile placed on top of the reference rock velocity profile.

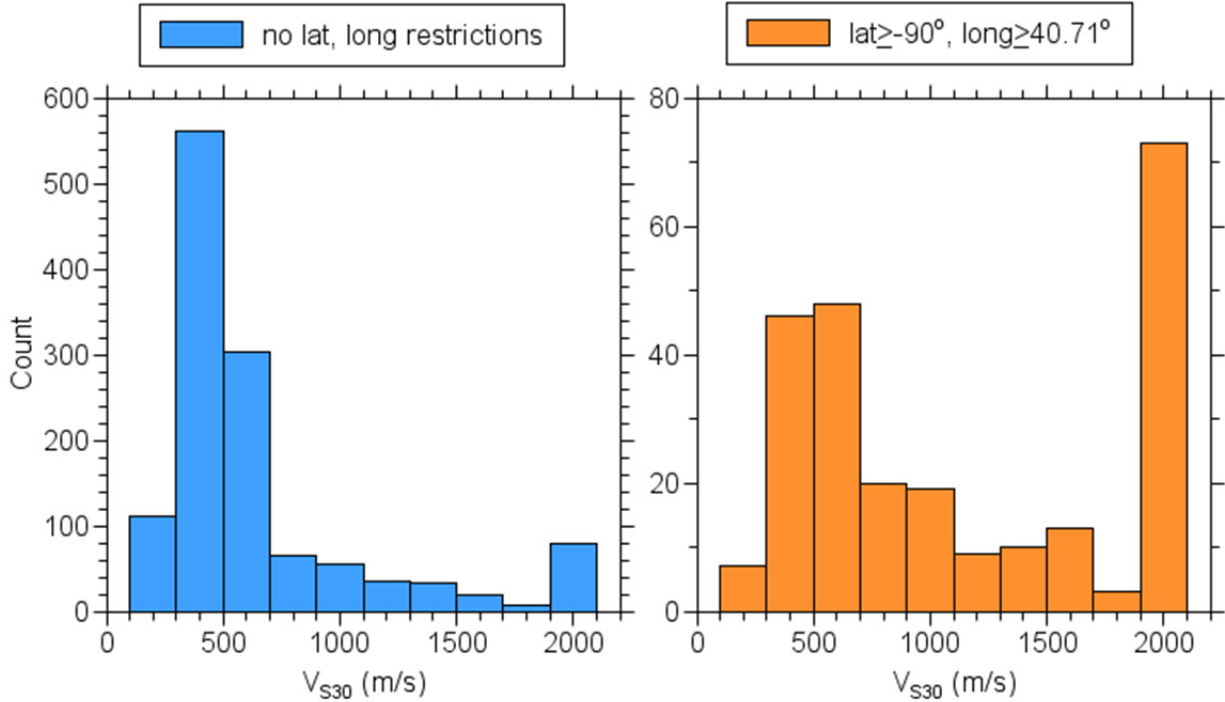


**Figure 1** Histograms of  $V_{S30}$  values in the NGA-East flatfile. The left graph includes all sites, whereas the right graph is the subset of sites east of St. Louis, Missouri, and north of New York City, New York (this is a rough way of choosing sites in northeastern U.S. and southeastern Canada).

In view of the dominance of sites in the NGA-East database with  $V_{S30}$  values less than 2000 m/sec, it is useful to adjust recorded motions to a reference-rock condition. This is useful for comparisons of simulations and observations. The adjustments in this report are developed for three types of GMIMs: 5%-damped pseudo-absolute response spectral acceleration (PSA), peak ground velocity (PGV), and peak ground acceleration (PGA). The method for adjusting observed motions to the reference-rock condition is straightforward. There are three steps to the method:

1. Adjust observed GMIMs to an intermediate reference condition (usually  $V_{S30} = 2000$  m/sec) using the site function that appears in ground-motion prediction equations (GMPEs). The function most commonly used is  $\ln GMIM \approx c \ln(V_{S30}/V_{REF})$ ; the coefficient  $c$  could come from studies such as those of Hollenback et al. [2015], regressing data in the NGA-East flatfile, or from other studies such as described by Stewart et al. [2012], in which amplifications from the PEER NGA-West2 GMPEs are adjusted based on residuals of the NGA-East data relative to the NGA-West2 GMPEs, or even from the NGA-West2 GMPEs, assuming the stiff soil/soft rock site responses are similar in eastern and western North America;
2. Simulate GMIMs for many magnitudes ( $M$ ), distances ( $R_{RUP}$ , the closest distance to the rupture surface), and oscillator periods ( $T$ ), one set of simulations using crustal amplifications for Fourier spectra obtained from models for which

$V_{S30} = 760$  m/sec, and a second set of simulations for crustal amplifications with  $V_{S30} = 3000$  m/sec; and

3. Form the ratios of the GMIMs for the two sets of amplifications. These ratios are the second set of adjustment factors to be applied to motions, the first set being discussed in step 1. The second set of adjustments is given here as tables, rather than as equations that are a function of magnitude, distance, and oscillator period. As will be discussed, the adjustment ratios are relatively constant for certain ranges of  $\mathbf{M}$ ,  $R_{RUP}$ , and  $T$ .

In this report, I discuss the crustal amplifications for the two values of  $V_{S30}$  (760 m/sec and 3000 m/sec) and then the ratios of GMIMs needed for step 2 (adjusting the GMIM values from sites with  $V_{S30} = 760$  m/sec to those with  $V_{S30} = 3000$  m/sec). Included in the section on the crustal amplifications is a discussion of the velocity profiles used for the amplifications. In addition to the ratios of GMIMs for  $V_{S30} = 3000$  m/sec divided by GMIMs for  $V_{S30} = 760$  m/sec, I also show GMIM ratios for  $V_{S30} = 3000$  m/sec divided by the GMIM for  $V_{S30} = 2000$  m/sec, because many of stations in the NGA-East flatfile have been assigned  $V_{S30} = 2000$  m/sec (as an aside, I would think that this argues for the reference velocity for NGA-East being 2000 m/sec, not 3000 m/sec).



## 2 CRUSTAL AMPLIFICATIONS FOR SITES WITH $V_{S30} = 760$ m/sec

### 2.1 VELOCITY PROFILES FOR SITES WITH $V_{S30} = 760$ M/SEC

I was provided with six profiles for which  $V_{S30} = 760$  m/sec. From here on, I sometimes refer to these sites as BC sites, named after the boundary between the National Earthquake Hazards Reduction Program [NEHRP] sites classes B and C (Chapter 3) [BSSC 2004]. Three profiles came from Walter Silva (S), and the other three came from Youssef Hashash and Joseph Harmon (HH). These models [note: I use “profiles” and “models” interchangeably] were guided by databases of velocity profiles. Sites with the same value of  $V_{S30}$  can be underlain by quite different velocity profiles; the multiplicity of profiles for each author is intended to include a range of those velocity-depth functions. The HH models have velocities of 3 km/sec within 100 m or so of the surface.

I was initially skeptical that such high velocities could occur at shallow depths, but a number of the models in Beresnev and Atkinson [1997] have velocities close to or greater than 3000 m/sec within 50 m of the surface. In addition, I used the BC site condition velocity model from Frankel et al. [1996] (Fea96). This model, derived by me and in collaboration with Art Frankel, replaces a western U.S. model that I used in 1986 with a model having a linear gradient in the upper 200 m with a slope such that  $V_{S30} = 760$  m/sec. These seven models are not from measurements at specific sites but are intended to represent generic sites. In addition to those seven models, I used velocity models based on measurements at three sites for which  $V_{S30}$  was close to 760 m/sec: HAIL, Harrisburg, IL,  $V_{S30} = 765$  m/sec, from Odum et al. [2010]; HATCH, Baxley, Georgia, Georgia Power Co.,  $V_{S30} = 762$  m/sec, from J. C. Chin [*Personal Communication*]; and OTT, Ottawa, Ontario,  $V_{S30} = 755$  m/sec, from Beresnev and Atkinson [1997]. The velocity profiles for the ten models are shown in Figures 2 and 3; the figures differ only in the maximum depth for each figure.

As is obvious from Figures 2 and 3, even though each model has a  $V_{S30}$  very close to 760 m/sec, the models differ significantly in detail. The models range from those represented by continuous functions of depth (e.g., Fea96) to those with large jumps in velocity at discrete interfaces (e.g., S760t), as well as a combination of these two characteristics (e.g., HH1000).

Because the simulations need velocity profiles extending to depths of at least 8 km, I had to merge the shallow profiles with deeper profiles. I did this by plotting the nine models that did not extend to 8 km (three Silva, three HH, HAIL, HATCH, and OTT) along with three shear-wave profiles extending to a depth of 8 km that I had available. These deeper profiles are the one

from Fea96, and the Boore and Joyner [1997] (BJ97) generic rock and very hard rock profiles. The combined velocity models, which were used in the calculations of crustal amplifications, are shown in Figures 4 and 5 for different maximum depths. In those figures, I have not distinguished between the original shallow models and the extended models, but the legends include the maximum depths of each shallow model.

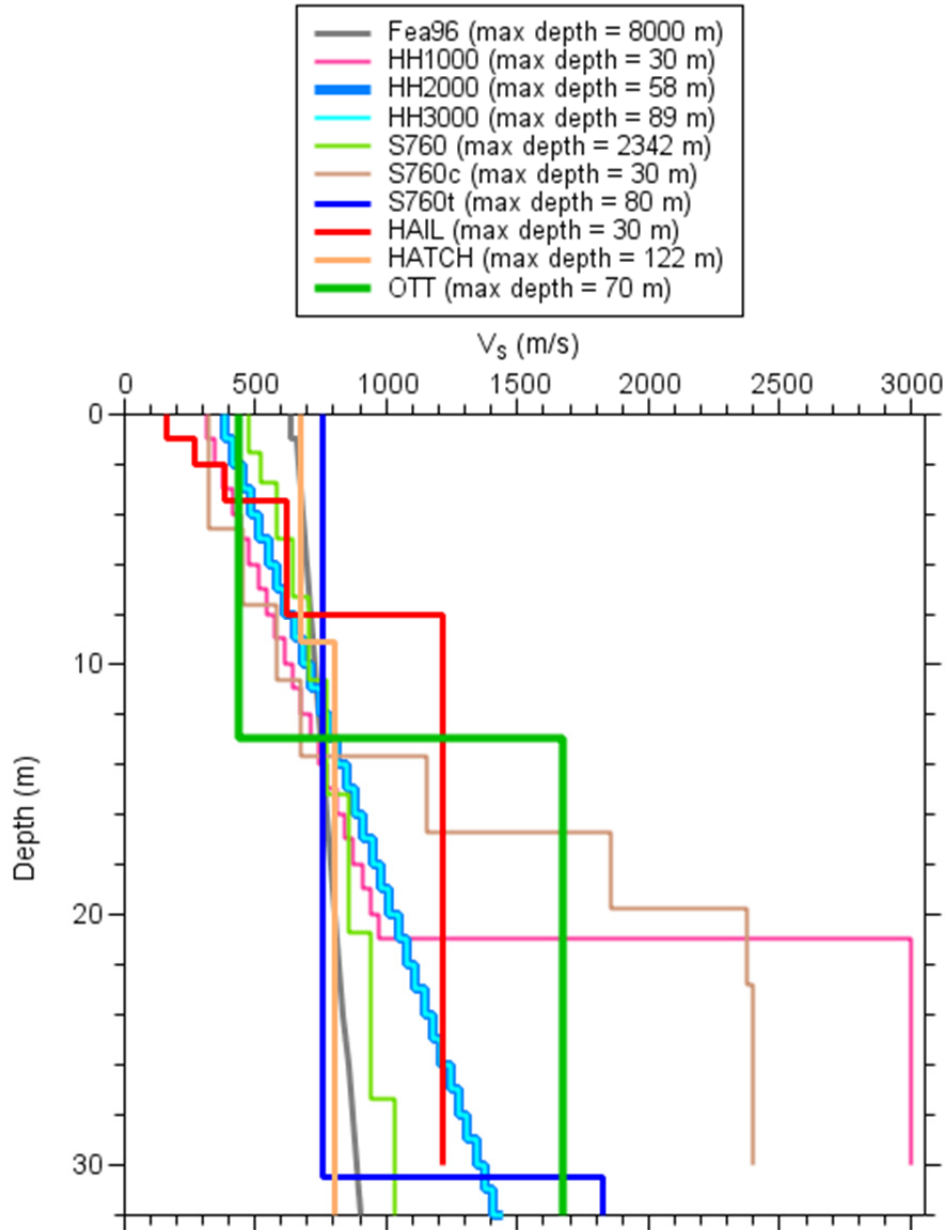
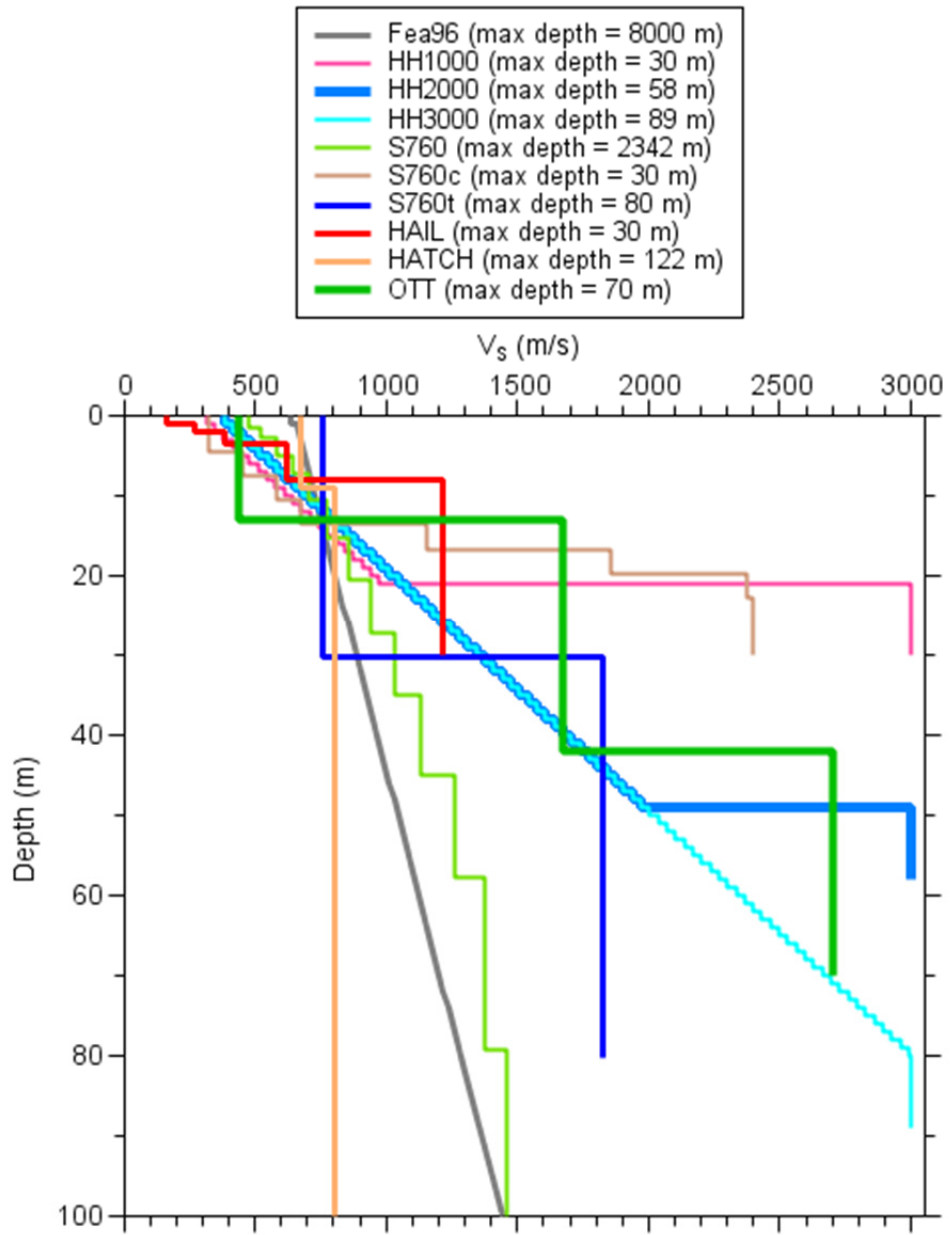
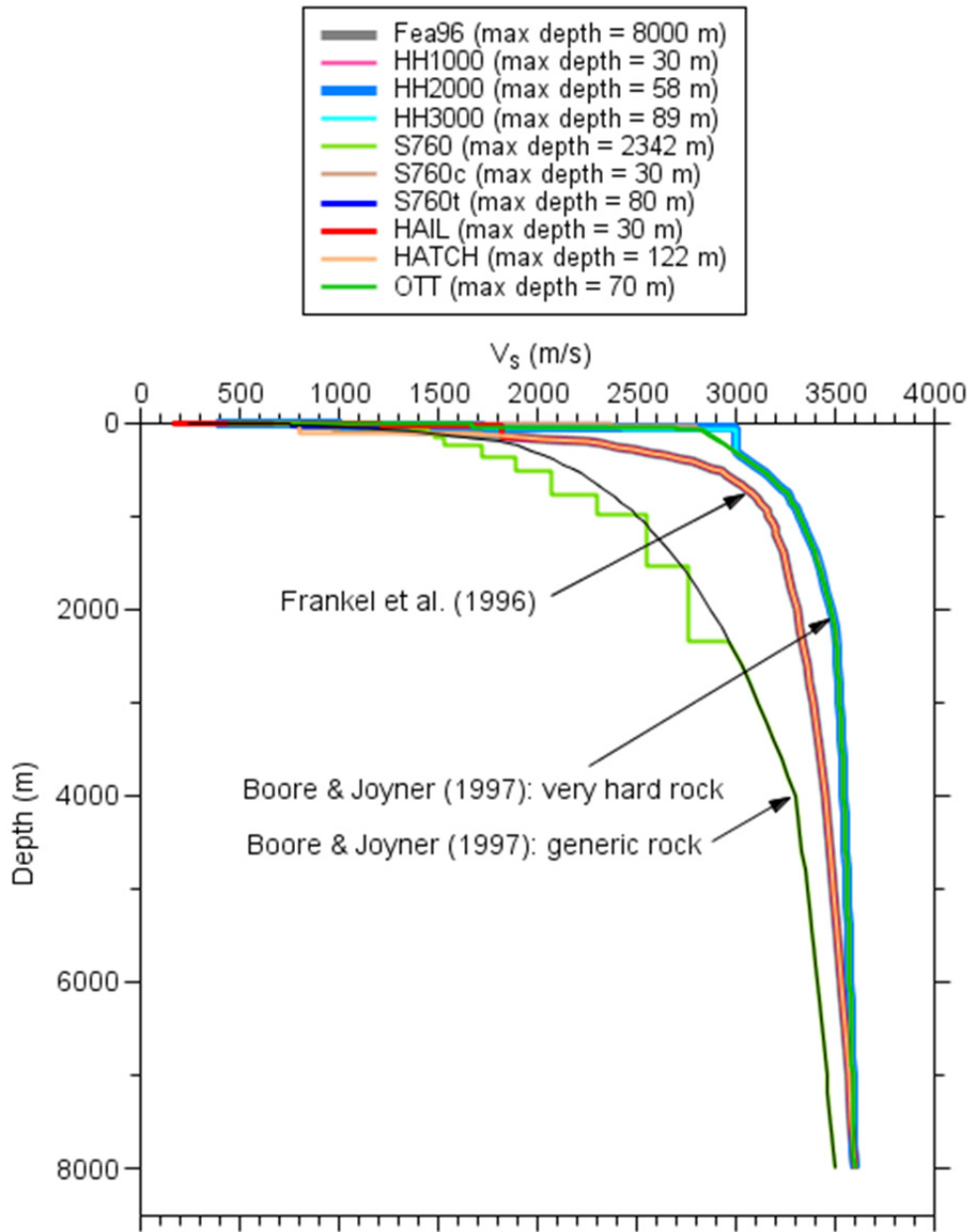


Figure 2 Models with  $V_{s30} = 760$  m/sec (Fea96=Frankel et al.; HH=Hashash and Harmon; S=Silva—see text for details). Some of the models extend below 32 m. The lowest depth of 32 m was chosen so that near-surface details can be seen.





**Figure 3** Models with  $V_{s30} = 760$  m/sec; see caption to Figure 2 for explanation of model abbreviations. Some of the models extend below 100 m. The lowest depth of 100 m was chosen so that details deeper than the 32 m used in the previous figure can be seen.



**Figure 4** Combined profiles; see caption to Figure 2 for explanation of model abbreviations. The maximum depth for the plot is 8500 m. The main purpose of this figure is to show the three profiles on to which the shallow profiles were merged.

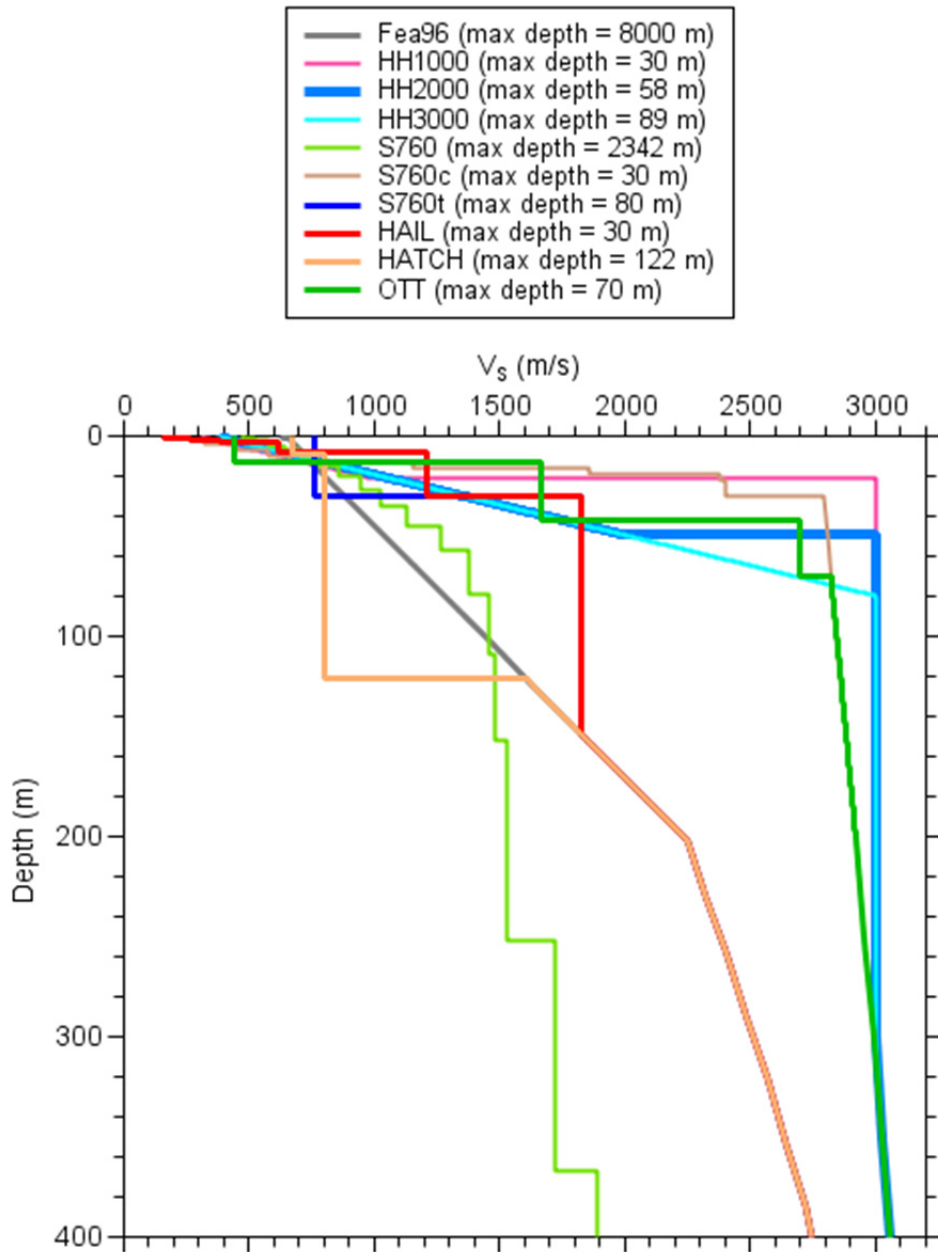


Figure 5 Combined profiles; see caption to Figure 2 for explanation of model abbreviations. The maximum depth of 400 m was chosen to show model details between those shown in Figure 4 and Figure 3.

## 2.2 AMPLIFICATIONS FOR SITES WITH $V_{s30} = 760$ M/SEC

I computed the square-root impedance (SRI) amplifications for each of the profiles, using the method described in Boore [2013]. The amplifications were computed assuming a source density and velocity of 2.8 g/cc and 3.7 km/sec, assuming a vertical angle of incidence and no attenuation (see Boore and Thompson [2015]). I also computed full resonant amplifications for

two Silva models, a gradient model (S760) and a model with a large change in velocity at a single interface (S760t); see Figure 3. All amplifications assume linear response. The amplifications assume no attenuation, but to show the effect of attenuation, curves have been added for two models in which the diminution operator  $\exp(-\pi\kappa f)$  has been applied, with  $\kappa=0.02$  sec. The results are shown in Figures 6 and 7 (where Figure 7 shows the subset of models from Figure 6 that were used in computing BC-to-reference rock adjustment factors described later).

Here are some comments on the amplifications shown in Figure 6:

1. The SRI amplifications all come together at a frequency corresponding to a quarter wavelength for 30 m, since each model has the same or almost the same  $V_{S30}$ ;
2. The amplifications at lower frequencies are controlled by the deeper parts of the profiles, and since there are three deeper profiles, the amplifications for the ten shallow models merge into one of three amplification curves;
3. At higher frequencies the amplifications are controlled by the shallow parts of the models, which can have significant variations—but the diminution operator will reduce the importance of these high frequencies when computing PSA at short periods; and
4. The full resonant amplifications are in reasonable agreement with both the gradient and step models (the underprediction of the resonant peaks for the step model is a well-known limitation of the SRI method (see Boore [2013])).

Although I could compute BC-to-reference rock ( $V_{S30} = 3000$  m/sec) adjustment factors for each of the BC models, I decided to compute adjustment factors for five models: Fea96, OTT, HH1000, HH3000, and a subjectively chosen weighted average of the amplifications, labeled as “Average BC Model” in Figures 6 and 7. The average BC model is the geometric mean of the amplifications for Fea96, HH1000, HH3000, and OTT; these models were chosen subjectively to incorporate both gradient and step models (in particular, that for OTT—till over glaciated rock). The crustal amplifications for the Fea96, OTT, and Average BC models are given in Table 1. The OTT model corresponds to one that might be encountered in glaciated regions, with a layer of glacial till on top of bedrock for which glaciation has removed any weathered layer. Such a site would be quite different than BC sites in other parts of the central and eastern North America (CENA). On the other hand, Figure 1 shows that most of the data in the NGA-East flatfile have a  $V_{S30}$  distribution that is quite different than those in NE U.S. and SE Canada; therefore, BC-to-reference rock adjustment factors for a BC model more representative of those sites is probably more useful for the NGA-East project. For this reason most of the results discussed in this report used the Fea96 model for the BC crustal amplifications. A comparison between the adjustment factors for the Fea96, OTT, HH1000, HH3000, and Average BC models is given in a later section.

On the other hand, Figure 1 shows that most of the data in the NGA-East flatfile have a  $V_{S30}$  distribution that is quite different than those in NE U.S. and SE Canada, and therefore BC-to-reference rock adjustment factors for a BC model more representative of those sites is probably more useful for the NGA-East project. For this reason most of the results discussed in this report used the Fea96 model for the BC crustal amplifications. A comparison between the

adjustment factors for the Fea96, OTT, HH1000, HH3000, and Average BC models is given in a later section.

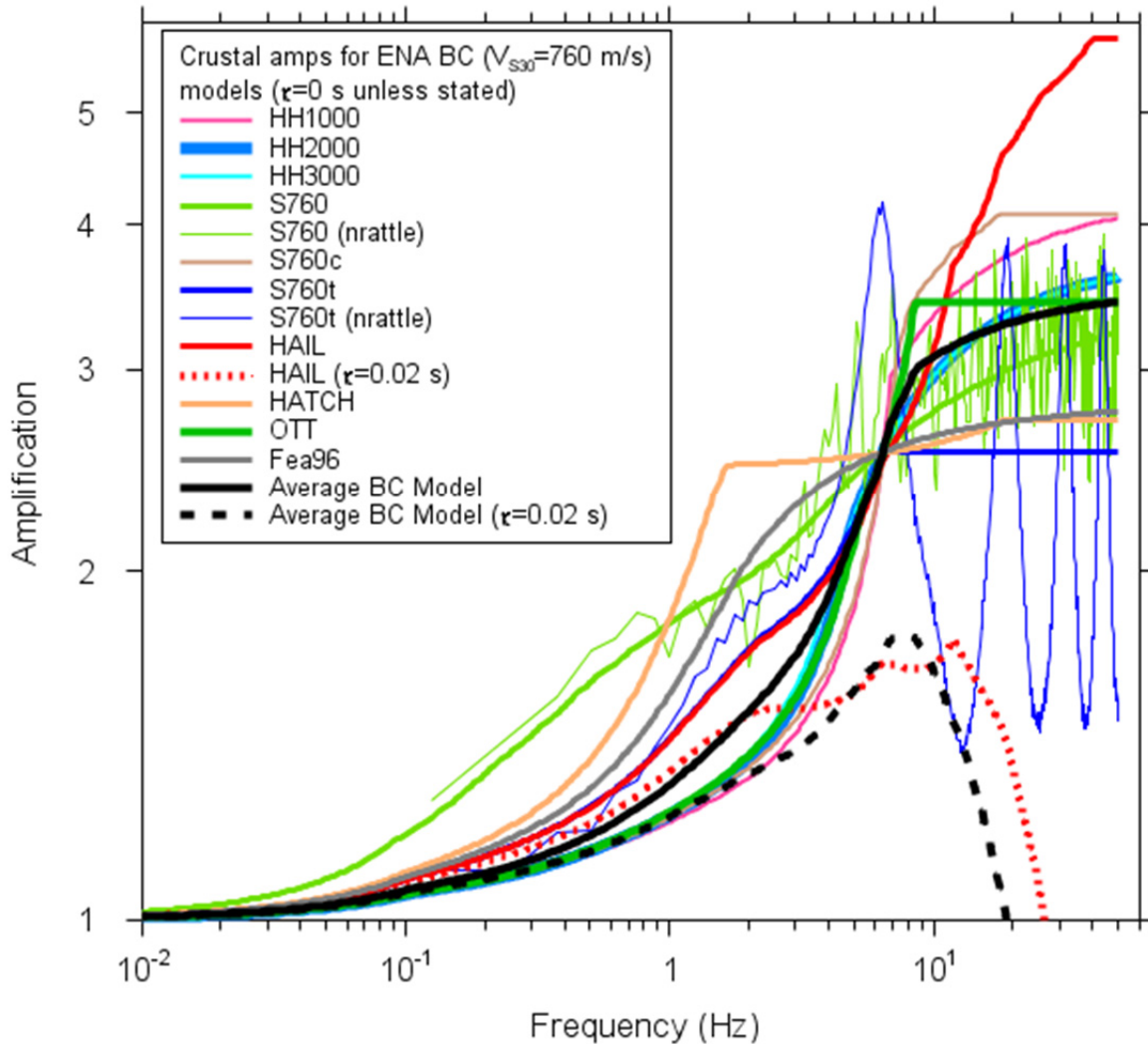


**Figure 6** Amplifications from the square-root-impedance method [Boore 2013] assuming an angle of incidence of 0 degrees; also shown are full-resonant amplifications (using the program *nrattle*) for two of the Silva profiles (one gradient-like and one step-like), assuming *SH* waves with a 30 degree angle of incidence. The effect of applying a kappa operator with  $\kappa = 0.02$  sec is also shown for two of the profiles. The Fea96 amplifications used a newer velocity-density relation than used to obtain the densities in Table A6 of Frankel et al. [1996] (Fea96), and therefore the amplifications shown in the figure are slightly different than those in Table A5 of Fea96.

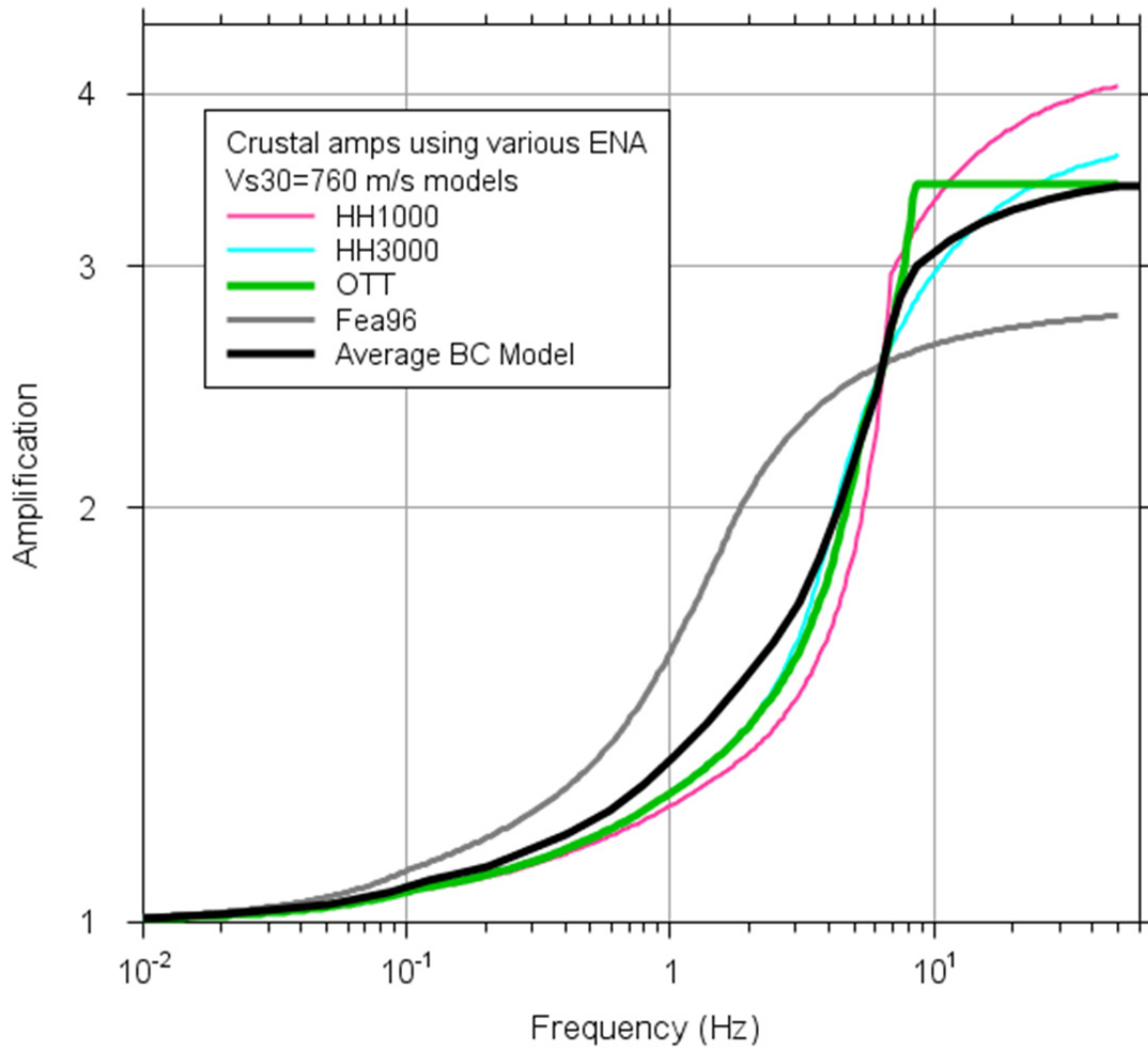


**Figure 7** The subset of crustal amplifications shown in Figure 6 that are used in computing the adjustment factors to go from sites with  $V_{S30} = 760$  m/sec to those with  $V_{S30} = 3000$  m/sec.

**Table 1** Crustal amplifications for three models with  $V_{S30}$  close to 760 m/sec\*.

F :Fea96	A:Fea96	F:Average	A:Average	F:OTT	A:OTT
0.005	1.000	0.001	1.001	0.010	1.009
0.010	1.019	0.007	1.004	0.030	1.014
0.022	1.031	0.020	1.011	0.060	1.031
0.053	1.054	0.051	1.029	0.111	1.056
0.120	1.104	0.085	1.051	0.195	1.081
0.223	1.167	0.121	1.070	0.377	1.123
0.362	1.234	0.203	1.098	0.635	1.175
0.541	1.321	0.401	1.155	1.027	1.245
0.789	1.450	0.586	1.205	1.575	1.328
1.179	1.667	0.789	1.256	2.294	1.437
1.657	1.928	1.035	1.316	3.105	1.573
2.273	2.135	1.395	1.395	3.786	1.731
3.156	2.314	1.879	1.493	4.617	1.974
4.772	2.470	2.465	1.597	5.233	2.250
8.149	2.595	3.062	1.705	6.057	2.430
15.522	2.677	3.702	1.837	6.937	2.745
32.987	2.736	4.356	1.998	7.863	3.086
59.130	2.761	5.266	2.240	8.459	3.436
76.330	2.761	6.031	2.429	42.663	3.436
—	—	6.542	2.581	—	—
—	—	6.907	2.704	—	—
—	—	7.447	2.852	—	—
—	—	8.580	3.000	—	—
—	—	11.562	3.134	—	—
—	—	15.163	3.226	—	—
—	—	19.886	3.296	—	—
—	—	26.798	3.354	—	—
—	—	36.112	3.397	—	—
—	—	50.000	3.432	—	—
—	—	100.000	3.432	—	—

\*F,A are frequencies and amplifications for each model. The frequencies are model dependent; they were chosen to give a good approximation of the amplifications shown in Figure 6, but using a smaller number of frequencies.





### **3 CRUSTAL AMPLIFICATIONS FOR SITES WITH $V_{S30} = 2000$ M/SEC and $V_{S30} = 3000$ M/SEC**

#### **3.1 VELOCITY PROFILES FOR SITES WITH $V_{S30} = 2000$ AND $V_{S30} = 3000$ M/SEC**

The velocity profiles used for the crustal amplifications are based on the very hard rock profile of Boore and Joyner [1997]. For  $V_{S30} = 3000$  m/sec, the top 300 m of the Boore and Joyner profile was replaced by a layer with a velocity of 3000 m/sec (see Boore and Thompson [2015]). For  $V_{S30} = 2000$  m/sec, the top 30 m of the profile had a shear-wave velocity of 2000 m/sec; this was underlain by material with a linear gradient, joining the standard profile at a depth of 300 m. The velocity models are shown in Figure 8. Figure 9(a), from Boore and Thompson [2015], compares the  $V_{S30} = 3000$  m/sec model used here with a different model having the same  $V_{S30}$ .

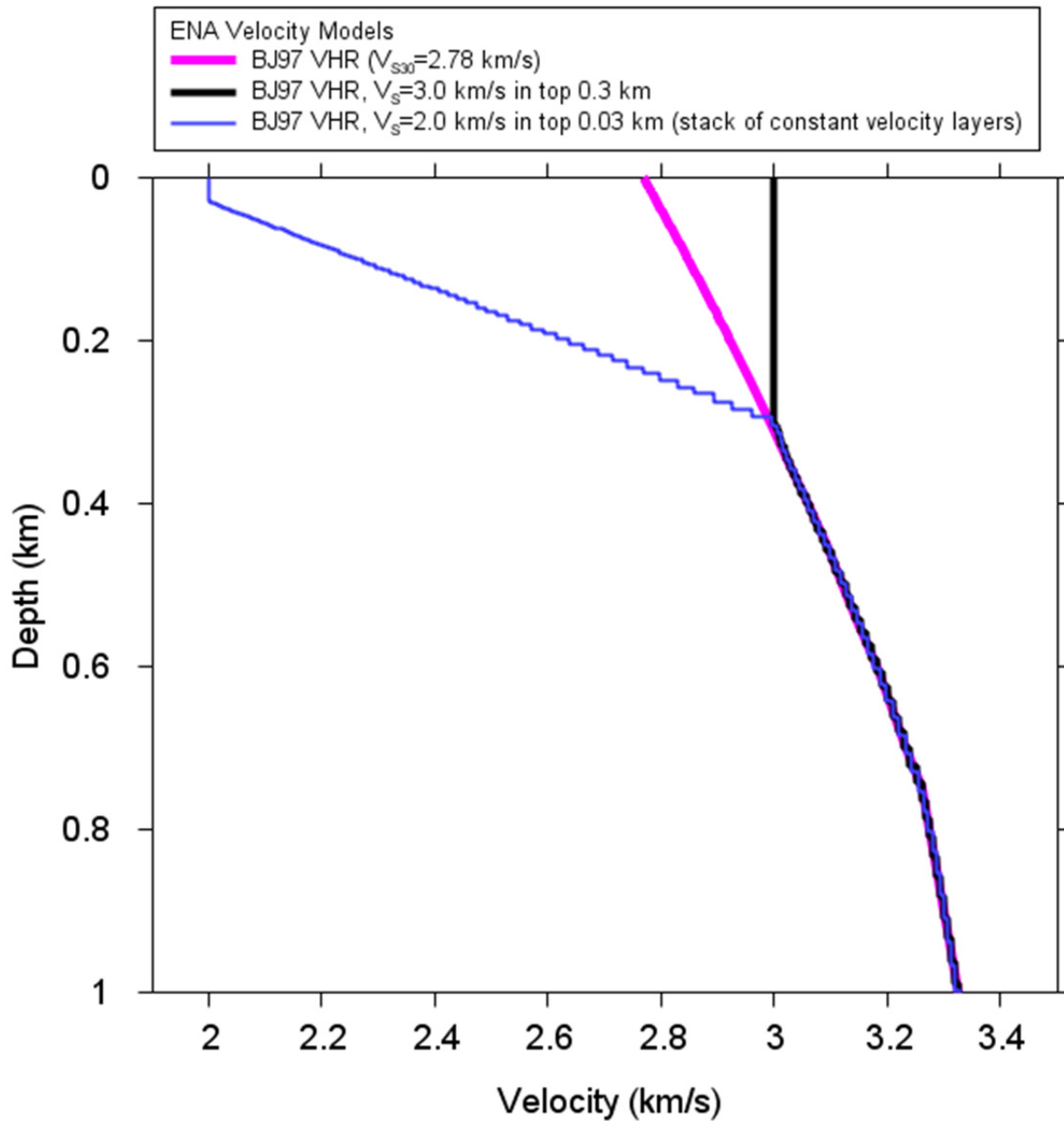


Figure 8 The Boore and Joyner [1997] (BJ97) very hard rock (VHR) velocity profile and the modifications to that profile such that  $V_{S30} = 2000$  m/sec and  $V_{S30} = 3000$  m/sec. The modified profiles were used to compute the crustal amplifications used in the simulations in this report.

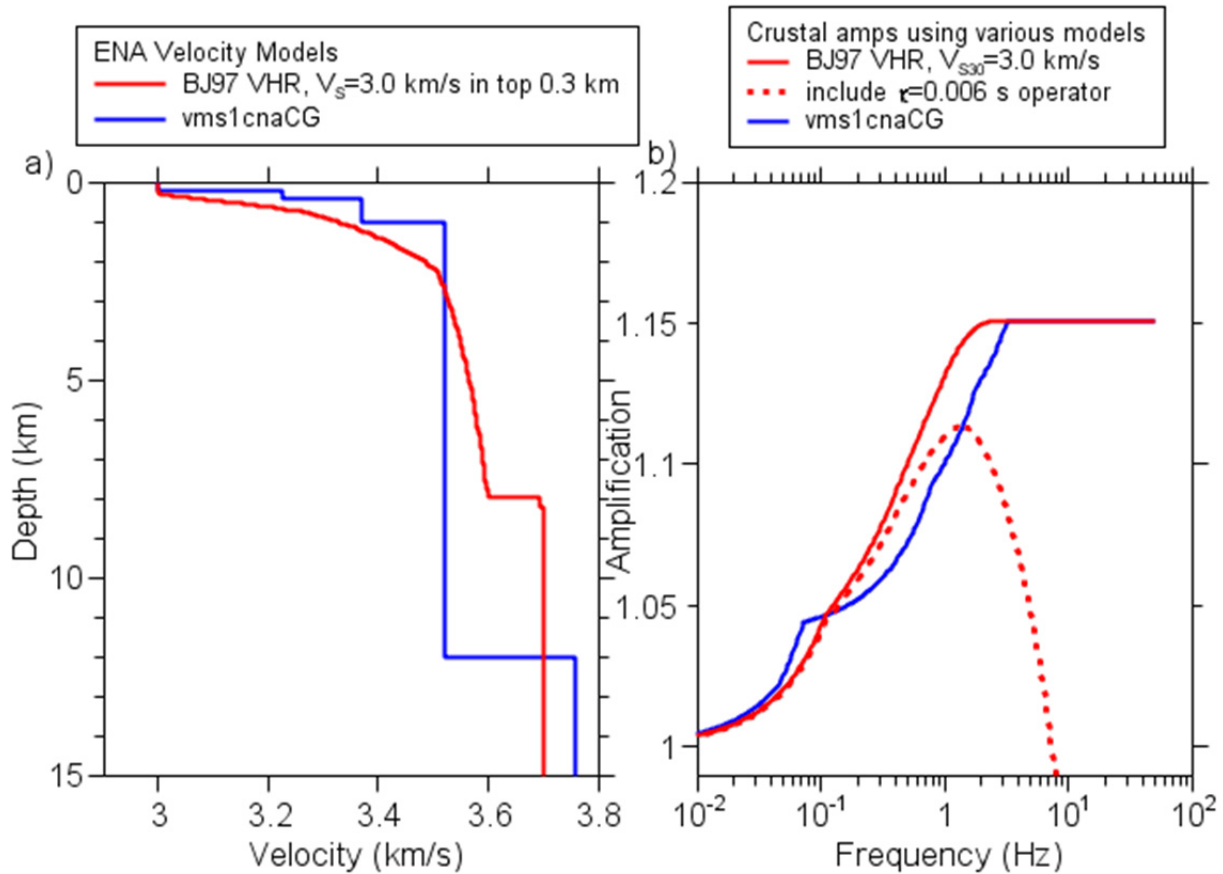


Figure 9 (a) Velocity models for a modification of the Boore and Joyner [1997] very hard rock (VHR) site in eastern North America (ENA); see Boore and Thompson [2015] for an explanation of the models. The BJ97 model ended at 8 km, without the step shown in the left graph; the step is due to the velocity near the source being 3.7 km/sec, rather than 3.6 km/sec; and (b) amplifications for the two models, without and with the  $\kappa$  attenuation operator for the modified BJ97 model. (Modified from Boore and Thompson [2015].)

### 3.2 AMPLIFICATIONS FOR SITES WITH $V_{S30} = 3000$ M/SEC

The amplifications were computed using the same method and assumptions as those for sites with  $V_{S30} = 760$  m/sec, with the results shown in Figure 9(b). In spite of the detailed differences in the two velocity models, the crustal amplifications for the two models are similar, and, more importantly, they are small.



#### **4 COMPARISON OF CRUSTAL AMPLIFICATIONS FOR SITES WITH $V_{S30} =$ 760 M/SEC, $V_{S30} = 2000$ M/SEC, and $V_{S30} =$ 3000 M/SEC**

The crustal amplifications for the three site conditions, without and with attenuation, are compared in Figure 10. Note that the combined amplification and diminution for sites with  $V_{S30} = 760$  m/sec is greater than for higher velocity sites except at high frequencies, where the decrease due to the diminution operator overwhelms the amplification. This has an impact on the BC-to-reference rock adjustment factors (defined as the ground motion intensity measure for a reference rock site divided by on for a BC site), which tend to become greater than unity at short periods as  $\kappa$  increases and  $\mathbf{M}$  decreases, as will be seen in the next section.

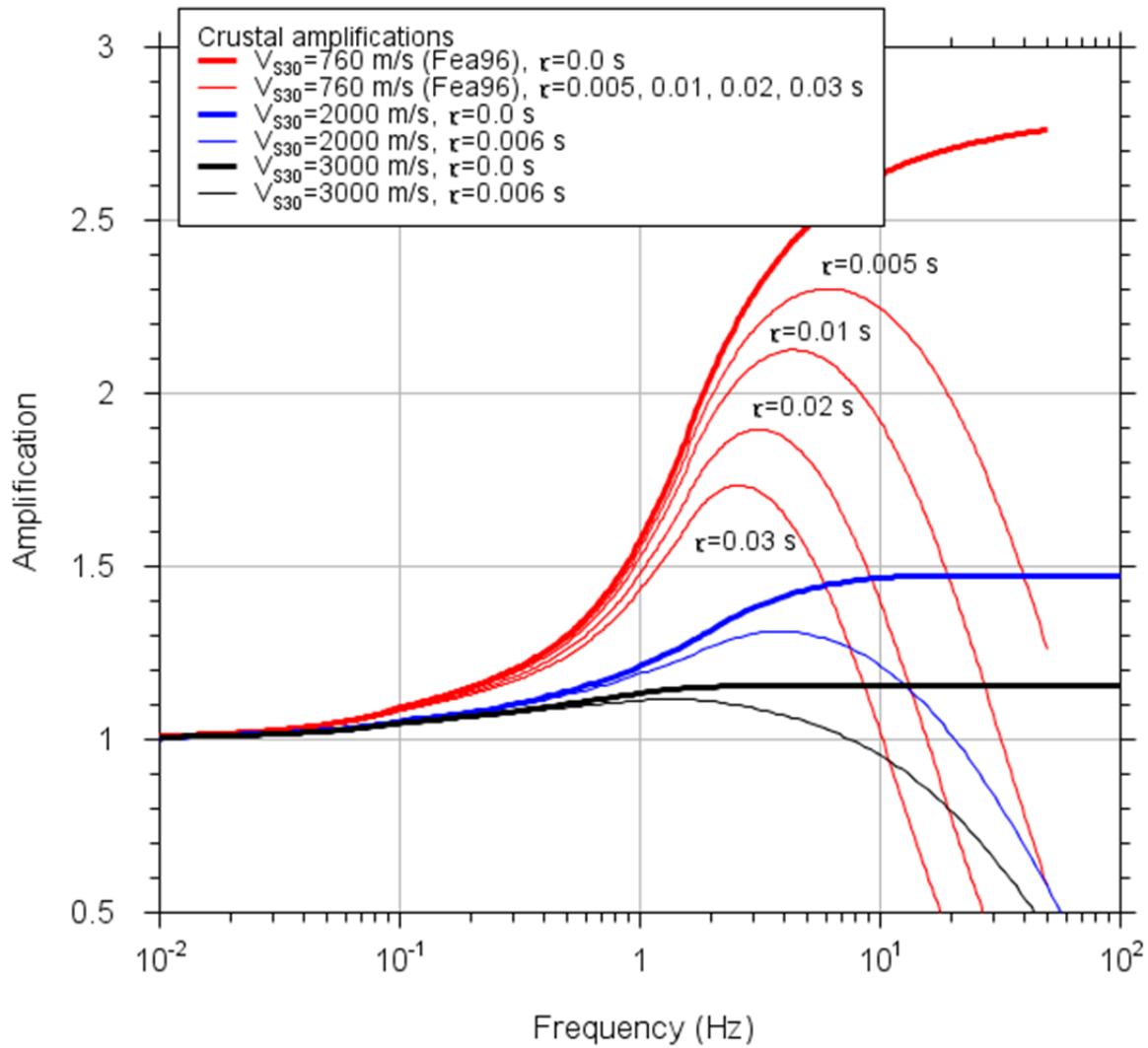


**Figure 10** Crustal amplifications for the three site conditions used in this report. The thin lines show the combined effect of the amplifications and kappa diminution operators [ $\exp(-\pi\kappa f)$ ].

## 5 COMPUTATION OF BC-TO-REFERENCE ROCK ADJUSTMENT FACTORS

The BC-to-reference rock adjustment factor (*BC2RRAF*) is defined as

$$BC2RRAF = \frac{Y(V_{S30} = 3000 \text{ m/sec})}{Y(V_{S30} = 760 \text{ m/sec})} \quad (1)$$

where  $Y$  is a GMIM for the indicated site condition. I defined the ratio with the BC GMIM in the denominator so that the adjustment of an observed motion is given by a multiplication of the observed motion, adjusted to the BC condition, by *BC2RRAF*. I computed  $Y$  and *BC2RRAFs* for two very different path attenuation models: Atkinson [2004] (A04), with a steep decay of  $1/R^{1.3}$  within the first 70 km, an increase going as  $R^{0.2}$  from 70 to 140 km, followed by a  $1/R^{0.5}$  decay, and the Boatwright and Seekins [2011] (BS11) model, with  $1/R^{1.0}$   $1/R^{1.0}$  within the first 50 km, followed by  $1/R^{0.5}$ . The  $Q(f)$  models differ for A04 and BS11. The Boore and Thompson [2015] path durations were used. The point-source stochastic method program *tmrs\_loop\_rv\_drvr*, part of the SMSIM suite of programs [Boore 2005], was used for the simulations. Other model parameters are contained in the SMSIM parameter files (these files are in the electronic appendix to this report). The Boore and Thompson [2015] finite-fault adjustment factor for earthquakes in stable continental regions was used in the computations. Also in the electronic appendix are files containing tables of the adjustment factors. Interpolation of these tables can be used to obtain the adjustment factors for non-tabulated periods, magnitudes, and distances.

### 5.1 ADJUSTMENTS OF GMIMS FOR SITES WITH $V_{S30} = 2000$ M/SEC TO THOSE WITH $V_{S30} = 3000$ M/SEC

Before showing the *BC2RRAFs*, I first discuss the adjustment factors from a site with  $V_{S30} = 2000$  m/sec to one with  $V_{S30} = 3000$  m/sec. This uses Equation (1), but with  $Y$  in the denominator computed for a  $V_{S30} = 2000$  m/sec crustal amplification. For both site conditions, the Campbell et al. [2014] reference value of 0.006 sec for  $\kappa$  was used in the simulations. The results are shown in Figure 11, where the adjustment factors are plotted against distance, with different GMIMs in each graph. As seen there, the adjustment factors are quite similar for the two attenuation models (A04 and BS11). Figure 11 also includes the ratio of the Fourier amplitude spectra (FAS) for the two crustal amplification models. Because the models only

differ in the amplifications, and thus the FAS ratios are the same as the ratios of the crustal amplifications themselves, they are not a function of magnitude or distance. Table 2 compiles these FAS ratios; because the possible use of this table, and subsequent ones for BC-to-reference rock, is as a simple substitute for the  $M$ - and  $R_{RUP}$ -dependent adjustment factors based on the stochastic method simulations in converting response spectra from on-site condition to another, the FAS ratios are tabulated versus period rather than frequency.

The FAS ratios and the adjustment factors are in good agreement for the larger magnitudes and for distances within some distance that depends on the period of the GMIM. The differences between the adjustment factors and the FAS ratios is understandable in terms of the combined effect of the frequency response of an oscillator (in particular, the fact that an oscillator can have a response at a frequency for which the ground motion itself has little or no energy), the magnitude- and frequency-dependent source spectral shape, the frequency-dependent amplification and diminution, and the distance- and magnitude-dependent path attenuation. A different way of showing the adjustments factors is given in Figure 12, where the adjustment factors are a function of period for a suite of magnitudes and two distances. Only the Boatwright and Seekins [2011] (BS11) attenuation model was used for the adjustment factors shown in this figure. This again shows the good comparison between the FAS ratios and the adjustment factors, particularly for the larger magnitudes (but note that at larger distances, Figure 11 shows that the short-period adjustment factors diverge significantly from the FAS ratio for the larger magnitudes).



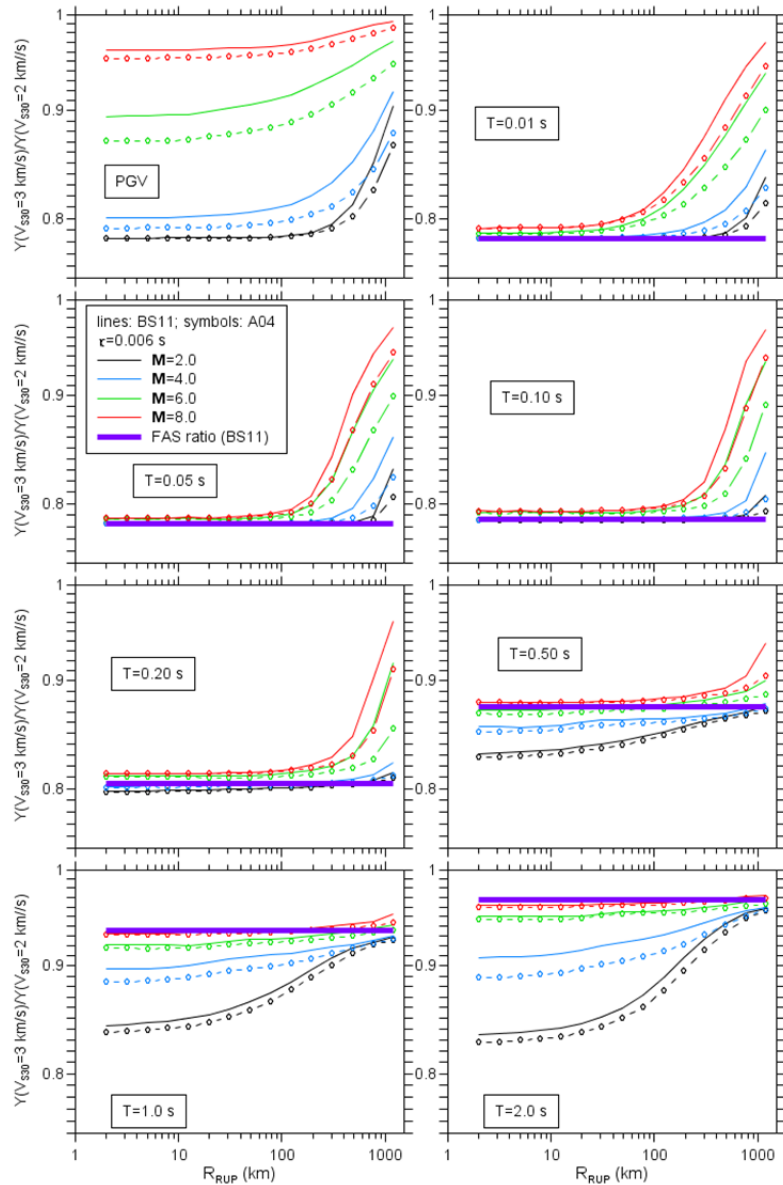


Figure 11

Ratios of PSA as a function of distance for  $V_{S30} = 3000$  m/sec and  $V_{S30} = 2000$  m/sec for the Atkinson [2004] (A04) and Boatwright and Seekins [2011] (BS11) attenuation models. Also shown are ratios of Fourier acceleration spectra (FAS) (no FAS ratio is shown for PGV). Each graph is for a single measure of ground motion (5%-damped PSA at the indicated periods and PGV) and a range of moment magnitudes (M).  $\kappa = 0.006$  sec for all ratios.

**Table 2**

**Ratio of Fourier amplitude spectra (FAS). FAS for a site with  $V_{S30} = 3000$  m/sec divided by the FAS of a site with  $V_{S30} = 2000$  m/sec.  $\kappa = 0.006$  sec for both sites.**

<i>T</i> (sec)	ratio (3kps/2kps)
0.010	0.782
0.020	0.782
0.025	0.782
0.030	0.782
0.040	0.782
0.050	0.782
0.075	0.783
0.100	0.786
0.150	0.795
0.200	0.805
0.250	0.816
0.300	0.827
0.400	0.852
0.500	0.877
0.750	0.918
1.000	0.936
1.500	0.956
2.000	0.970
3.000	0.980
4.000	0.985
5.000	0.988
7.500	0.991
10.000	0.994

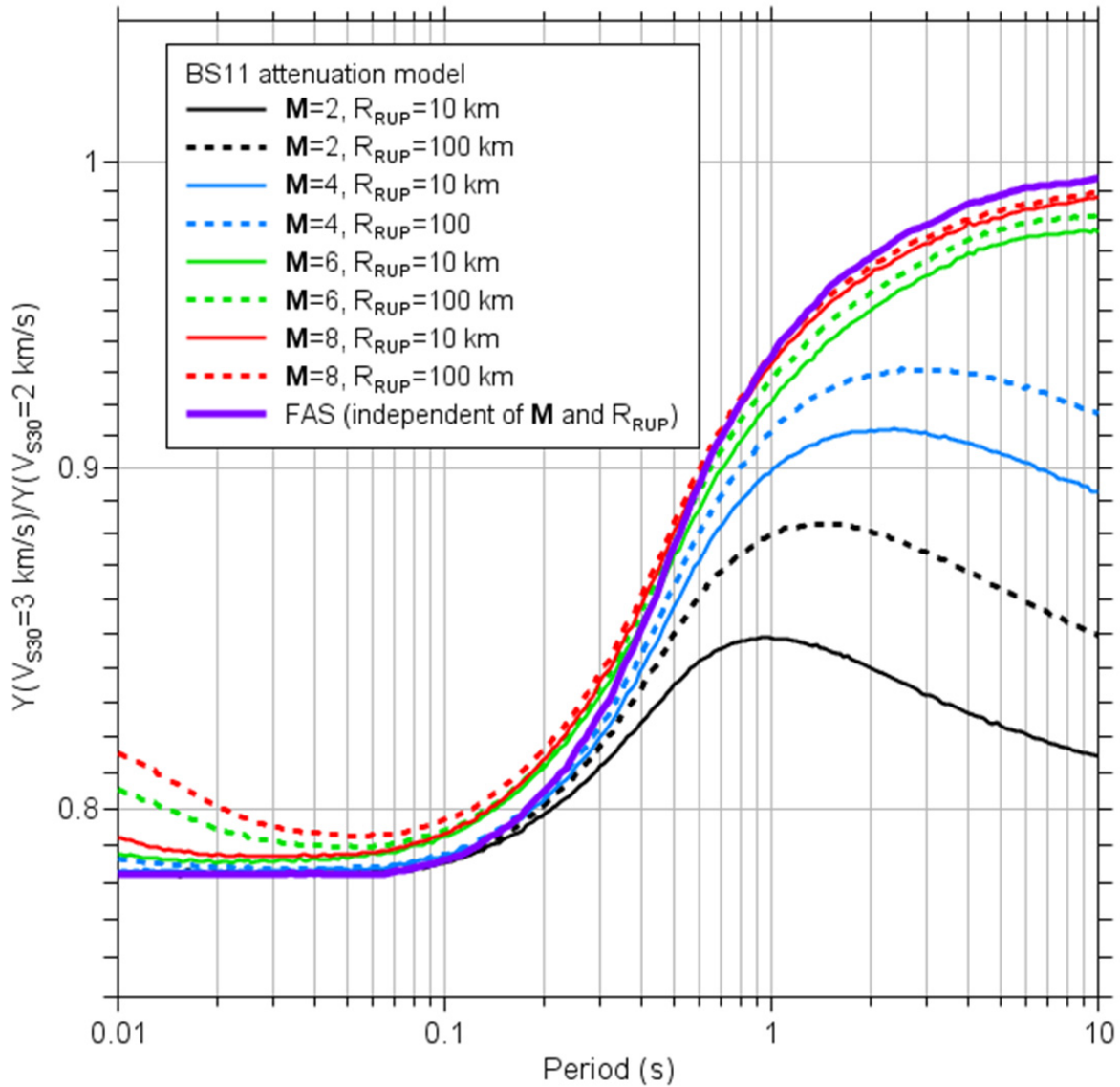


Figure 12 Ratios of PSA for  $V_{S30} = 3000$  m/sec and  $V_{S30} = 2000$  m/sec as a function of period, for distances of 10 km and 100 km. The Boatwright and Seekins [2011] (BS11) attenuation model and a diminution operator with  $\kappa = 0.006$  sec was used for the both site conditions. Also shown are ratios of Fourier acceleration spectra (FAS).

## 5.2 ADJUSTMENTS OF GMIMS FOR SITES WITH $V_{S30} = 760$ M/SEC TO THOSE WITH $V_{S30} = 3000$ M/SEC

There is uncertainty about what value to use for  $\kappa$  for the  $V_{S30} = 760$  m/sec model. Frankel et al. [1996] assumed 0.01 sec, Silva et al. [1999] and Atkinson and Boore [2006] used 0.02 sec, Darragh et al. [2015] found 0.005 sec from inverting data, and Yenier and Atkinson [2015] used 0.025 sec. As will be seen in the *BC2RRAF* plots, the conversion factor from a BC condition to a very hard rock condition can be quite sensitive to the choice of  $\kappa$  for short period motions at close distances. For this report, I show ratios for  $\kappa$  equal to 0.005, 0.01, 0.02, and 0.03 sec. The *BC2RRAF* plots for these values of  $\kappa$  are shown in Figures 13, 14, 15, and 16 as a function of distance, for the Fea96 BC model. As in the previous section, the figures show that the *BC2RRAFs* are not sensitive to the attenuation model (A04 and BS11), and that the factors are in reasonable agreement with the FAS ratios for larger magnitudes and closer distances, particularly for longer period motions. (The FAS ratios for the Fea96 model are given in Table 3.) Direct comparisons of the *BC2RRAFs*, for the BS11 attenuation model, are shown in Figure 17 (to avoid clutter, the results for  $\kappa = 0.005$  sec are not shown in that figure). It is not surprising that the short-period adjustment factors are quite sensitive to  $\kappa$ . The question of what  $\kappa$  to use is beyond the scope of this report. I have tried to find BC sites in central and eastern U.S. and Canada with measured ground motions, with no success. But this was prior to the compilation of the NGA-East database, and it could be that such recordings are now available. I suspect that the  $\kappa$  to be used at a BC site similar to OTT will be smaller than those for BC sites that have a less rapid increase velocities at shallow depths than at OTT.

A comparison of the *BC2RRAFs* as a function of period is shown in Figures 18, 19, 20, and 21, one figure per  $\kappa$ . Each figure shows the *BC2RRAFs* for two distances and a suite of magnitudes. Unlike the previous figures, each of these figures uses the same  $y$ -axis scale for ease of inter-comparison.

Here I summarize a few observations from Figures 13 through 21:

1. The ratios for very small  $\mathbf{M}$  are quite different than for those from larger  $\mathbf{M}$ ;
2. In general, the ratios are similar for the two path attenuation models;
3. Ignoring  $\mathbf{M} = 2$ , the ratios are somewhat insensitive to  $\mathbf{M}$  and  $R_{RUP}$ , except for short periods and larger distances. This is good news, as it suggests that a simple period-dependent adjustment factor can be used for a wide range of  $\mathbf{M}$  and  $R_{RUP}$ ; and
4. The ratios for short-period motions are very sensitive to the value of  $\kappa$ . For example, the *BC2RRAFs* for  $\mathbf{M} = 6$  for  $\kappa = 0.005$  sec and 0.03 sec differ by a factors of 2.1 and 1.1 for  $T = 0.1$  sec and  $T = 1.0$  sec, respectively, for distances out to several hundred km.

**Table 3** Ratio of Fourier amplitude spectra (FAS): FAS for a site with  $V_{S30} = 3000$  m/sec and  $\kappa = 0.006$  sec divided by the FAS of a site with  $V_{S30} = 760$  m/sec for the modified Frankel et al. [1996] (Fea) model and four values of  $\kappa$ .

$T$ (sec)	ratio (3kps/Fea; $\kappa = 0.005$ sec)	ratio (3kps/Fea; $\kappa = 0.01$ sec)	ratio (3kps/Fea; $\kappa = 0.02$ sec)	ratio (3kps/Fea; $\kappa = 0.03$ sec)
0.010	0.304	1.465	33.893	784.310
0.020	0.357	0.784	3.771	18.140
0.025	0.370	0.694	2.438	8.565
0.030	0.379	0.639	1.822	5.193
0.040	0.393	0.582	1.276	2.798
0.050	0.402	0.550	1.030	1.931
0.075	0.416	0.513	0.780	1.186
0.100	0.426	0.499	0.683	0.935
0.150	0.444	0.493	0.608	0.749
0.200	0.457	0.495	0.579	0.677
0.250	0.475	0.506	0.573	0.650
0.300	0.489	0.515	0.572	0.635
0.400	0.524	0.545	0.589	0.638
0.500	0.560	0.578	0.615	0.655
0.750	0.651	0.665	0.693	0.723
1.000	0.720	0.732	0.755	0.779
1.500	0.800	0.808	0.825	0.843
2.000	0.845	0.851	0.865	0.878
3.000	0.886	0.891	0.901	0.910
4.000	0.907	0.911	0.918	0.925
5.000	0.922	0.925	0.930	0.936
7.500	0.945	0.947	0.951	0.955
10.000	0.958	0.959	0.962	0.965

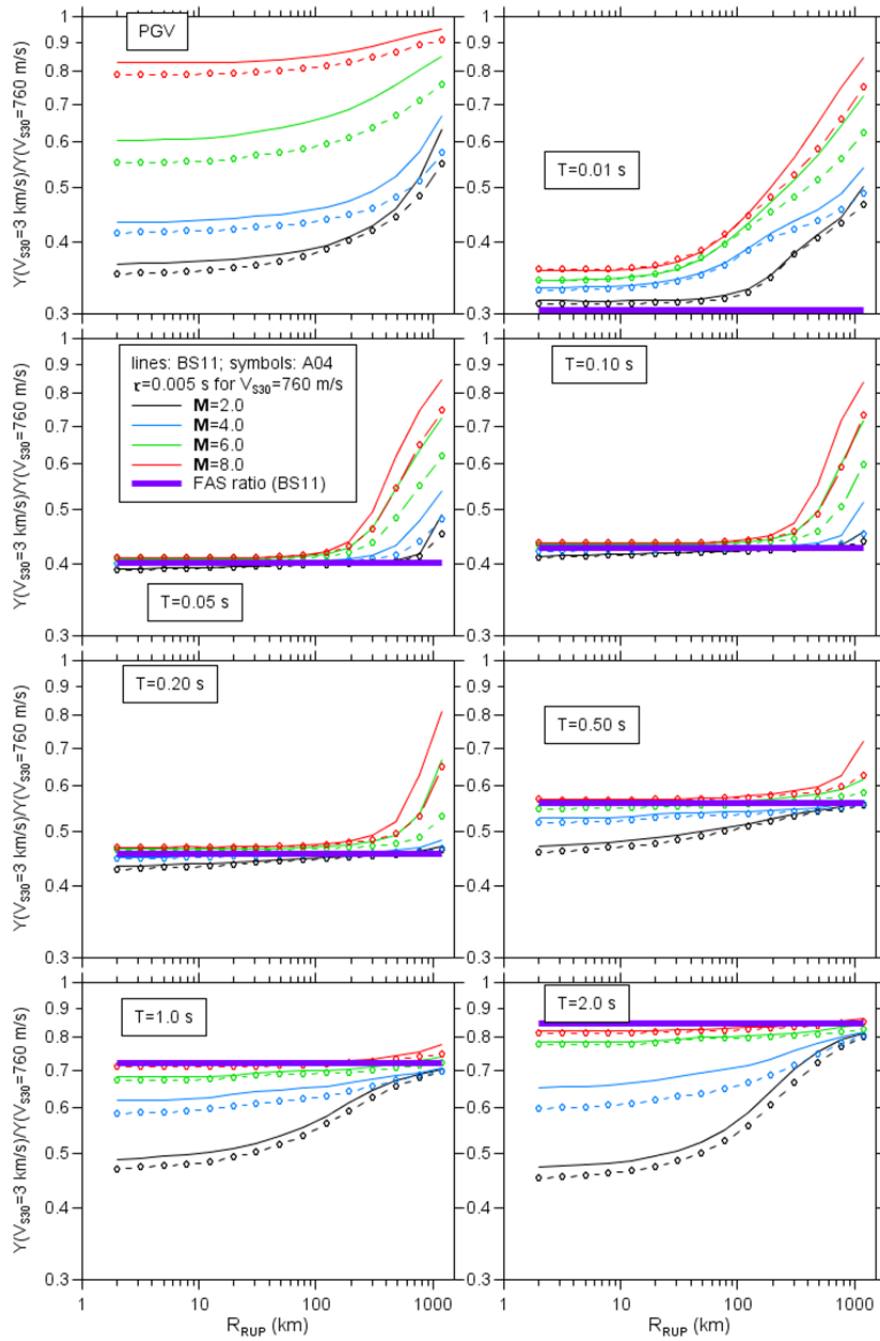


Figure 13

Ratios of PSA as a function of distance for  $V_{S30} = 3000$  m/sec and  $V_{S30} = 760$  m/sec for the Atkinson [2004] (A04) and Boatwright and Seekins [2011] (BS11) attenuation models. Also shown are ratios of Fourier acceleration spectra (FAS) (no FAS ratio is shown for PGV). Each graph is for a single measure of ground motion (5%-damped PSA at the indicated periods and PGV) and a range of moment magnitudes ( $M$ ).  $\kappa = 0.006$  sec for  $V_{S30} = 3000$  m/sec and  $\kappa = 0.005$  sec for  $V_{S30} = 760$  m/sec. The modified Frankel et al. [1996] model was used for the  $V_{S30} = 760$  m/sec crustal amplifications.

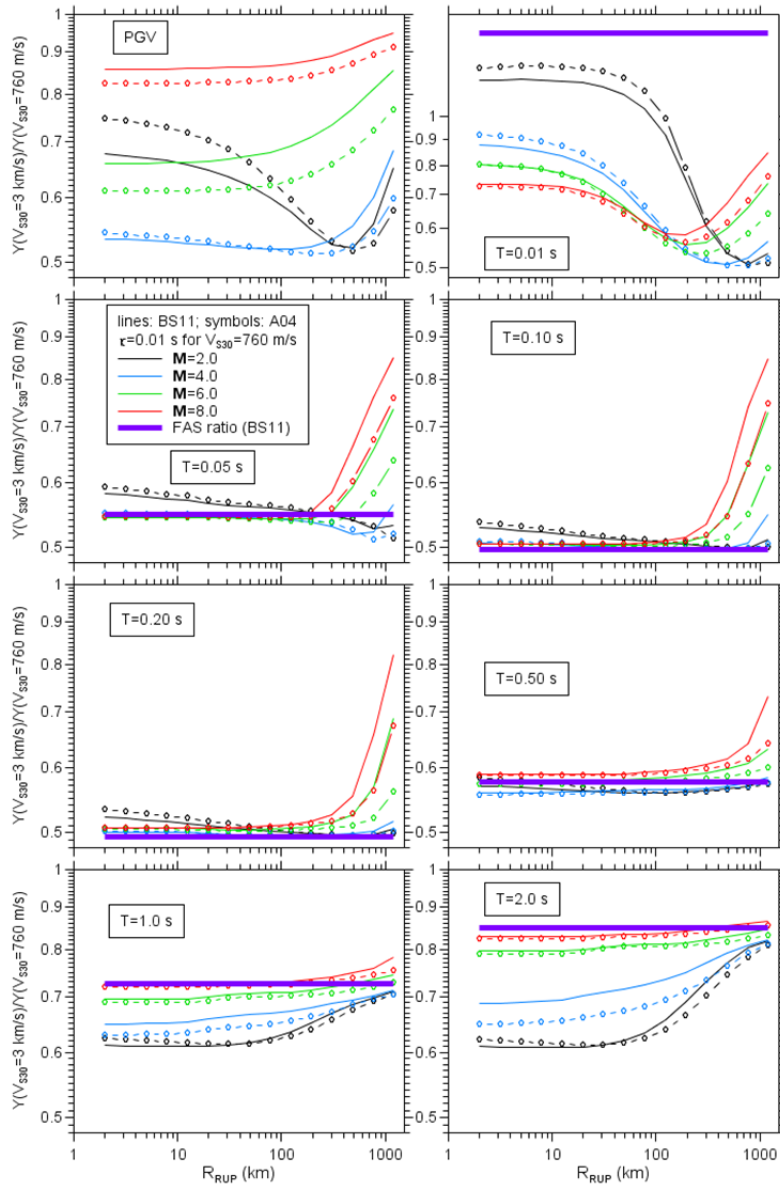


Figure 14

Ratios of PSA as a function of distance for  $V_{S30} = 3000$  m/sec and  $V_{S30} = 760$  m/sec for the Atkinson [2004] (A04) and Boatwright and Seekins [2011] (BS11) attenuation models. Also shown are ratios of Fourier acceleration spectra (FAS) (no FAS ratio is shown for PGV). Each graph is for a single measure of ground motion (5%-damped PSA at the indicated periods and PGV) and a range of moment magnitudes ( $M$ ).  $\kappa = 0.006$  sec for  $V_{S30} = 3000$  m/sec and  $\kappa = 0.010$  sec for  $V_{S30} = 760$  m/sec. The modified Frankel et al. [1996] model was used for the  $V_{S30} = 760$  m/sec crustal amplifications.

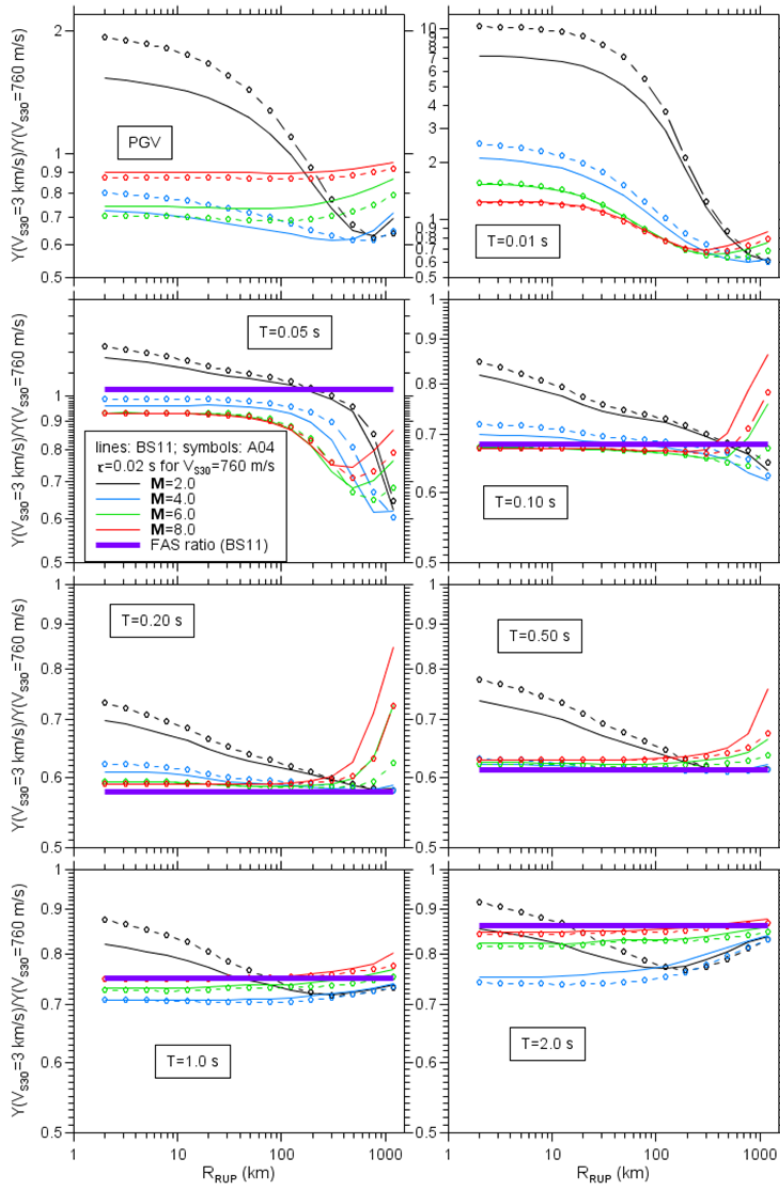


Figure 15

Ratios of PSA as a function of distance for  $V_{S30} = 3000 \text{ m/sec}$  and  $V_{S30} = 760 \text{ m/sec}$  for the Atkinson [2004] (A04) and Boatwright and Seekins [2011] (BS11) attenuation models. Also shown are ratios of Fourier acceleration spectra (FAS) [no FAS ratio is shown for PGV, and it is off the top of the graph (33.9) for  $T = 0.01 \text{ sec}$ ]. Each graph is for a single measure of ground motion (5%-damped PSA at the indicated periods and PGV) and a range of moment magnitudes ( $M$ ).  $\kappa = 0.006 \text{ sec}$  for  $V_{S30} = 3000 \text{ m/sec}$  and  $\kappa = 0.020 \text{ sec}$  for  $V_{S30} = 760 \text{ m/sec}$ . The modified Frankel et al. [1996] model was used for the  $V_{S30} = 760 \text{ m/sec}$  crustal amplifications.



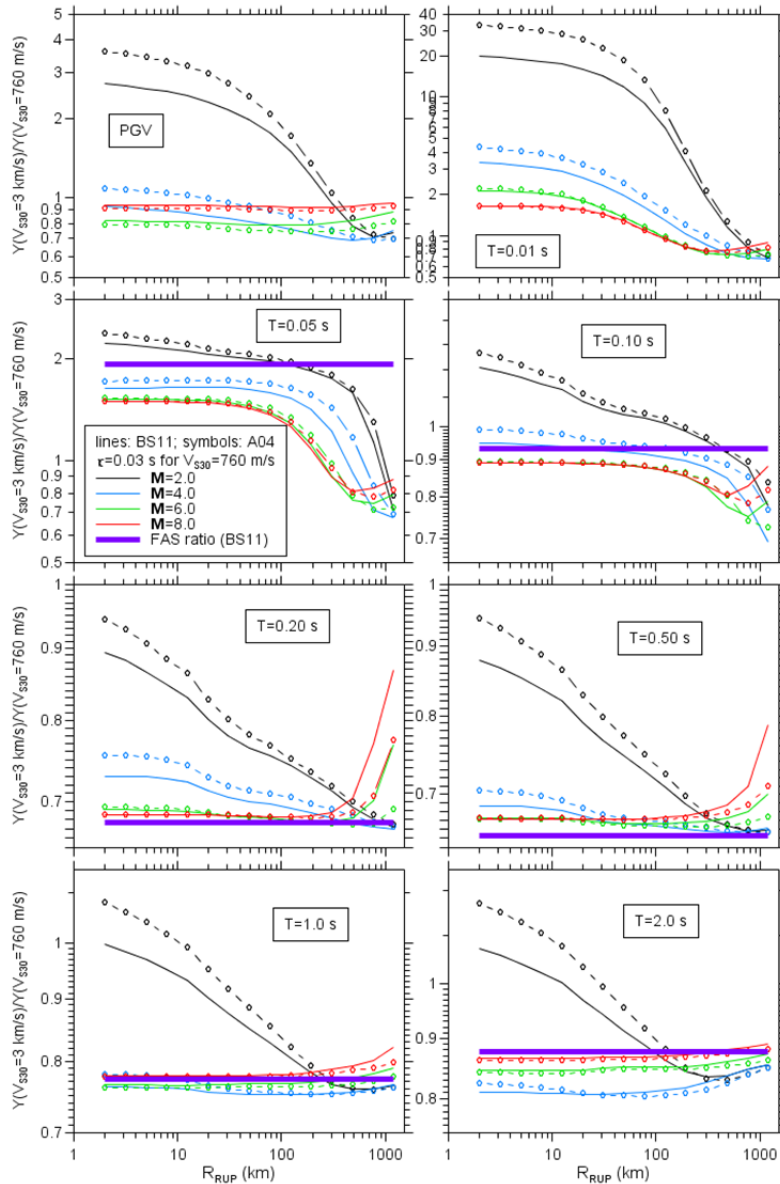


Figure 16

Ratios of PSA as a function of distance for  $V_{S30} = 3000$  m/sec and  $V_{S30} = 760$  m/sec for the Atkinson [2004] (A04) and Boatwright and Seekins [2011] (BS11) attenuation models. Also shown are ratios of Fourier acceleration spectra (FAS) [no FAS ratio is shown for PGV, and it is off the top of the graph (784) for  $T = 0.01$  sec]. Each graph is for a single measure of ground motion (5%-damped PSA at the indicated periods and PGV) and a range of moment magnitudes ( $M$ ).  $\kappa = 0.006$  sec for  $V_{S30} = 3000$  m/sec and  $\kappa = 0.020$  sec for  $V_{S30} = 760$  m/sec. The modified Frankel et al. [1996] model was used for the  $V_{S30} = 760$  m/sec crustal amplifications.

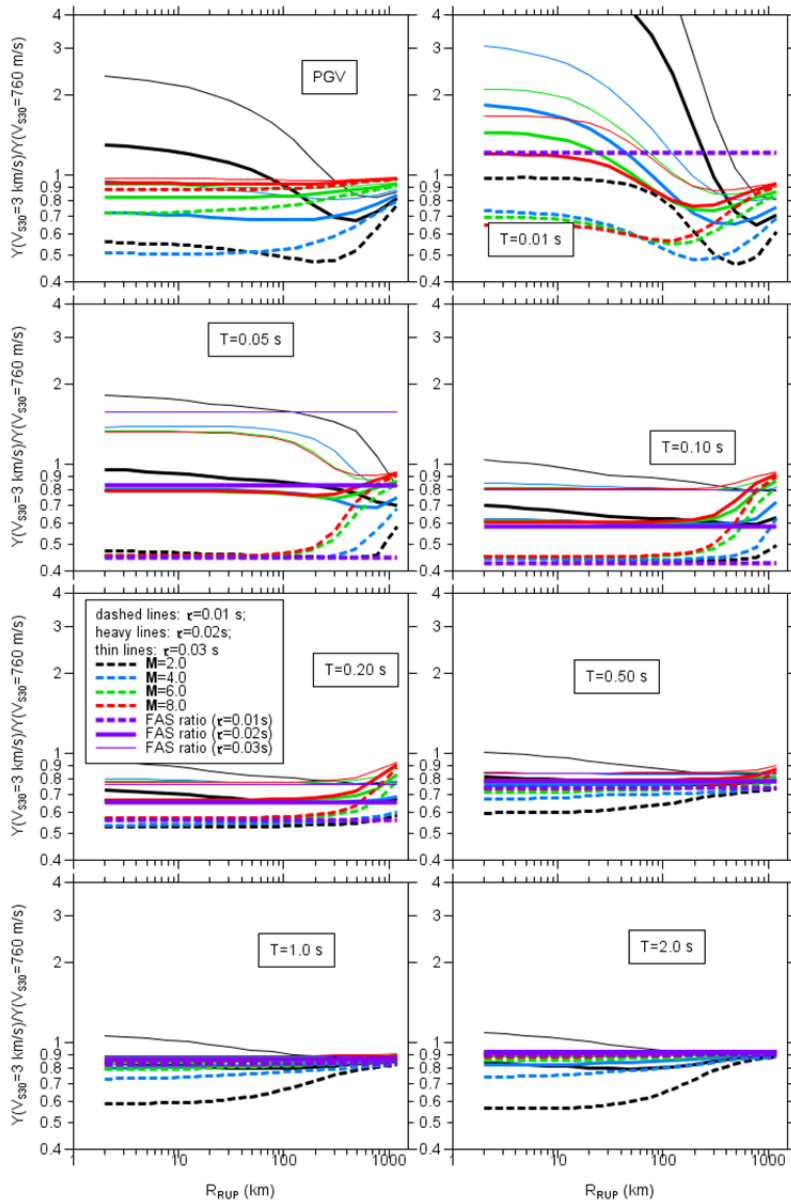


Figure 17

Ratios of PSA as a function of distance for  $V_{S30} = 3000 \text{ m/sec}$  and  $V_{S30} = 760 \text{ m/sec}$  for the Atkinson [2004] (A04) and Boatwright and Seekins [2011] (BS11) attenuation model and the three values of  $\kappa$  (0.01 sec, 0.02 sec, and 0.03 sec) used for the  $V_{S30} = 760 \text{ m/sec}$  site condition. The modified Frankel et al. [1996] model was used for the  $V_{S30} = 760 \text{ m/sec}$  crustal amplifications. Also shown are ratios of Fourier acceleration spectra (FAS) [no FAS ratio is shown for PGV, and the ratios for  $\kappa = 0.02 \text{ sec}$  and  $0.03 \text{ sec}$  are off the top of the graph for  $T = 0.01 \text{ sec}$ ]. Each graph is for a single measure of ground motion (5%-damped PSA at the indicated periods and PGV) and a range of moment magnitudes (M).  $\kappa = 0.006 \text{ sec}$  for  $V_{S30} = 3000 \text{ m/sec}$ . To make the period-dependent sensitivity of the ratios clear, all graphs have the same scale for the ordinate (sacrificing the ratios for  $M=2$  and  $T = 0.01 \text{ sec}$ , which are off scale).

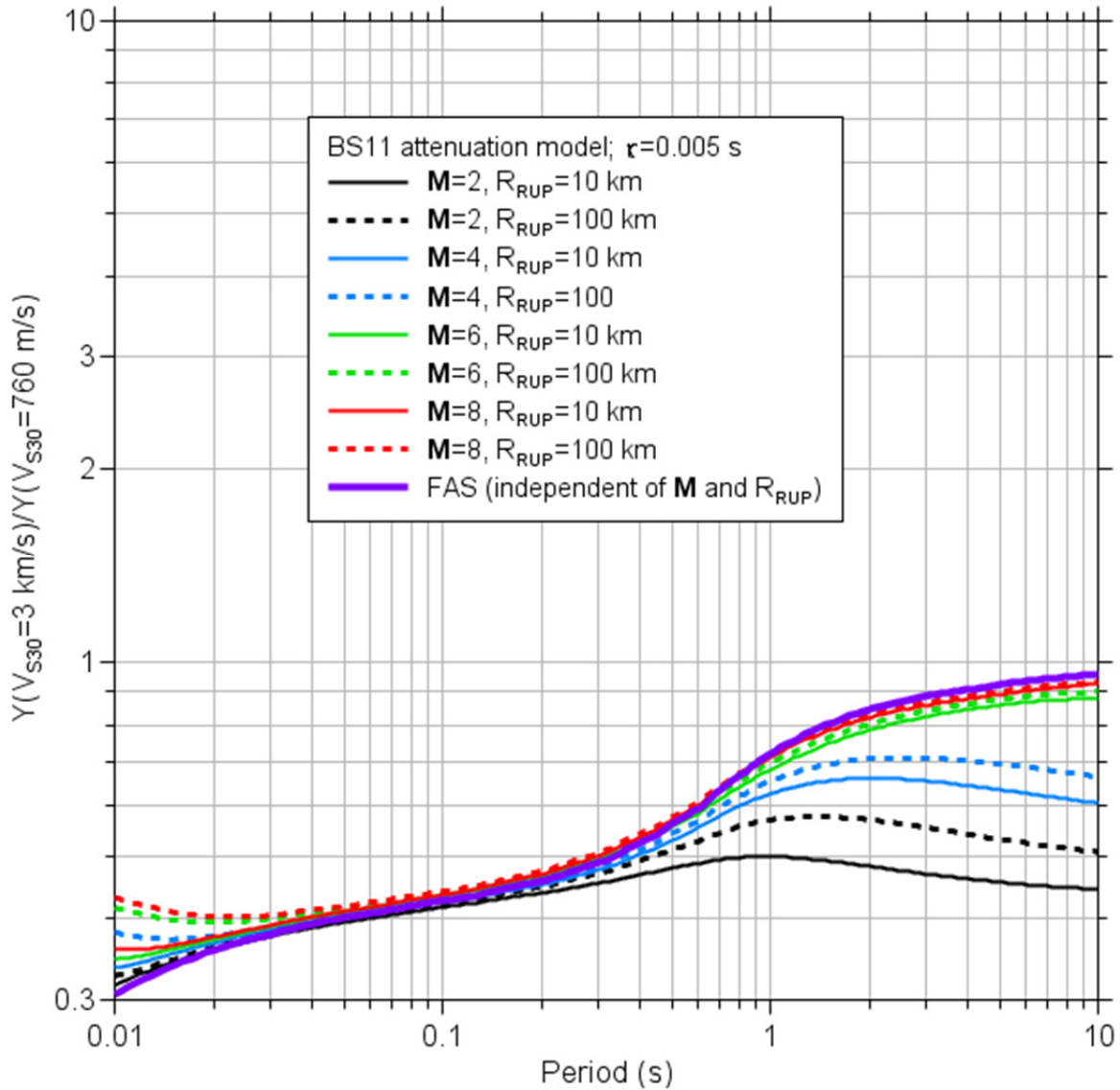


Figure 18

Ratios of PSA for  $V_{S30} = 3000$  m/sec and  $V_{S30} = 760$  m/sec as a function of period for distances of 10 km and 100 km. The Boatwright and Seekins [2011] (BS11) attenuation model and a diminution operation with  $\kappa = 0.005$  sec was used for the  $V_{S30} = 760$  m/sec site condition. The modified Frankel et al. [1996] model was used for the  $V_{S30} = 760$  m/sec crustal amplifications. Also shown are ratios of Fourier acceleration spectra (FAS).

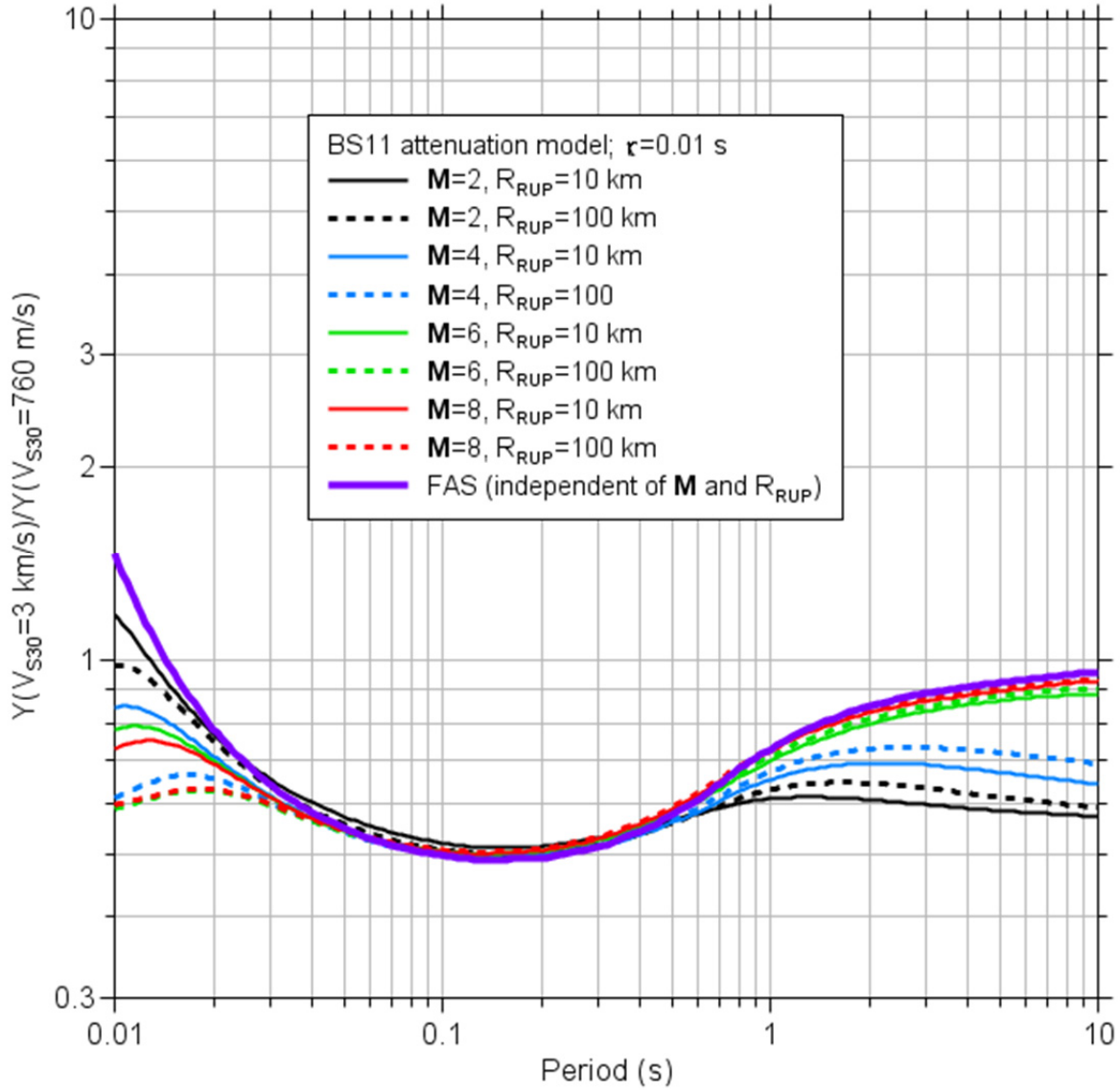


Figure 19

Ratios of PSA for  $V_{S30} = 3000$  m/sec and  $V_{S30} = 760$  m/sec as a function of period for distances of 10 km and 100 km. The Boatwright and Seekins [2011] (BS11) attenuation model and a diminution operation with  $\kappa = 0.01$  sec was used for the  $V_{S30} = 760$  m/sec site condition. The modified Frankel et al. [1996] model was used for the  $V_{S30} = 760$  m/sec crustal amplifications. Also shown are ratios of Fourier acceleration spectra (FAS).

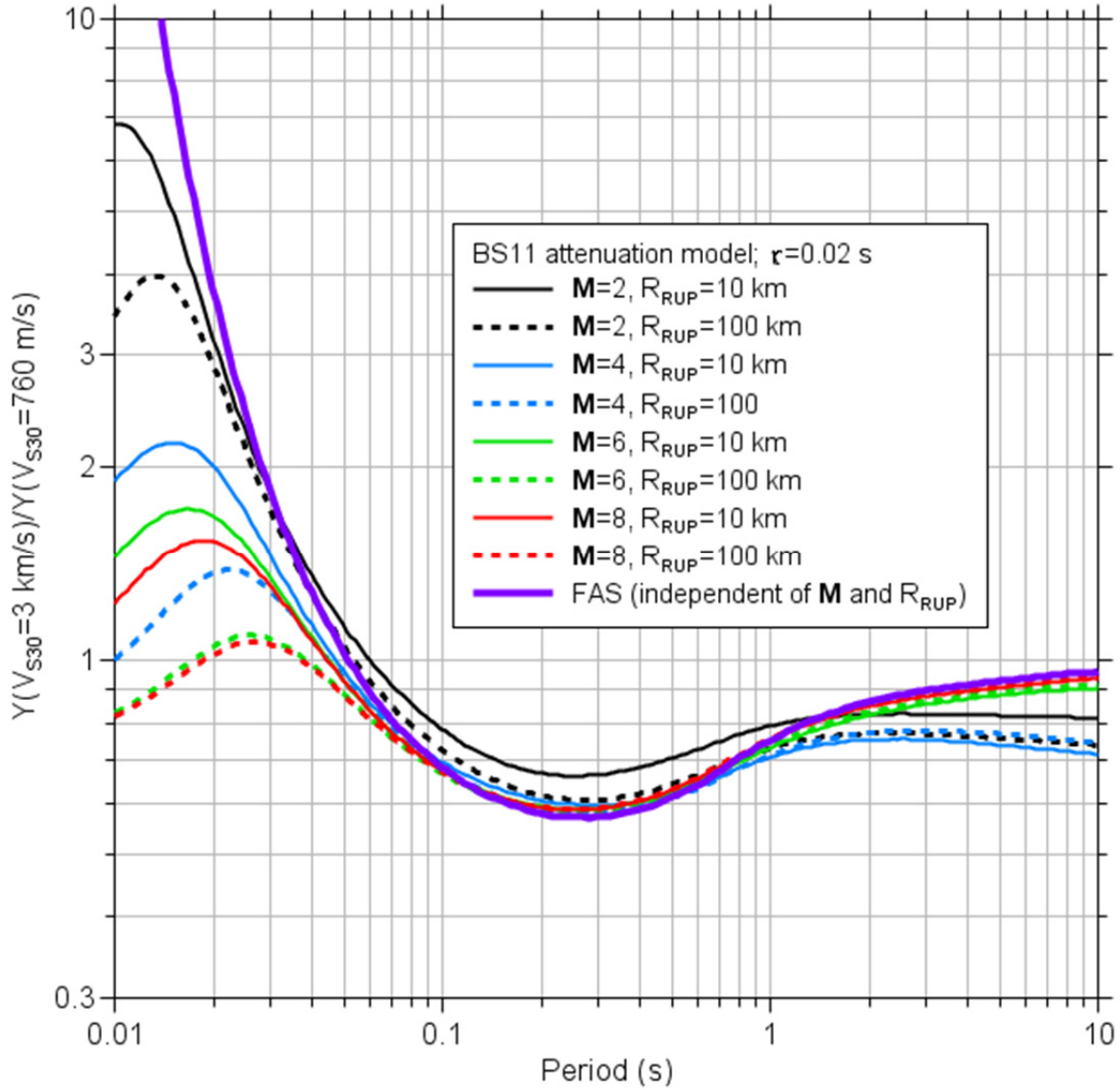


Figure 20

Ratios of PSA for  $V_{S30} = 3000$  m/sec and  $V_{S30} = 760$  m/sec as a function of period for distances of 10 km and 100 km. The Boatwright and Seekins [2011] (BS11) attenuation model and a diminution operation with  $\kappa = 0.02$  sec was used for the  $V_{S30} = 760$  m/sec site condition. The modified Frankel et al. [1996] model was used for the  $V_{S30} = 760$  m/sec crustal amplifications. Also shown are ratios of Fourier acceleration spectra (FAS).

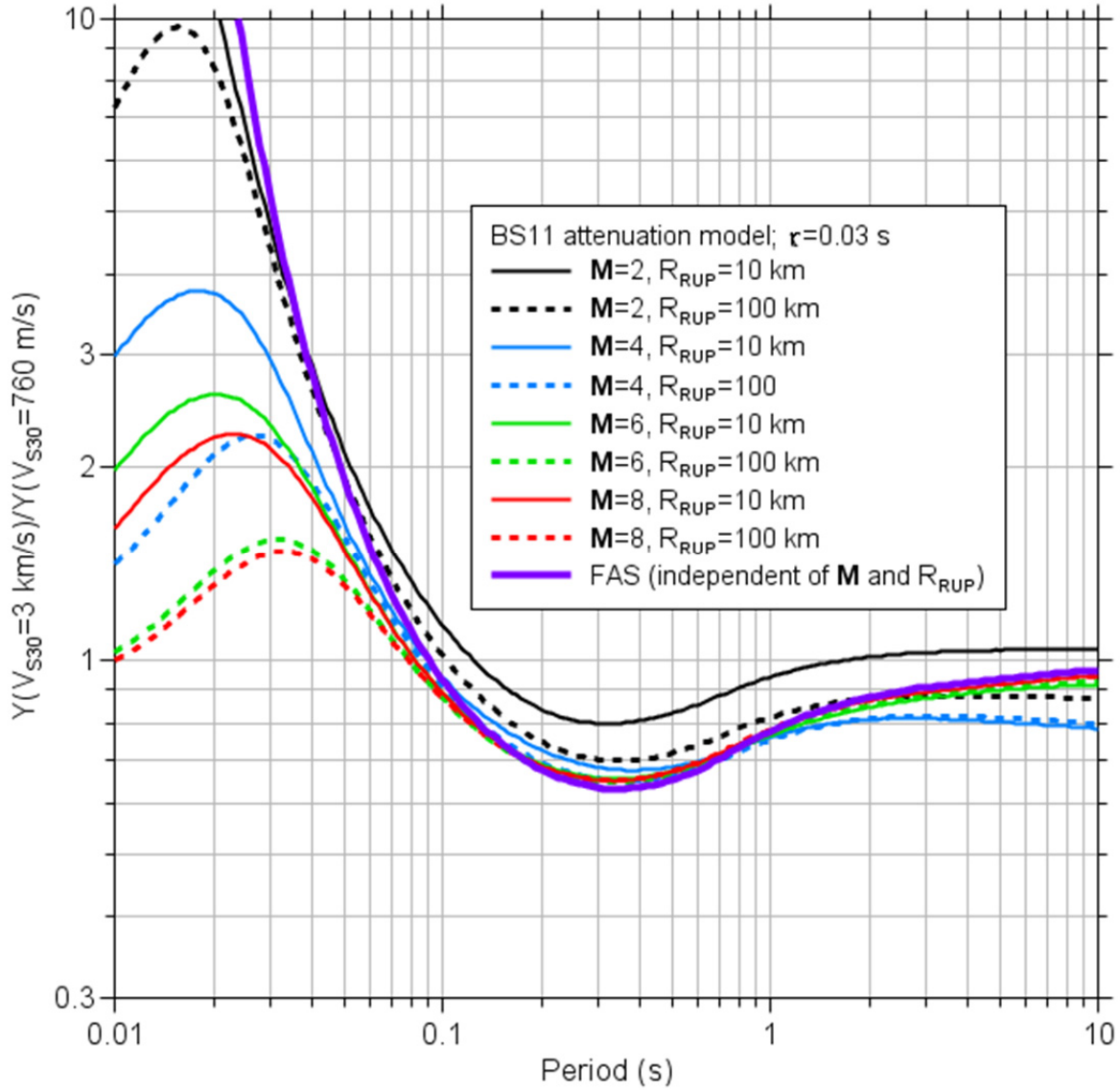


Figure 21 Ratios of PSA for  $V_{S30} = 3000$  m/sec and  $V_{S30} = 760$  m/sec as a function of period for distances of 10 km and 100 km. The Boatwright and Seekins [2011] (BS11) attenuation model and a diminution operation with  $\kappa = 0.03$  sec was used for the  $V_{S30} = 760$  m/sec site condition. The modified Frankel et al. [1996] model was used for the  $V_{S30} = 760$  m/sec crustal amplifications. Also shown are ratios of Fourier acceleration spectra (FAS).

## 6 VARIABILITY OF THE *BC2RRAFs*

The *BC2RRAFs* for several different BC models are compared in Figures 22 through 25. Each figure shows the adjustment factors as a function of period for a fixed distance and a suite of magnitudes; no FAS ratios are given in the figures. Figures 22 and 23 compare BC models HH1000, HH3000, and OTT. The *BC2RRAFs* are similar for these three BC models, which is expected from the similarity of the crustal amplifications in Figure 7. The adjustment factors are not sensitive to the distances used in the figures (10 km and 100 km), although earlier figures (e.g., Figure 17) shows a distance dependence of the *BC2RRAFs* for greater distances and short periods. On the other hand, Figure 7 shows that the crustal amplifications for the Fea96, Average BC and OTT models are different, and this maps the differences in amplitude and shape of the *BC2RRAFs* shown in Figures 24 and 25. Although not shown in the figures, for completeness I provide the FAS ratios for the Average BC and the OTT BC models in Tables 4 and 5. A direct comparison of the *BC2RRAFs* for the Fea96, Average BC and OTT models are given in Figure 26, which shows the ratio of the *BC2RRAFs* for the Fea96 and OTT models relative to that of the Average BC model. Also included in Figure 26 are the ratios of the FAS ratios for the three models. This figure shows that the *BC2RRAFs* are generally within 20% of one another; it also shows that the FAS ratios are a good predictor of the variation in *BC2RRAFs* except for short periods.

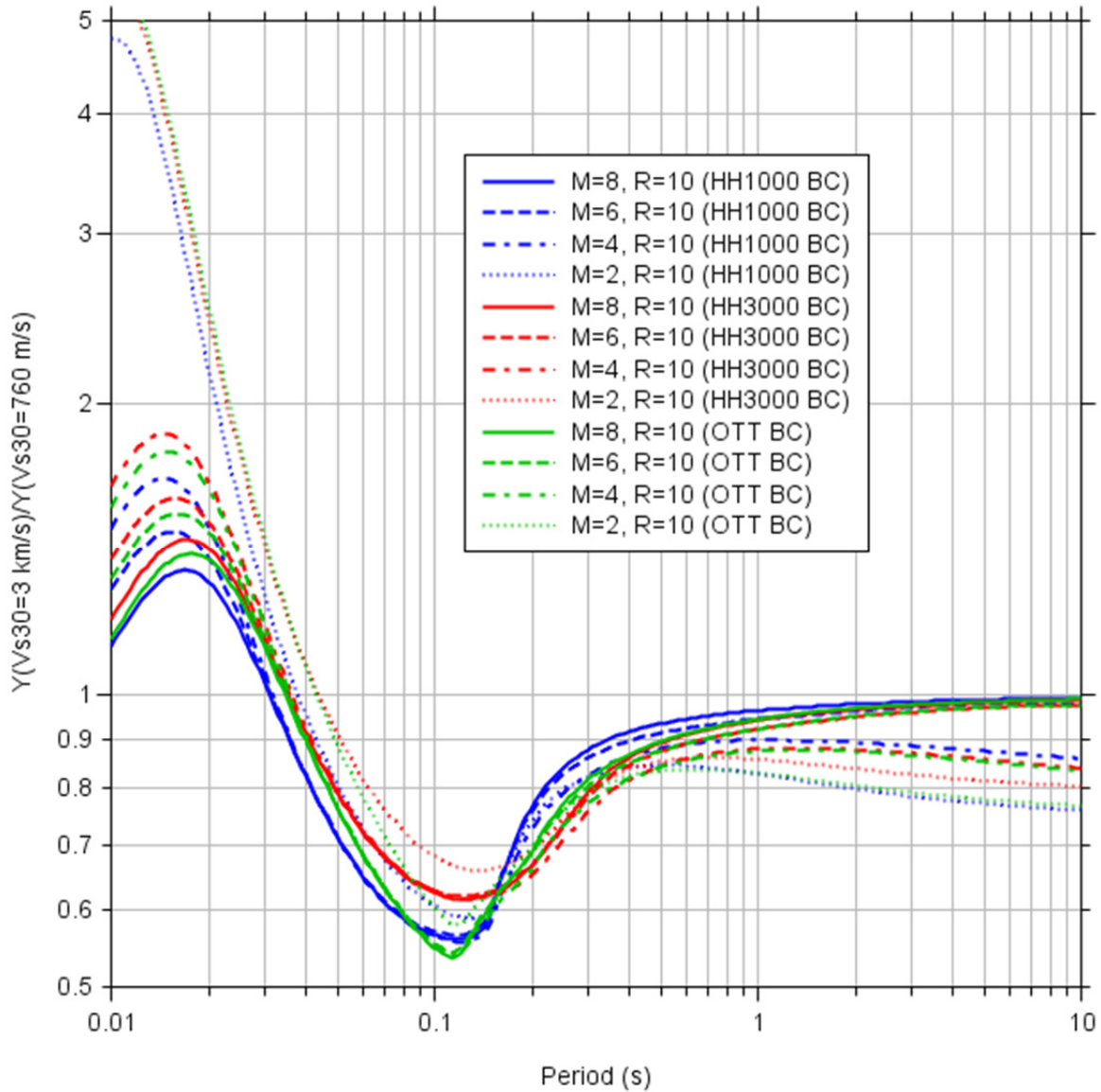


Figure 22

Ratios of PSA for  $V_{S30} = 3000$  m/sec and  $V_{S30} = 760$  m/sec as a function of period for a distance of 10 km. The Boatwright and Seekins [2011] (BS11) attenuation model and a diminution operation with  $\kappa = 0.02$  sec was used for the  $V_{S30} = 760$  m/sec site condition. Three models were used for the  $V_{S30} = 760$  m/sec crustal amplifications: Hashash and Harmon models HH1000 and HH3000, and the OTT model of Beresnev and Atkinson [1997].



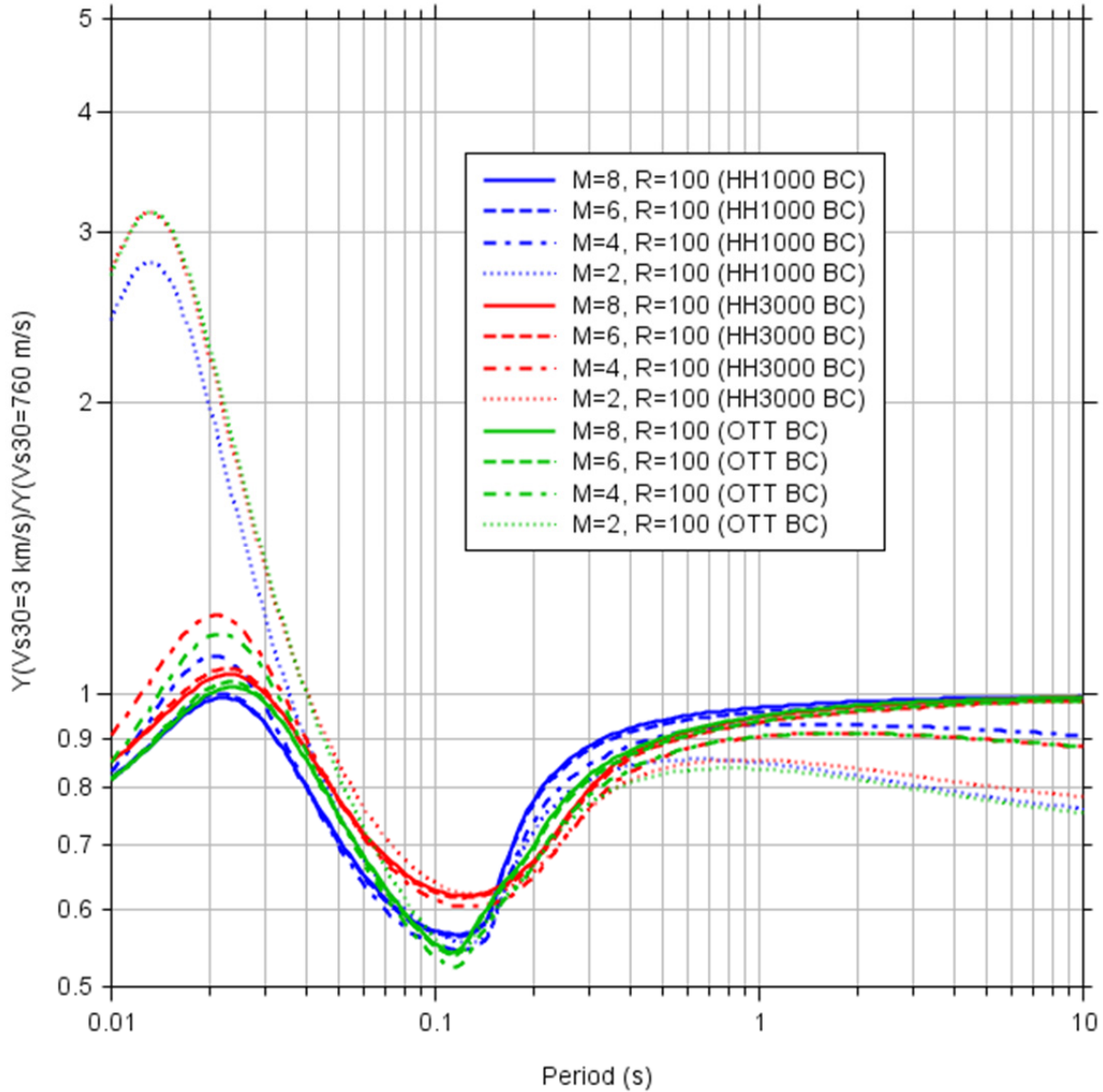


Figure 23

Ratios of PSA for  $V_{S30} = 3000$  m/sec and  $V_{S30} = 760$  m/sec as a function of period for a distance of 100 km. The Boatwright and Seekins [2011] (BS11) attenuation model and a diminution operation with  $\kappa = 0.02$  sec was used for the  $V_{S30} = 760$  m/sec site condition. Three models were used for the  $V_{S30} = 760$  m/sec crustal amplifications: Hashash and Harmon models HH1000 and HH3000, and the OTT model of Beresnev and Atkinson [1997].

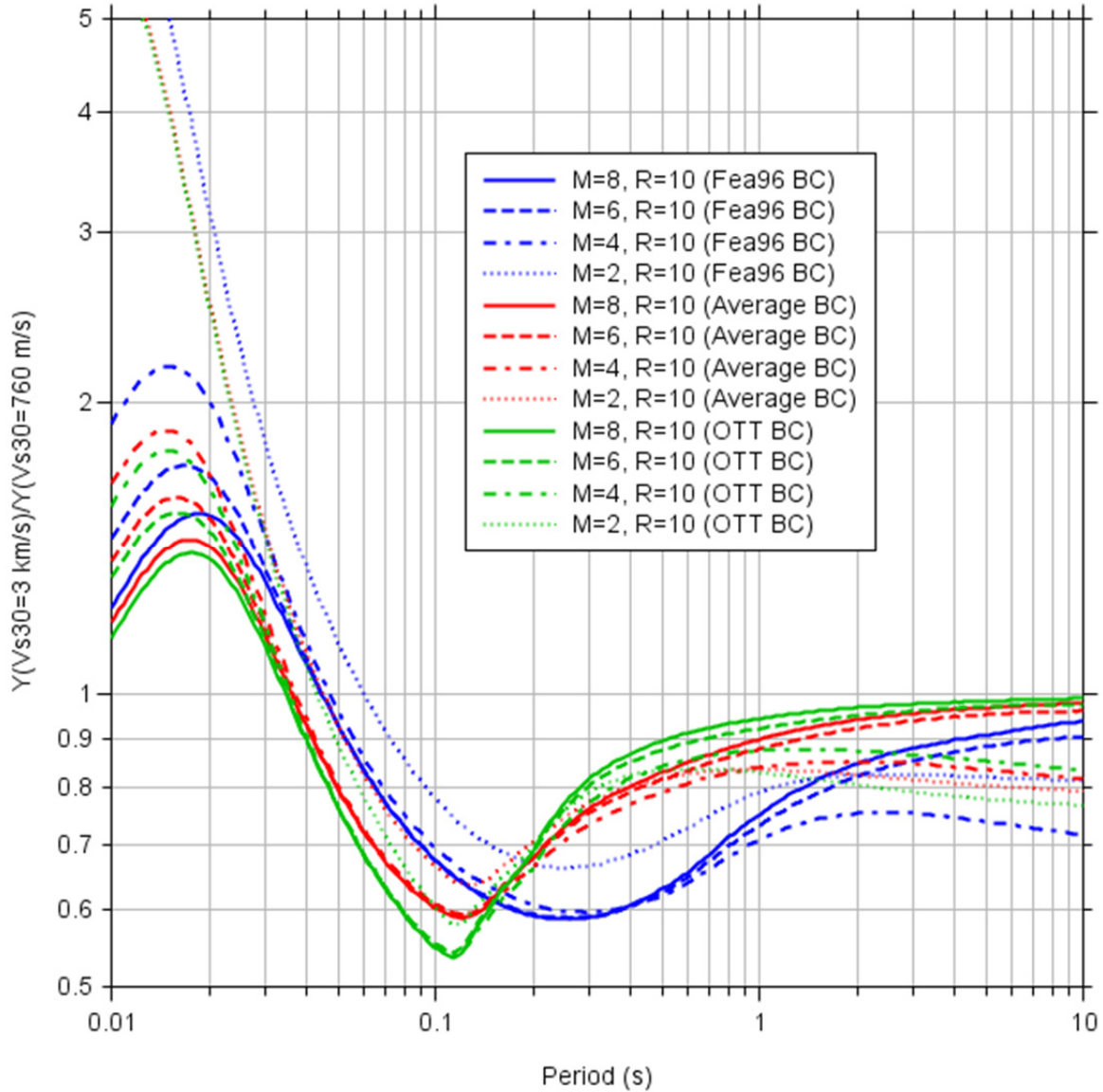


Figure 24

Ratios of PSA for  $V_{S30} = 3000$  m/sec and  $V_{S30} = 760$  m/sec as a function of period for a distance of 10 km. The Boatwright and Seekins [2011] (BS11) attenuation model and a diminution operation with  $\kappa = 0.02$  sec was used for the  $V_{S30} = 760$  m/sec site condition. Three models were used for the  $V_{S30} = 760$  m/sec crustal amplifications: Frankel et al. [1996] (Fea96), the average BC model derived in this report (Average BC), and the OTT model of Beresnev and Atkinson [1997].

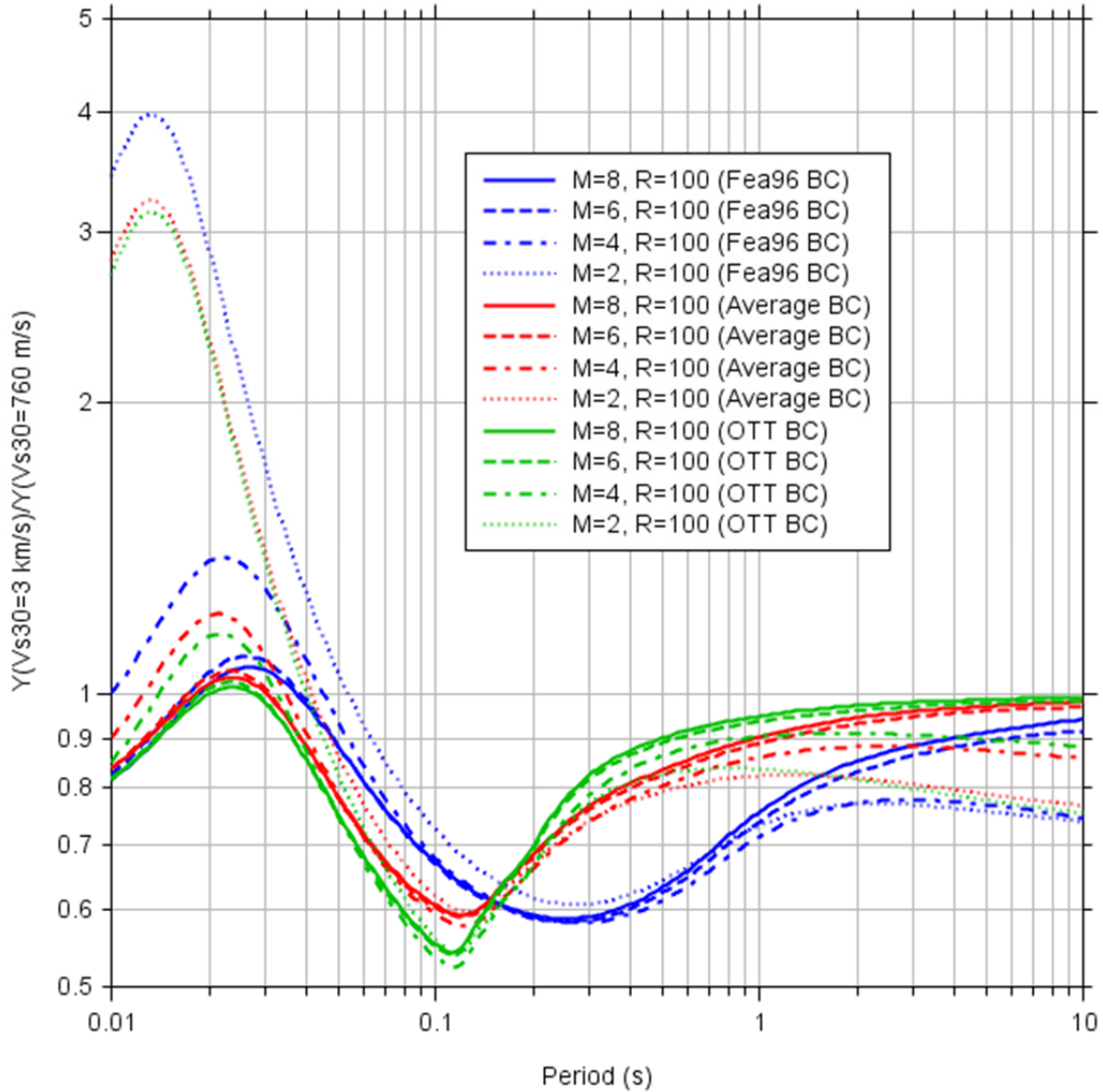


Figure 25

Ratios of PSA for  $V_{S30} = 3000$  m/sec and  $V_{S30} = 760$  m/sec as a function of period for a distance of 100 km. The Boatwright and Seekins [2011] (BS11) attenuation model and a diminution operation with  $\kappa = 0.02$  sec was used for the  $V_{S30} = 760$  m/sec site condition. Three models were used for the  $V_{S30} = 760$  m/sec crustal amplifications: Frankel et al. [1996] (Fea96), the average BC model derived in this report (Average BC), and the OTT model of Beresnev and Atkinson [1997].

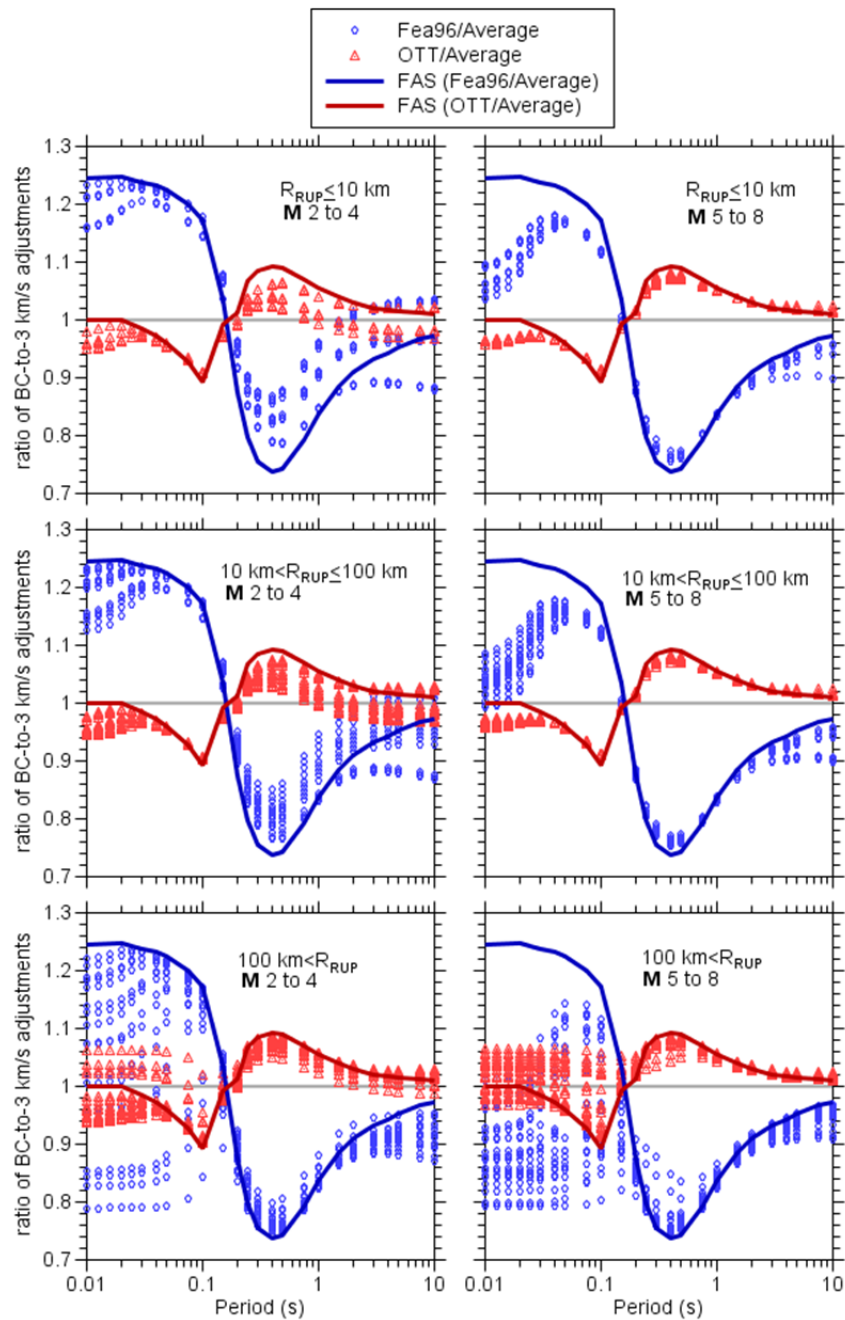


Figure 26

Ratios of PSA for  $V_{S30} = 3000$  m/sec and  $V_{S30} = 760$  m/sec as a function of period for distances of 10 km and 100 km. The Boatwright and Seekins [2011] (BS11) attenuation model and a diminution operation with  $\kappa = 0.03$  sec was used for the  $V_{S30} = 760$  m/sec site condition. The modified Frankel et al. [1996] model was used for the  $V_{S30} = 760$  m/sec crustal amplifications. Also shown are ratios of Fourier acceleration spectra (FAS).

**Table 4** Ratio of Fourier amplitude spectra (FAS): FAS for a site with  $V_{S30} = 3000$  m/sec and  $\kappa = 0.006$  sec divided by the FAS of a site with  $V_{S30} = 760$  m/sec for the Average BC model and four values of  $\kappa$ .

$T$ (sec)	ratio (3kps/Avg; $\kappa = 0.005$ sec)	ratio (3kps/Avg; $\kappa = 0.01$ sec)	ratio (3kps/Avg; $\kappa = 0.02$ sec)	ratio (3kps/Avg; $\kappa = 0.03$ sec)
0.010	0.245	1.178	27.268	630.990
0.020	0.287	0.629	3.024	14.547
0.025	0.298	0.559	1.962	6.895
0.030	0.306	0.517	1.473	4.199
0.040	0.319	0.472	1.035	2.270
0.050	0.328	0.449	0.841	1.577
0.075	0.347	0.428	0.651	0.989
0.100	0.364	0.426	0.583	0.799
0.150	0.430	0.477	0.588	0.726
0.200	0.523	0.566	0.662	0.775
0.250	0.595	0.634	0.719	0.815
0.300	0.647	0.682	0.757	0.841
0.400	0.712	0.741	0.801	0.867
0.500	0.755	0.779	0.830	0.883
0.750	0.823	0.841	0.877	0.914
1.000	0.861	0.875	0.903	0.932
1.500	0.904	0.914	0.933	0.953
2.000	0.930	0.937	0.952	0.967
3.000	0.953	0.958	0.968	0.978
4.000	0.963	0.967	0.975	0.982
5.000	0.968	0.972	0.978	0.984
7.500	0.978	0.980	0.985	0.989
10.000	0.985	0.987	0.990	0.993

**Table 5** Ratio of Fourier amplitude spectra (FAS): FAS for a site with  $V_{S30} = 3000$  m/sec and  $\kappa = 0.006$  sec divided by the FAS of a site with  $V_{S30} = 760$  m/sec for the OTT model and four values of  $\kappa$ .

$T$ (sec)	ratio (3kps/OTT; $\kappa = 0.005$ sec)	ratio (3kps/OTT; $\kappa = 0.01$ sec)	ratio (3kps/OTT; $\kappa = 0.02$ sec)	ratio (3kps/OTT; $\kappa = 0.03$ sec)
0.010	0.245	1.177	27.235	630.235
0.020	0.286	0.628	3.020	14.530
0.025	0.295	0.554	1.946	6.836
0.030	0.302	0.509	1.451	4.135
0.040	0.310	0.459	1.006	2.206
0.050	0.315	0.431	0.807	1.513
0.075	0.321	0.396	0.602	0.915
0.100	0.325	0.380	0.520	0.712
0.150	0.426	0.473	0.584	0.720
0.200	0.529	0.572	0.670	0.784
0.250	0.635	0.676	0.766	0.869
0.300	0.701	0.739	0.821	0.911
0.400	0.777	0.808	0.874	0.945
0.500	0.821	0.848	0.903	0.961
0.750	0.881	0.900	0.938	0.978
1.000	0.908	0.923	0.952	0.982
1.500	0.938	0.948	0.968	0.989
2.000	0.957	0.965	0.980	0.996
3.000	0.972	0.977	0.987	0.998
4.000	0.979	0.983	0.990	0.998
5.000	0.982	0.985	0.991	0.997
7.500	0.989	0.991	0.995	0.999
10.000	0.993	0.994	0.998	1.001

## 7 Conclusions

None of the ground motions in the NGA-East database were recorded on sites with a  $V_{S30}$  as high as that for the reference-rock site condition (3000 m/sec). Most of the motions come from sites with estimated values of  $V_{S30}$  near 500 m/sec. A procedure to adjust these motions to the reference-rock condition is given here. The first step is to adjust the observed motions to a  $V_{S30} = 760$  m/sec site condition, and then use adjustment factors to convert that motion to a site with  $V_{S30} = 3000$  m/sec. The conversion to  $V_{S30} = 760$  m/sec is not given here, as it can be based on existing ground-motion models. This study focuses on the adjustments from  $V_{S30} = 760$  m/sec to  $V_{S30} = 3000$  m/sec, but I also provide adjustments for sites with  $V_{S30} = 2000$  m/sec to those with  $V_{S30} = 3000$  m/sec, as a number of the recordings in northeastern U.S. and southeastern Canada are on sites for which the estimated  $V_{S30}$  is 2000 m/sec. The adjustment factors are based on stochastic-method simulations, using crustal amplifications derived in this report. Adjustment factors are provided as tables of ratios of simulated ground-motion intensity measures for sites with  $V_{S30} = 3000$  m/sec and either 760 m/sec or 2000 m/sec. The adjustment factors are for magnitudes ranging from 2 to 8, rupture distances from 2 km to 1200 km, and periods from 0.01 sec to 10 sec, in addition to PGA and PGV. One model was considered for  $V_{S30} = 3000$  m/sec, as the amplifications are not sensitive to the details of hard-rock velocity profiles. In contrast, 10 models that have been used in CENA, all with  $V_{S30}$  very close to 760 m/sec, were considered. I provide adjustment factors for two of those models that approximately span the range of models, as well as an average model (for the convenience of the user). For each of the models with  $V_{S30} = 760$  m/sec, adjustment factors are provided for four values of  $\kappa$ : 0.005 sec, 0.01 sec, 0.02 sec, and 0.03 sec.

The adjustment factors for the three models of the crustal amplifications for sites with  $V_{S30} = 760$  m/sec are generally within 20% of one another for a given value of the diminution parameter  $\kappa$ . On the other hand, the adjustment factors for each model are sensitive to  $\kappa$  at short periods. For a given period, the adjustment factors can be a function of magnitude and distance, but except for short-period motions, small magnitudes, and distances greater than about 200 km, the factors are relatively insensitive to magnitude and distance. In these cases, the ratios of the Fourier spectra of the ground motions (which are essentially ratios of the site amplifications) are a convenient substitute for the adjustment factors based on the ratios of simulated ground-motion intensity measures. These Fourier spectral ratios are given in tables.





## 8 Data and Resources

The square-root-impedance and full resonant amplifications were computed using the programs *site\_amp* and *nrattle*, respectively; they and various utility programs used in the computations are part of the SMSIM suite of programs, available from the online software link at [www.daveboore.com](http://www.daveboore.com) [last accessed 10 April 2015]. *nrattle* is a modification by R. Herrmann of C. Mueller's program *rattle*; *nrattle* is included in the SMSIM suite of software with their permission. The densities used in some of the models were obtained from velocity-density relations given in *daves\_notes\_on\_relating\_density\_to\_velocity\_v1.2.pdf*, available from [www.daveboore.com/daves\\_notes.html](http://www.daveboore.com/daves_notes.html) [last accessed 10 April 2015]. The ground-motion intensity measures and the Fourier spectra were computed using the SMSIM programs *tmrs\_loop\_rv\_drvr* and *fmrs\_loop\_fas\_drvr*, respectively. The figures were prepared using CoPlot (<http://www.cohort.com>).



## REFERENCES

- Atkinson G.M. (2004). Empirical attenuation of ground-motion spectral amplitudes in southeastern Canada and the northeastern United States, *Bull. Seism. Soc. Am.* 94: 1079–1095.
- Atkinson G.M., Boore D.M. (2006). Earthquake ground-motion prediction equations for eastern North America, *Bull. Seismol. Soc. Am.*, 96: 2181–2205. (also see the erratum published in Vol. 97, No. 3, p. 1032).
- Beresnev I.A., Atkinson G.M. (1997). Shear-wave velocity survey of seismographic sites in eastern Canada calibration of empirical regression method of estimating site response, *Seismol. Res. Lett.*, 68: 981–987.
- Boatwright J., Seekins L. (2011). Regional spectral analysis of three moderate earthquakes in northeastern North America, *Bull. Seismol. Soc. Am.*, 101: 1769–1782.
- Boore D.M. (2005). SMSIM---Fortran Programs for Simulating Ground Motions from Earthquakes: Version 2.3---A Revision of OFR 96-80-A, U.S. Geological Survey Open-File Report, *U. S. Geological Survey Open-File Report 00-509*, 55 pg. The most recent revision was created on 15 August 2005; it is available from the online publications link on <http://www.daveboore.com>.
- Boore D.M. (2013). The uses and limitations of the square-root impedance method for computing site amplification, *Bull. Seismol. Soc. Am.*, 103: 2356–2368.
- Boore D.M., Joyner W.B. (1997). Site amplifications for generic rock sites, *Bull. Seismol. Soc. Am.*, 87: 327–341.
- Boore D.M., Thompson E.M. (2015). Revisions to some parameters used in stochastic-method simulations of ground motion, *Bull. Seismol. Soc. Am.*, 105: 1029–1041.
- BSSC (2004). *NEHRP Recommended Provisions for Seismic Regulations for New Buildings and other Structures (FEMA 450), 2003 Edition, Part 1 - Provisions, Part 2 - Commentary*, prepared by the Building Seismic Safety Council for the Federal Emergency Management Agency, Building Seismic Safety Council, National Institute of Building Sciences, Washington, D.C.  
(available from [http://www.nibs.org/?page=bssc\\_2003pubs#FEMA450](http://www.nibs.org/?page=bssc_2003pubs#FEMA450)).
- Campbell K.W., Hashash Y.M.A., Kim B., Kottke A.R., Rathje E.M., Silva W.J., Stewart J.P. (2014). Reference-rock site conditions for central and Eastern North America: Part II – attenuation definition, *PEER Report 2014-12*, Pacific Earthquake Engineering Research Center, University of California, Berkeley, CA, 80 pg.
- Darragh R.B., Abrahamson N.A., Silva W.J., Gregor N. (2015). Development of hard rock ground motion models for region 2 of central and eastern North America, Chapter 3 in in *NGA-East: Median Ground Motion Models for the Central and Eastern North America Region, PEER Report No. 2015/04*, Pacific Earthquake Engineering Research Center, University of California, Berkeley, CA, 345 pg.
- Frankel A., Mueller C., Barnhard T., Perkins D., Leyendecker E., Dickman N., Hanson S., Hopper M. (1996). National seismic hazard maps: documentation June 1996, *U.S. Geological. Survey Open-File Report. 96-532*, 69 pg.
- Goulet C.A., Kishida T. Ancheta T D., Cramer C.H., Darragh R.B., Silva W.J., Hashash Y.M.A., Harmon J., Stewart J.P., Wooddell K.E., Youngs R.R. (2014). PEER NGA-East database, *PEER Report No. 2014/17*, Pacific Earthquake Engineering Research Center, University of California, Berkeley, CA.
- Hashash Y.M.A., Kottke A.R., Stewart J.P., Campbell K.W., Kim B., Rathje E.M., Silva W.J. (2014). Reference-rock site conditions for central and eastern North America: Part I – velocity definition, *PEER Report No. 2014-11*, Pacific Earthquake Engineering Research Center, University of California, Berkeley, CA, 188 pg.
- Hollenback J., Kuehn N., Goulet C.A., Abrahamson N.A. (2015). PEER NGA-East median ground motion models, Chapter 11 in *NGA-East: median ground motion models for the central and eastern North America region, PEER Report No. 2015/04*, Pacific Earthquake Engineering Research Center, University of California, Berkeley, CA, 345 pg.

- Odum J.K., Stephenson W.J., Williams R.A. (2010). Predicted and observed spectral response from collocated shallow, active and passive-source Vs data at five ANSS Sites, Illinois and Indiana, USA, *Seismol. Res. Lett.*, 81: 955–964.
- Silva W.J., Darragh R.B., and Gregor N. (1999). Reassessment of site coefficients and near-fault factors for building code provisions, *U.S. Geological Survey Award 98-HQ-GR-1010*, final report.
- Stewart J.P., Hashash Y.M.A., Kim B., Harmon J. (2012). Preliminary site corrections for NGA-East project, memo to Christine Goulet, dated November 3, 2012.
- Yenier E., Atkinson G.M. (2015). Regionally-adjustable generic ground-motion prediction equation based on equivalent point-source simulations: application to central and eastern North America, Chapter 4 in NGA-East: Median Ground Motion Models for the Central and Eastern North America Region, *PEER Report No. 2015/04*, Pacific Earthquake Engineering Research Center, University of California, Berkeley, CA, 345 pg.

## **Appendix A      SMSIM Parameters Files Used in the Simulations**

Appendix A contains the Electronic Appendix SMSIM parameters files used in the simulations.



## **Appendix B      Tables of PGV, PGA, and PSA $V_{S30} = 760$ m/sec to $V_{S30} = 3000$ m/sec Adjustment Factors**

Appendix B contains the Electronic Appendix tables of PGV, PGA, and PSA  $V_{S30} = 760$  m/sec-to- $V_{S30} = 3000$  m/sec adjustment factors. Separate files are given for the Atkinson [2004] (A04) and Boatwright and Seekins [2011] (BS11) attenuation models, and for each model, separate files are given for each BC kappa (0.005, 0.010, 0.020, and 0.030 sec). In addition, adjustment factors are given for  $V_{S30} = 2000$  m/sec to  $V_{S30} = 3000$  m/sec.





## PEER REPORTS

PEER reports are available as a free PDF download from [http://peer.berkeley.edu/publications/peer\\_reports\\_complete.html](http://peer.berkeley.edu/publications/peer_reports_complete.html). Printed hard copies of PEER reports can be ordered directly from our printer by following the instructions at [http://peer.berkeley.edu/publications/peer\\_reports.html](http://peer.berkeley.edu/publications/peer_reports.html). For other related questions about the PEER Report Series, contact the Pacific Earthquake Engineering Research Center, 325 Davis Hall mail code 1792, Berkeley, CA 94720. Tel.: (510) 642-3437; Fax: (510) 665-1655; Email: [peer\\_editor@berkeley.edu](mailto:peer_editor@berkeley.edu)

- PEER 2015/06** *Adjusting Ground-Motion Intensity Measures to a Reference Site for which  $V_{s30} = 3000$  m/sec.* David M. Boore. May 2015.
- PEER 2015/05** *Hybrid Simulation of Seismic Isolation Systems Applied to an APR-1400 Nuclear Power Plant.* Andreas H. Schellenberg, Alireza Sarebanha, Matthew J. Schoettler, Gilberto Mosqueda, Gianmario Benzoni, and Stephen A. Mahin. April 2015.
- PEER 2015/04** *NGA-East: Median Ground-Motion Models for the Central and Eastern North America Region.* April 2015.
- PEER 2015/03** *Single Series Solution for the Rectangular Fiber-Reinforced Elastomeric Isolator Compression Modulus.* James M. Kelly and Niel C. Van Engelen. March 2015.
- PEER 2015/02** *A Full-Scale, Single-Column Bridge Bent Tested by Shake-Table Excitation.* Matthew J. Schoettler, José I. Restrepo, Gabriele Guerrini, David E. Duck, and Francesco Carrea. March 2015.
- PEER 2015/01** *Concrete Column Blind Prediction Contest 2010: Outcomes and Observations.* Vesna Terzic, Matthew J. Schoettler, José I. Restrepo, and Stephen A Mahin. March 2015.
- PEER 2014/20** *Stochastic Modeling and Simulation of Near-Fault Ground Motions for Performance-Based Earthquake Engineering.* Mayssa Dabaghi and Armen Der Kiureghian. December 2014.
- PEER 2014/19** *Seismic Response of a Hybrid Fiber-Reinforced Concrete Bridge Column Detailed for Accelerated Bridge Construction.* Wilson Nguyen, William Trono, Marios Panagiotou, and Claudia P. Ostertag. December 2014.
- PEER 2014/18** *Three-Dimensional Beam-Truss Model for Reinforced Concrete Walls and Slabs Subjected to Cyclic Static or Dynamic Loading.* Yuan Lu, Marios Panagiotou, and Ioannis Koutromanos. December 2014.
- PEER 2014/17** *PEER NGA-East Database.* Christine A. Goulet, Tadahiro Kishida, Timothy D. Ancheta, Chris H. Cramer, Robert B. Darragh, Walter J. Silva, Youssef M.A. Hashash, Joseph Harmon, Jonathan P. Stewart, Katie E. Wooddell, and Robert R. Youngs. October 2014.
- PEER 2014/16** *Guidelines for Performing Hazard-Consistent One-Dimensional Ground Response Analysis for Ground Motion Prediction.* Jonathan P. Stewart, Kioumars Afshari, and Youssef M.A. Hashash. October 2014.
- PEER 2014/15** *NGA-East Regionalization Report: Comparison of Four Crustal Regions within Central and Eastern North America using Waveform Modeling and 5%-Damped Pseudo-Spectral Acceleration Response.* Jennifer Dreiling, Marius P. Isken, Walter D. Mooney, Martin C. Chapman, and Richard W. Godbee. October 2014.
- PEER 2014/14** *Scaling Relations between Seismic Moment and Rupture Area of Earthquakes in Stable Continental Regions.* Paul Somerville. August 2014.
- PEER 2014/13** *PEER Preliminary Notes and Observations on the August 24, 2014, South Napa Earthquake.* Grace S. Kang (Editor), Stephen A. Mahin (Editors). September 2014.
- PEER 2014/12** *Reference-Rock Site Conditions for Central and Eastern North America: Part II – Attenuation (Kappa) Definition.* Kenneth W. Campbell, Youssef M.A. Hashash, Byungmin Kim, Albert R. Kottke, Ellen M. Rathje, Walter J. Silva, and Jonathan P. Stewart. August 2014.
- PEER 2014/11** *Reference-Rock Site Conditions for Central and Eastern North America: Part I - Velocity Definition.* Youssef M.A. Hashash, Albert R. Kottke, Jonathan P. Stewart, Kenneth W. Campbell, Byungmin Kim, Ellen M. Rathje, Walter J. Silva, Sissy Nikolaou, and Cheryl Moss. August 2014.
- PEER 2014/10** *Evaluation of Collapse and Non-Collapse of Parallel Bridges Affected by Liquefaction and Lateral Spreading.* Benjamin Turner, Scott J. Brandenberg, and Jonathan P. Stewart. August 2014.
- PEER 2014/09** *PEER Arizona Strong-Motion Database and GMPEs Evaluation.* Tadahiro Kishida, Robert E. Kayen, Olga-Joan Ktenidou, Walter J. Silva, Robert B. Darragh, and Jennie Watson-Lamprey. June 2014.
- PEER 2014/08** *Unbonded Pretensioned Bridge Columns with Rocking Detail.* Jeffrey A. Schaefer, Bryan Kennedy, Marc O. Eberhard, John F. Stanton. June 2014.
- PEER 2014/07** *Northridge 20 Symposium Summary Report: Impacts, Outcomes, and Next Steps.* May 2014.

- PEER 2014/06** *Report of the Tenth Planning Meeting of NEES/E-Defense Collaborative Research on Earthquake Engineering.* December 2013.
- PEER 2014/05** *Seismic Velocity Site Characterization of Thirty-One Chilean Seismometer Stations by Spectral Analysis of Surface Wave Dispersion.* Robert Kayen, Brad D. Carkin, Skye Corbet, Camilo Pinilla, Allan Ng, Edward Gorbis, and Christine Truong. April 2014.
- PEER 2014/04** *Effect of Vertical Acceleration on Shear Strength of Reinforced Concrete Columns.* Hyerin Lee and Khalid M. Mosalam. April 2014.
- PEER 2014/03** *Retest of Thirty-Year-Old Neoprene Isolation Bearings.* James M. Kelly and Niel C. Van Engelen. March 2014.
- PEER 2014/02** *Theoretical Development of Hybrid Simulation Applied to Plate Structures.* Ahmed A. Bakhty, Khalid M. Mosalam, and Sanjay Govindjee. January 2014.
- PEER 2014/01** *Performance-Based Seismic Assessment of Skewed Bridges.* Peyman Kaviani, Farzin Zareian, and Ertugrul Taciroglu. January 2014.
- PEER 2013/26** *Urban Earthquake Engineering. Proceedings of the U.S.-Iran Seismic Workshop.* December 2013.
- PEER 2013/25** *Earthquake Engineering for Resilient Communities: 2013 PEER Internship Program Research Report Collection.* Heidi Tremayne (Editor), Stephen A. Mahin (Editor), Jorge Archbold Monterossa, Matt Brosman, Shelly Dean, Katherine deLaveaga, Curtis Fong, Donovan Holder, Rakeeb Khan, Elizabeth Jachens, David Lam, Daniela Martinez Lopez, Mara Minner, Geffen Oren, Julia Pavicic, Melissa Quinonez, Lorena Rodriguez, Sean Salazar, Kelli Slaven, Vivian Steyert, Jenny Taing, and Salvador Tena. December 2013.
- PEER 2013/24** *NGA-West2 Ground Motion Prediction Equations for Vertical Ground Motions.* September 2013.
- PEER 2013/23** *Coordinated Planning and Preparedness for Fire Following Major Earthquakes.* Charles Scawthorn. November 2013.
- PEER 2013/22** *GEM-PEER Task 3 Project: Selection of a Global Set of Ground Motion Prediction Equations.* Jonathan P. Stewart, John Douglas, Mohammad B. Javanbarg, Carola Di Alessandro, Yousef Bozorgnia, Norman A. Abrahamson, David M. Boore, Kenneth W. Campbell, Elise Delavaud, Mustafa Erdik and Peter J. Stafford. December 2013.
- PEER 2013/21** *Seismic Design and Performance of Bridges with Columns on Rocking Foundations.* Grigorios Antonellis and Marios Panagiotou. September 2013.
- PEER 2013/20** *Experimental and Analytical Studies on the Seismic Behavior of Conventional and Hybrid Braced Frames.* Jiun-Wei Lai and Stephen A. Mahin. September 2013.
- PEER 2013/19** *Toward Resilient Communities: A Performance-Based Engineering Framework for Design and Evaluation of the Built Environment.* Michael William Mieler, Bozidar Stojadinovic, Robert J. Budnitz, Stephen A. Mahin and Mary C. Comerio. September 2013.
- PEER 2013/18** *Identification of Site Parameters that Improve Predictions of Site Amplification.* Ellen M. Rathje and Sara Navidi. July 2013.
- PEER 2013/17** *Response Spectrum Analysis of Concrete Gravity Dams Including Dam-Water-Foundation Interaction.* Arnkjell Løkke and Anil K. Chopra. July 2013.
- PEER 2013/16** *Effect of hoop reinforcement spacing on the cyclic response of large reinforced concrete special moment frame beams.* Marios Panagiotou, Tea Visnjic, Grigorios Antonellis, Panagiotis Galanis, and Jack P. Moehle. June 2013.
- PEER 2013/15** *A Probabilistic Framework to Include the Effects of Near-Fault Directivity in Seismic Hazard Assessment.* Shrey Kumar Shahi, Jack W. Baker. October 2013.
- PEER 2013/14** *Hanging-Wall Scaling using Finite-Fault Simulations.* Jennifer L. Donahue and Norman A. Abrahamson. September 2013.
- PEER 2013/13** *Semi-Empirical Nonlinear Site Amplification and its Application in NEHRP Site Factors.* Jonathan P. Stewart and Emel Seyhan. November 2013.
- PEER 2013/12** *Nonlinear Horizontal Site Response for the NGA-West2 Project.* Ronnie Kamai, Norman A. Abramson, Walter J. Silva. May 2013.
- PEER 2013/11** *Epistemic Uncertainty for NGA-West2 Models.* Linda Al Atik and Robert R. Youngs. May 2013.
- PEER 2013/10** *NGA-West 2 Models for Ground-Motion Directionality.* Shrey K. Shahi and Jack W. Baker. May 2013.
- PEER 2013/09** *Final Report of the NGA-West2 Directivity Working Group.* Paul Spudich, Jeffrey R. Bayless, Jack W. Baker, Brian S.J. Chiou, Badie Rowshandel, Shrey Shahi, and Paul Somerville. May 2013.
- PEER 2013/08** *NGA-West2 Model for Estimating Average Horizontal Values of Pseudo-Absolute Spectral Accelerations Generated by Crustal Earthquakes.* I. M. Idriss. May 2013.

- PEER 2013/07** *Update of the Chiou and Youngs NGA Ground Motion Model for Average Horizontal Component of Peak Ground Motion and Response Spectra.* Brian Chiou and Robert Youngs. May 2013.
- PEER 2013/06** *NGA-West2 Campbell-Bozorgnia Ground Motion Model for the Horizontal Components of PGA, PGV, and 5%-Damped Elastic Pseudo-Acceleration Response Spectra for Periods Ranging from 0.01 to 10 sec.* Kenneth W. Campbell and Yousef Bozorgnia. May 2013.
- PEER 2013/05** *NGA-West 2 Equations for Predicting Response Spectral Accelerations for Shallow Crustal Earthquakes.* David M. Boore, Jonathan P. Stewart, Emel Seyhan, Gail M. Atkinson. May 2013.
- PEER 2013/04** *Update of the AS08 Ground-Motion Prediction Equations Based on the NGA-West2 Data Set.* Norman Abrahamson, Walter Silva, and Ronnie Kamai. May 2013.
- PEER 2013/03** *PEER NGA-West2 Database.* Timothy D. Ancheta, Robert B. Darragh, Jonathan P. Stewart, Emel Seyhan, Walter J. Silva, Brian S.J. Chiou, Katie E. Wooddell, Robert W. Graves, Albert R. Kottke, David M. Boore, Tadahiro Kishida, and Jennifer L. Donahue. May 2013.
- PEER 2013/02** *Hybrid Simulation of the Seismic Response of Squat Reinforced Concrete Shear Walls.* Catherine A. Whyte and Bozidar Stojadinovic. May 2013.
- PEER 2013/01** *Housing Recovery in Chile: A Qualitative Mid-program Review.* Mary C. Comerio. February 2013.
- PEER 2012/08** *Guidelines for Estimation of Shear Wave Velocity.* Bernard R. Wair, Jason T. DeJong, and Thomas Shantz. December 2012.
- PEER 2012/07** *Earthquake Engineering for Resilient Communities: 2012 PEER Internship Program Research Report Collection.* Heidi Tremayne (Editor), Stephen A. Mahin (Editor), Collin Anderson, Dustin Cook, Michael Erceg, Carlos Esparza, Jose Jimenez, Dorian Krausz, Andrew Lo, Stephanie Lopez, Nicole McCurdy, Paul Shipman, Alexander Strum, Eduardo Vega. December 2012.
- PEER 2012/06** *Fragilities for Precarious Rocks at Yucca Mountain.* Matthew D. Purvance, Rasool Anooshehpour, and James N. Brune. December 2012.
- PEER 2012/05** *Development of Simplified Analysis Procedure for Piles in Laterally Spreading Layered Soils.* Christopher R. McGann, Pedro Arduino, and Peter Mackenzie-Helnwein. December 2012.
- PEER 2012/04** *Unbonded Pre-Tensioned Columns for Bridges in Seismic Regions.* Phillip M. Davis, Todd M. Janes, Marc O. Eberhard, and John F. Stanton. December 2012.
- PEER 2012/03** *Experimental and Analytical Studies on Reinforced Concrete Buildings with Seismically Vulnerable Beam-Column Joints.* Sangjoon Park and Khalid M. Mosalam. October 2012.
- PEER 2012/02** *Seismic Performance of Reinforced Concrete Bridges Allowed to Uplift during Multi-Directional Excitation.* Andres Oscar Espinoza and Stephen A. Mahin. July 2012.
- PEER 2012/01** *Spectral Damping Scaling Factors for Shallow Crustal Earthquakes in Active Tectonic Regions.* Sanaz Rezaeian, Yousef Bozorgnia, I. M. Idriss, Kenneth Campbell, Norman Abrahamson, and Walter Silva. July 2012.
- PEER 2011/10** *Earthquake Engineering for Resilient Communities: 2011 PEER Internship Program Research Report Collection.* Eds. Heidi Faison and Stephen A. Mahin. December 2011.
- PEER 2011/09** *Calibration of Semi-Stochastic Procedure for Simulating High-Frequency Ground Motions.* Jonathan P. Stewart, Emel Seyhan, and Robert W. Graves. December 2011.
- PEER 2011/08** *Water Supply in regard to Fire Following Earthquake.* Charles Scawthorn. November 2011.
- PEER 2011/07** *Seismic Risk Management in Urban Areas. Proceedings of a U.S.-Iran-Turkey Seismic Workshop.* September 2011.
- PEER 2011/06** *The Use of Base Isolation Systems to Achieve Complex Seismic Performance Objectives.* Troy A. Morgan and Stephen A. Mahin. July 2011.
- PEER 2011/05** *Case Studies of the Seismic Performance of Tall Buildings Designed by Alternative Means.* Task 12 Report for the Tall Buildings Initiative. Jack Moehle, Yousef Bozorgnia, Nirmal Jayaram, Pierson Jones, Mohsen Rahnama, Nilesh Shome, Zeynep Tuna, John Wallace, Tony Yang, and Farzin Zareian. July 2011.
- PEER 2011/04** *Recommended Design Practice for Pile Foundations in Laterally Spreading Ground.* Scott A. Ashford, Ross W. Boulanger, and Scott J. Brandenburg. June 2011.
- PEER 2011/03** *New Ground Motion Selection Procedures and Selected Motions for the PEER Transportation Research Program.* Jack W. Baker, Ting Lin, Shrey K. Shahi, and Nirmal Jayaram. March 2011.
- PEER 2011/02** *A Bayesian Network Methodology for Infrastructure Seismic Risk Assessment and Decision Support.* Michelle T. Bensi, Armen Der Kiureghian, and Daniel Straub. March 2011.

- PEER 2011/01** *Demand Fragility Surfaces for Bridges in Liquefied and Laterally Spreading Ground.* Scott J. Brandenberg, Jian Zhang, Pirooz Kashighandi, Yili Huo, and Minxing Zhao. March 2011.
- PEER 2010/05** *Guidelines for Performance-Based Seismic Design of Tall Buildings.* Developed by the Tall Buildings Initiative. November 2010.
- PEER 2010/04** *Application Guide for the Design of Flexible and Rigid Bus Connections between Substation Equipment Subjected to Earthquakes.* Jean-Bernard Dastous and Armen Der Kiureghian. September 2010.
- PEER 2010/03** *Shear Wave Velocity as a Statistical Function of Standard Penetration Test Resistance and Vertical Effective Stress at Caltrans Bridge Sites.* Scott J. Brandenberg, Naresh Bellana, and Thomas Shantz. June 2010.
- PEER 2010/02** *Stochastic Modeling and Simulation of Ground Motions for Performance-Based Earthquake Engineering.* Sanaz Rezaeian and Armen Der Kiureghian. June 2010.
- PEER 2010/01** *Structural Response and Cost Characterization of Bridge Construction Using Seismic Performance Enhancement Strategies.* Ady Aviram, Božidar Stojadinović, Gustavo J. Parra-Montesinos, and Kevin R. Mackie. March 2010.
- PEER 2009/03** *The Integration of Experimental and Simulation Data in the Study of Reinforced Concrete Bridge Systems Including Soil-Foundation-Structure Interaction.* Matthew Dryden and Gregory L. Fenves. November 2009.
- PEER 2009/02** *Improving Earthquake Mitigation through Innovations and Applications in Seismic Science, Engineering, Communication, and Response. Proceedings of a U.S.-Iran Seismic Workshop.* October 2009.
- PEER 2009/01** *Evaluation of Ground Motion Selection and Modification Methods: Predicting Median Interstory Drift Response of Buildings.* Curt B. Haselton, Ed. June 2009.
- PEER 2008/10** *Technical Manual for Strata.* Albert R. Kottke and Ellen M. Rathje. February 2009.
- PEER 2008/09** *NGA Model for Average Horizontal Component of Peak Ground Motion and Response Spectra.* Brian S.-J. Chiou and Robert R. Youngs. November 2008.
- PEER 2008/08** *Toward Earthquake-Resistant Design of Concentrically Braced Steel Structures.* Patxi Uriz and Stephen A. Mahin. November 2008.
- PEER 2008/07** *Using OpenSees for Performance-Based Evaluation of Bridges on Liquefiable Soils.* Stephen L. Kramer, Pedro Arduino, and HyungSuk Shin. November 2008.
- PEER 2008/06** *Shaking Table Tests and Numerical Investigation of Self-Centering Reinforced Concrete Bridge Columns.* Hyung IL Jeong, Junichi Sakai, and Stephen A. Mahin. September 2008.
- PEER 2008/05** *Performance-Based Earthquake Engineering Design Evaluation Procedure for Bridge Foundations Undergoing Liquefaction-Induced Lateral Ground Displacement.* Christian A. Ledezma and Jonathan D. Bray. August 2008.
- PEER 2008/04** *Benchmarking of Nonlinear Geotechnical Ground Response Analysis Procedures.* Jonathan P. Stewart, Annie On-Lei Kwok, Youssef M. A. Hashash, Neven Matasovic, Robert Pyke, Zhiliang Wang, and Zhaohui Yang. August 2008.
- PEER 2008/03** *Guidelines for Nonlinear Analysis of Bridge Structures in California.* Ady Aviram, Kevin R. Mackie, and Božidar Stojadinović. August 2008.
- PEER 2008/02** *Treatment of Uncertainties in Seismic-Risk Analysis of Transportation Systems.* Evangelos Stergiou and Anne S. Kiremidjian. July 2008.
- PEER 2008/01** *Seismic Performance Objectives for Tall Buildings.* William T. Holmes, Charles Kircher, William Petak, and Nabih Youssef. August 2008.
- PEER 2007/12** *An Assessment to Benchmark the Seismic Performance of a Code-Conforming Reinforced Concrete Moment-Frame Building.* Curt Haselton, Christine A. Goulet, Judith Mitrani-Reiser, James L. Beck, Gregory G. Deierlein, Keith A. Porter, Jonathan P. Stewart, and Ertugrul Taciroglu. August 2008.
- PEER 2007/11** *Bar Buckling in Reinforced Concrete Bridge Columns.* Wayne A. Brown, Dawn E. Lehman, and John F. Stanton. February 2008.
- PEER 2007/10** *Computational Modeling of Progressive Collapse in Reinforced Concrete Frame Structures.* Mohamed M. Talaat and Khalid M. Mosalam. May 2008.
- PEER 2007/09** *Integrated Probabilistic Performance-Based Evaluation of Benchmark Reinforced Concrete Bridges.* Kevin R. Mackie, John-Michael Wong, and Božidar Stojadinović. January 2008.
- PEER 2007/08** *Assessing Seismic Collapse Safety of Modern Reinforced Concrete Moment-Frame Buildings.* Curt B. Haselton and Gregory G. Deierlein. February 2008.
- PEER 2007/07** *Performance Modeling Strategies for Modern Reinforced Concrete Bridge Columns.* Michael P. Berry and Marc O. Eberhard. April 2008.

- PEER 2007/06** *Development of Improved Procedures for Seismic Design of Buried and Partially Buried Structures.* Linda Al Atik and Nicholas Sitar. June 2007.
- PEER 2007/05** *Uncertainty and Correlation in Seismic Risk Assessment of Transportation Systems.* Renee G. Lee and Anne S. Kiremidjian. July 2007.
- PEER 2007/04** *Numerical Models for Analysis and Performance-Based Design of Shallow Foundations Subjected to Seismic Loading.* Sivapalan Gajan, Tara C. Hutchinson, Bruce L. Kutter, Prishati Raychowdhury, José A. Ugalde, and Jonathan P. Stewart. May 2008.
- PEER 2007/03** *Beam-Column Element Model Calibrated for Predicting Flexural Response Leading to Global Collapse of RC Frame Buildings.* Curt B. Haselton, Abbie B. Liel, Sarah Taylor Lange, and Gregory G. Deierlein. May 2008.
- PEER 2007/02** *Campbell-Bozorgnia NGA Ground Motion Relations for the Geometric Mean Horizontal Component of Peak and Spectral Ground Motion Parameters.* Kenneth W. Campbell and Yousef Bozorgnia. May 2007.
- PEER 2007/01** *Boore-Atkinson NGA Ground Motion Relations for the Geometric Mean Horizontal Component of Peak and Spectral Ground Motion Parameters.* David M. Boore and Gail M. Atkinson. May 2007.
- PEER 2006/12** *Societal Implications of Performance-Based Earthquake Engineering.* Peter J. May. May 2007.
- PEER 2006/11** *Probabilistic Seismic Demand Analysis Using Advanced Ground Motion Intensity Measures, Attenuation Relationships, and Near-Fault Effects.* Polsak Tothong and C. Allin Cornell. March 2007.
- PEER 2006/10** *Application of the PEER PBEE Methodology to the I-880 Viaduct.* Sashi Kunnath. February 2007.
- PEER 2006/09** *Quantifying Economic Losses from Travel Forgone Following a Large Metropolitan Earthquake.* James Moore, Sungbin Cho, Yue Yue Fan, and Stuart Werner. November 2006.
- PEER 2006/08** *Vector-Valued Ground Motion Intensity Measures for Probabilistic Seismic Demand Analysis.* Jack W. Baker and C. Allin Cornell. October 2006.
- PEER 2006/07** *Analytical Modeling of Reinforced Concrete Walls for Predicting Flexural and Coupled-Shear-Flexural Responses.* Kutay Orakcal, Leonardo M. Massone, and John W. Wallace. October 2006.
- PEER 2006/06** *Nonlinear Analysis of a Soil-Drilled Pier System under Static and Dynamic Axial Loading.* Gang Wang and Nicholas Sitar. November 2006.
- PEER 2006/05** *Advanced Seismic Assessment Guidelines.* Paolo Bazzurro, C. Allin Cornell, Charles Menun, Maziar Motahari, and Nicolas Luco. September 2006.
- PEER 2006/04** *Probabilistic Seismic Evaluation of Reinforced Concrete Structural Components and Systems.* Tae Hyung Lee and Khalid M. Mosalam. August 2006.
- PEER 2006/03** *Performance of Lifelines Subjected to Lateral Spreading.* Scott A. Ashford and Teerawut Juirnarongrit. July 2006.
- PEER 2006/02** *Pacific Earthquake Engineering Research Center Highway Demonstration Project.* Anne Kiremidjian, James Moore, Yue Yue Fan, Nesrin Basoz, Ozgur Yazali, and Meredith Williams. April 2006.
- PEER 2006/01** *Bracing Berkeley. A Guide to Seismic Safety on the UC Berkeley Campus.* Mary C. Comerio, Stephen Tوبرiner, and Ariane Fehrenkamp. January 2006.
- PEER 2005/16** *Seismic Response and Reliability of Electrical Substation Equipment and Systems.* Junho Song, Armen Der Kiureghian, and Jerome L. Sackman. April 2006.
- PEER 2005/15** *CPT-Based Probabilistic Assessment of Seismic Soil Liquefaction Initiation.* R. E. S. Moss, R. B. Seed, R. E. Kayen, J. P. Stewart, and A. Der Kiureghian. April 2006.
- PEER 2005/14** *Workshop on Modeling of Nonlinear Cyclic Load-Deformation Behavior of Shallow Foundations.* Bruce L. Kutter, Geoffrey Martin, Tara Hutchinson, Chad Harden, Sivapalan Gajan, and Justin Phalen. March 2006.
- PEER 2005/13** *Stochastic Characterization and Decision Bases under Time-Dependent Aftershock Risk in Performance-Based Earthquake Engineering.* Gee Liek Yeo and C. Allin Cornell. July 2005.
- PEER 2005/12** *PEER Testbed Study on a Laboratory Building: Exercising Seismic Performance Assessment.* Mary C. Comerio, editor. November 2005.
- PEER 2005/11** *Van Nuys Hotel Building Testbed Report: Exercising Seismic Performance Assessment.* Helmut Krawinkler, editor. October 2005.
- PEER 2005/10** *First NEES/E-Defense Workshop on Collapse Simulation of Reinforced Concrete Building Structures.* September 2005.
- PEER 2005/09** *Test Applications of Advanced Seismic Assessment Guidelines.* Joe Maffei, Karl Telleen, Danya Mohr, William Holmes, and Yuki Nakayama. August 2006.

- PEER 2005/08** *Damage Accumulation in Lightly Confined Reinforced Concrete Bridge Columns.* R. Tyler Ranf, Jared M. Nelson, Zach Price, Marc O. Eberhard, and John F. Stanton. April 2006.
- PEER 2005/07** *Experimental and Analytical Studies on the Seismic Response of Freestanding and Anchored Laboratory Equipment.* Dimitrios Konstantinidis and Nicos Makris. January 2005.
- PEER 2005/06** *Global Collapse of Frame Structures under Seismic Excitations.* Luis F. Ibarra and Helmut Krawinkler. September 2005.
- PEER 2005/05** *Performance Characterization of Bench- and Shelf-Mounted Equipment.* Samit Ray Chaudhuri and Tara C. Hutchinson. May 2006.
- PEER 2005/04** *Numerical Modeling of the Nonlinear Cyclic Response of Shallow Foundations.* Chad Harden, Tara Hutchinson, Geoffrey R. Martin, and Bruce L. Kutter. August 2005.
- PEER 2005/03** *A Taxonomy of Building Components for Performance-Based Earthquake Engineering.* Keith A. Porter. September 2005.
- PEER 2005/02** *Fragility Basis for California Highway Overpass Bridge Seismic Decision Making.* Kevin R. Mackie and Božidar Stojadinović. June 2005.
- PEER 2005/01** *Empirical Characterization of Site Conditions on Strong Ground Motion.* Jonathan P. Stewart, Yoojoong Choi, and Robert W. Graves. June 2005.
- PEER 2004/09** *Electrical Substation Equipment Interaction: Experimental Rigid Conductor Studies.* Christopher Stearns and André Filiatrault. February 2005.
- PEER 2004/08** *Seismic Qualification and Fragility Testing of Line Break 550-kV Disconnect Switches.* Shakhzod M. Takhirov, Gregory L. Fenves, and Eric Fujisaki. January 2005.
- PEER 2004/07** *Ground Motions for Earthquake Simulator Qualification of Electrical Substation Equipment.* Shakhzod M. Takhirov, Gregory L. Fenves, Eric Fujisaki, and Don Clyde. January 2005.
- PEER 2004/06** *Performance-Based Regulation and Regulatory Regimes.* Peter J. May and Chris Koski. September 2004.
- PEER 2004/05** *Performance-Based Seismic Design Concepts and Implementation: Proceedings of an International Workshop.* Peter Fajfar and Helmut Krawinkler, editors. September 2004.
- PEER 2004/04** *Seismic Performance of an Instrumented Tilt-up Wall Building.* James C. Anderson and Vitelmo V. Bertero. July 2004.
- PEER 2004/03** *Evaluation and Application of Concrete Tilt-up Assessment Methodologies.* Timothy Graf and James O. Malley. October 2004.
- PEER 2004/02** *Analytical Investigations of New Methods for Reducing Residual Displacements of Reinforced Concrete Bridge Columns.* Junichi Sakai and Stephen A. Mahin. August 2004.
- PEER 2004/01** *Seismic Performance of Masonry Buildings and Design Implications.* Kerri Anne Taeko Tokoro, James C. Anderson, and Vitelmo V. Bertero. February 2004.
- PEER 2003/18** *Performance Models for Flexural Damage in Reinforced Concrete Columns.* Michael Berry and Marc Eberhard. August 2003.
- PEER 2003/17** *Predicting Earthquake Damage in Older Reinforced Concrete Beam-Column Joints.* Catherine Pagni and Laura Lowes. October 2004.
- PEER 2003/16** *Seismic Demands for Performance-Based Design of Bridges.* Kevin Mackie and Božidar Stojadinović. August 2003.
- PEER 2003/15** *Seismic Demands for Nondeteriorating Frame Structures and Their Dependence on Ground Motions.* Ricardo Antonio Medina and Helmut Krawinkler. May 2004.
- PEER 2003/14** *Finite Element Reliability and Sensitivity Methods for Performance-Based Earthquake Engineering.* Terje Haukaas and Armen Der Kiureghian. April 2004.
- PEER 2003/13** *Effects of Connection Hysteretic Degradation on the Seismic Behavior of Steel Moment-Resisting Frames.* Janise E. Rodgers and Stephen A. Mahin. March 2004.
- PEER 2003/12** *Implementation Manual for the Seismic Protection of Laboratory Contents: Format and Case Studies.* William T. Holmes and Mary C. Comerio. October 2003.
- PEER 2003/11** *Fifth U.S.-Japan Workshop on Performance-Based Earthquake Engineering Methodology for Reinforced Concrete Building Structures.* February 2004.
- PEER 2003/10** *A Beam-Column Joint Model for Simulating the Earthquake Response of Reinforced Concrete Frames.* Laura N. Lowes, Nilanjan Mitra, and Arash Altoontash. February 2004.

- PEER 2003/09** *Sequencing Repairs after an Earthquake: An Economic Approach.* Marco Casari and Simon J. Wilkie. April 2004.
- PEER 2003/08** *A Technical Framework for Probability-Based Demand and Capacity Factor Design (DCFD) Seismic Formats.* Fatemeh Jalayer and C. Allin Cornell. November 2003.
- PEER 2003/07** *Uncertainty Specification and Propagation for Loss Estimation Using FOSM Methods.* Jack W. Baker and C. Allin Cornell. September 2003.
- PEER 2003/06** *Performance of Circular Reinforced Concrete Bridge Columns under Bidirectional Earthquake Loading.* Mahmoud M. Hachem, Stephen A. Mahin, and Jack P. Moehle. February 2003.
- PEER 2003/05** *Response Assessment for Building-Specific Loss Estimation.* Eduardo Miranda and Shahram Taghavi. September 2003.
- PEER 2003/04** *Experimental Assessment of Columns with Short Lap Splices Subjected to Cyclic Loads.* Murat Melek, John W. Wallace, and Joel Conte. April 2003.
- PEER 2003/03** *Probabilistic Response Assessment for Building-Specific Loss Estimation.* Eduardo Miranda and Hesameddin Aslani. September 2003.
- PEER 2003/02** *Software Framework for Collaborative Development of Nonlinear Dynamic Analysis Program.* Jun Peng and Kincho H. Law. September 2003.
- PEER 2003/01** *Shake Table Tests and Analytical Studies on the Gravity Load Collapse of Reinforced Concrete Frames.* Kenneth John Elwood and Jack P. Moehle. November 2003.
- PEER 2002/24** *Performance of Beam to Column Bridge Joints Subjected to a Large Velocity Pulse.* Natalie Gibson, André Filiatrault, and Scott A. Ashford. April 2002.
- PEER 2002/23** *Effects of Large Velocity Pulses on Reinforced Concrete Bridge Columns.* Greg L. Orozco and Scott A. Ashford. April 2002.
- PEER 2002/22** *Characterization of Large Velocity Pulses for Laboratory Testing.* Kenneth E. Cox and Scott A. Ashford. April 2002.
- PEER 2002/21** *Fourth U.S.-Japan Workshop on Performance-Based Earthquake Engineering Methodology for Reinforced Concrete Building Structures.* December 2002.
- PEER 2002/20** *Barriers to Adoption and Implementation of PBEE Innovations.* Peter J. May. August 2002.
- PEER 2002/19** *Economic-Engineered Integrated Models for Earthquakes: Socioeconomic Impacts.* Peter Gordon, James E. Moore II, and Harry W. Richardson. July 2002.
- PEER 2002/18** *Assessment of Reinforced Concrete Building Exterior Joints with Substandard Details.* Chris P. Pantelides, Jon Hansen, Justin Nadauld, and Lawrence D. Reaveley. May 2002.
- PEER 2002/17** *Structural Characterization and Seismic Response Analysis of a Highway Overcrossing Equipped with Elastomeric Bearings and Fluid Dampers: A Case Study.* Nicos Makris and Jian Zhang. November 2002.
- PEER 2002/16** *Estimation of Uncertainty in Geotechnical Properties for Performance-Based Earthquake Engineering.* Allen L. Jones, Steven L. Kramer, and Pedro Arduino. December 2002.
- PEER 2002/15** *Seismic Behavior of Bridge Columns Subjected to Various Loading Patterns.* Asadollah Esmaeily-Gh. and Yan Xiao. December 2002.
- PEER 2002/14** *Inelastic Seismic Response of Extended Pile Shaft Supported Bridge Structures.* T.C. Hutchinson, R.W. Boulanger, Y.H. Chai, and I.M. Idriss. December 2002.
- PEER 2002/13** *Probabilistic Models and Fragility Estimates for Bridge Components and Systems.* Paolo Gardoni, Armen Der Kiureghian, and Khalid M. Mosalam. June 2002.
- PEER 2002/12** *Effects of Fault Dip and Slip Rake on Near-Source Ground Motions: Why Chi-Chi Was a Relatively Mild M7.6 Earthquake.* Brad T. Aagaard, John F. Hall, and Thomas H. Heaton. December 2002.
- PEER 2002/11** *Analytical and Experimental Study of Fiber-Reinforced Strip Isolators.* James M. Kelly and Shakhzod M. Takhirov. September 2002.
- PEER 2002/10** *Centrifuge Modeling of Settlement and Lateral Spreading with Comparisons to Numerical Analyses.* Sivapalan Gajan and Bruce L. Kutter. January 2003.
- PEER 2002/09** *Documentation and Analysis of Field Case Histories of Seismic Compression during the 1994 Northridge, California, Earthquake.* Jonathan P. Stewart, Patrick M. Smith, Daniel H. Whang, and Jonathan D. Bray. October 2002.
- PEER 2002/08** *Component Testing, Stability Analysis and Characterization of Buckling-Restrained Unbonded Braces™.* Cameron Black, Nicos Makris, and Ian Aiken. September 2002.

- PEER 2002/07** *Seismic Performance of Pile-Wharf Connections*. Charles W. Roeder, Robert Graff, Jennifer Soderstrom, and Jun Han Yoo. December 2001.
- PEER 2002/06** *The Use of Benefit-Cost Analysis for Evaluation of Performance-Based Earthquake Engineering Decisions*. Richard O. Zerbe and Anthony Falit-Baiamonte. September 2001.
- PEER 2002/05** *Guidelines, Specifications, and Seismic Performance Characterization of Nonstructural Building Components and Equipment*. André Filiatrault, Constantin Christopoulos, and Christopher Stearns. September 2001.
- PEER 2002/04** *Consortium of Organizations for Strong-Motion Observation Systems and the Pacific Earthquake Engineering Research Center Lifelines Program: Invited Workshop on Archiving and Web Dissemination of Geotechnical Data, 4–5 October 2001*. September 2002.
- PEER 2002/03** *Investigation of Sensitivity of Building Loss Estimates to Major Uncertain Variables for the Van Nuys Testbed*. Keith A. Porter, James L. Beck, and Rustem V. Shaikhutdinov. August 2002.
- PEER 2002/02** *The Third U.S.-Japan Workshop on Performance-Based Earthquake Engineering Methodology for Reinforced Concrete Building Structures*. July 2002.
- PEER 2002/01** *Nonstructural Loss Estimation: The UC Berkeley Case Study*. Mary C. Comerio and John C. Stallmeyer. December 2001.
- PEER 2001/16** *Statistics of SDF-System Estimate of Roof Displacement for Pushover Analysis of Buildings*. Anil K. Chopra, Rakesh K. Goel, and Chatpan Chintanapakdee. December 2001.
- PEER 2001/15** *Damage to Bridges during the 2001 Nisqually Earthquake*. R. Tyler Ranf, Marc O. Eberhard, and Michael P. Berry. November 2001.
- PEER 2001/14** *Rocking Response of Equipment Anchored to a Base Foundation*. Nicos Makris and Cameron J. Black. September 2001.
- PEER 2001/13** *Modeling Soil Liquefaction Hazards for Performance-Based Earthquake Engineering*. Steven L. Kramer and Ahmed-W. Elgamal. February 2001.
- PEER 2001/12** *Development of Geotechnical Capabilities in OpenSees*. Boris Jeremić. September 2001.
- PEER 2001/11** *Analytical and Experimental Study of Fiber-Reinforced Elastomeric Isolators*. James M. Kelly and Shakhzod M. Takhirov. September 2001.
- PEER 2001/10** *Amplification Factors for Spectral Acceleration in Active Regions*. Jonathan P. Stewart, Andrew H. Liu, Yoojoong Choi, and Mehmet B. Baturay. December 2001.
- PEER 2001/09** *Ground Motion Evaluation Procedures for Performance-Based Design*. Jonathan P. Stewart, Shyh-Jeng Chiou, Jonathan D. Bray, Robert W. Graves, Paul G. Somerville, and Norman A. Abrahamson. September 2001.
- PEER 2001/08** *Experimental and Computational Evaluation of Reinforced Concrete Bridge Beam-Column Connections for Seismic Performance*. Clay J. Naito, Jack P. Moehle, and Khalid M. Mosalam. November 2001.
- PEER 2001/07** *The Rocking Spectrum and the Shortcomings of Design Guidelines*. Nicos Makris and Dimitrios Konstantinidis. August 2001.
- PEER 2001/06** *Development of an Electrical Substation Equipment Performance Database for Evaluation of Equipment Fragilities*. Thalia Agnanos. April 1999.
- PEER 2001/05** *Stiffness Analysis of Fiber-Reinforced Elastomeric Isolators*. Hsiang-Chuan Tsai and James M. Kelly. May 2001.
- PEER 2001/04** *Organizational and Societal Considerations for Performance-Based Earthquake Engineering*. Peter J. May. April 2001.
- PEER 2001/03** *A Modal Pushover Analysis Procedure to Estimate Seismic Demands for Buildings: Theory and Preliminary Evaluation*. Anil K. Chopra and Rakesh K. Goel. January 2001.
- PEER 2001/02** *Seismic Response Analysis of Highway Overcrossings Including Soil-Structure Interaction*. Jian Zhang and Nicos Makris. March 2001.
- PEER 2001/01** *Experimental Study of Large Seismic Steel Beam-to-Column Connections*. Egor P. Popov and Shakhzod M. Takhirov. November 2000.
- PEER 2000/10** *The Second U.S.-Japan Workshop on Performance-Based Earthquake Engineering Methodology for Reinforced Concrete Building Structures*. March 2000.
- PEER 2000/09** *Structural Engineering Reconnaissance of the August 17, 1999 Earthquake: Kocaeli (Izmit), Turkey*. Halil Sezen, Kenneth J. Elwood, Andrew S. Whittaker, Khalid Mosalam, John J. Wallace, and John F. Stanton. December 2000.



- PEER 2000/08** *Behavior of Reinforced Concrete Bridge Columns Having Varying Aspect Ratios and Varying Lengths of Confinement.* Anthony J. Calderone, Dawn E. Lehman, and Jack P. Moehle. January 2001.
- PEER 2000/07** *Cover-Plate and Flange-Plate Reinforced Steel Moment-Resisting Connections.* Taejin Kim, Andrew S. Whittaker, Amir S. Gilani, Vitelmo V. Bertero, and Shakhzod M. Takhirov. September 2000.
- PEER 2000/06** *Seismic Evaluation and Analysis of 230-kV Disconnect Switches.* Amir S. J. Gilani, Andrew S. Whittaker, Gregory L. Fenves, Chun-Hao Chen, Henry Ho, and Eric Fujisaki. July 2000.
- PEER 2000/05** *Performance-Based Evaluation of Exterior Reinforced Concrete Building Joints for Seismic Excitation.* Chandra Clyde, Chris P. Pantelides, and Lawrence D. Reaveley. July 2000.
- PEER 2000/04** *An Evaluation of Seismic Energy Demand: An Attenuation Approach.* Chung-Che Chou and Chia-Ming Uang. July 1999.
- PEER 2000/03** *Framing Earthquake Retrofitting Decisions: The Case of Hillside Homes in Los Angeles.* Detlof von Winterfeldt, Nels Roselund, and Alicia Kitsuse. March 2000.
- PEER 2000/02** *U.S.-Japan Workshop on the Effects of Near-Field Earthquake Shaking.* Andrew Whittaker, ed. July 2000.
- PEER 2000/01** *Further Studies on Seismic Interaction in Interconnected Electrical Substation Equipment.* Armen Der Kiureghian, Kee-Jeung Hong, and Jerome L. Sackman. November 1999.
- PEER 1999/14** *Seismic Evaluation and Retrofit of 230-kV Porcelain Transformer Bushings.* Amir S. Gilani, Andrew S. Whittaker, Gregory L. Fenves, and Eric Fujisaki. December 1999.
- PEER 1999/13** *Building Vulnerability Studies: Modeling and Evaluation of Tilt-up and Steel Reinforced Concrete Buildings.* John W. Wallace, Jonathan P. Stewart, and Andrew S. Whittaker, editors. December 1999.
- PEER 1999/12** *Rehabilitation of Nonductile RC Frame Building Using Encasement Plates and Energy-Dissipating Devices.* Mehrdad Sasani, Vitelmo V. Bertero, James C. Anderson. December 1999.
- PEER 1999/11** *Performance Evaluation Database for Concrete Bridge Components and Systems under Simulated Seismic Loads.* Yael D. Hose and Frieder Seible. November 1999.
- PEER 1999/10** *U.S.-Japan Workshop on Performance-Based Earthquake Engineering Methodology for Reinforced Concrete Building Structures.* December 1999.
- PEER 1999/09** *Performance Improvement of Long Period Building Structures Subjected to Severe Pulse-Type Ground Motions.* James C. Anderson, Vitelmo V. Bertero, and Raul Bertero. October 1999.
- PEER 1999/08** *Envelopes for Seismic Response Vectors.* Charles Menun and Armen Der Kiureghian. July 1999.
- PEER 1999/07** *Documentation of Strengths and Weaknesses of Current Computer Analysis Methods for Seismic Performance of Reinforced Concrete Members.* William F. Cofer. November 1999.
- PEER 1999/06** *Rocking Response and Overturning of Anchored Equipment under Seismic Excitations.* Nicos Makris and Jian Zhang. November 1999.
- PEER 1999/05** *Seismic Evaluation of 550 kV Porcelain Transformer Bushings.* Amir S. Gilani, Andrew S. Whittaker, Gregory L. Fenves, and Eric Fujisaki. October 1999.
- PEER 1999/04** *Adoption and Enforcement of Earthquake Risk-Reduction Measures.* Peter J. May, Raymond J. Burby, T. Jens Feeley, and Robert Wood.
- PEER 1999/03** *Task 3 Characterization of Site Response General Site Categories.* Adrian Rodriguez-Marek, Jonathan D. Bray, and Norman Abrahamson. February 1999.
- PEER 1999/02** *Capacity-Demand-Diagram Methods for Estimating Seismic Deformation of Inelastic Structures: SDF Systems.* Anil K. Chopra and Rakesh Goel. April 1999.
- PEER 1999/01** *Interaction in Interconnected Electrical Substation Equipment Subjected to Earthquake Ground Motions.* Armen Der Kiureghian, Jerome L. Sackman, and Kee-Jeung Hong. February 1999.
- PEER 1998/08** *Behavior and Failure Analysis of a Multiple-Frame Highway Bridge in the 1994 Northridge Earthquake.* Gregory L. Fenves and Michael Ellery. December 1998.
- PEER 1998/07** *Empirical Evaluation of Inertial Soil-Structure Interaction Effects.* Jonathan P. Stewart, Raymond B. Seed, and Gregory L. Fenves. November 1998.
- PEER 1998/06** *Effect of Damping Mechanisms on the Response of Seismic Isolated Structures.* Nicos Makris and Shih-Po Chang. November 1998.
- PEER 1998/05** *Rocking Response and Overturning of Equipment under Horizontal Pulse-Type Motions.* Nicos Makris and Yiannis Roussos. October 1998.

- PEER 1998/04** *Pacific Earthquake Engineering Research Invitational Workshop Proceedings, May 14–15, 1998: Defining the Links between Planning, Policy Analysis, Economics and Earthquake Engineering.* Mary Comerio and Peter Gordon. September 1998.
- PEER 1998/03** *Repair/Upgrade Procedures for Welded Beam to Column Connections.* James C. Anderson and Xiaojing Duan. May 1998.
- PEER 1998/02** *Seismic Evaluation of 196 kV Porcelain Transformer Bushings.* Amir S. Gilani, Juan W. Chavez, Gregory L. Fennes, and Andrew S. Whittaker. May 1998.
- PEER 1998/01** *Seismic Performance of Well-Confined Concrete Bridge Columns.* Dawn E. Lehman and Jack P. Moehle. December 2000.

## ONLINE PEER REPORTS

The following PEER reports are available by Internet only at [http://peer.berkeley.edu/publications/peer\\_reports\\_complete.html](http://peer.berkeley.edu/publications/peer_reports_complete.html).

- PEER 2012/103** *Performance-Based Seismic Demand Assessment of Concentrically Braced Steel Frame Buildings.* Chui-Hsin Chen and Stephen A. Mahin. December 2012.
- PEER 2012/102** *Procedure to Restart an Interrupted Hybrid Simulation: Addendum to PEER Report 2010/103.* Vesna Terzic and Božidar Stojadinovic. October 2012.
- PEER 2012/101** *Mechanics of Fiber Reinforced Bearings.* James M. Kelly and Andrea Calabrese. February 2012.
- PEER 2011/107** *Nonlinear Site Response and Seismic Compression at Vertical Array Strongly Shaken by 2007 Niigata-ken Chuetsu-oki Earthquake.* Eric Yee, Jonathan P. Stewart, and Kohji Tokimatsu. December 2011.
- PEER 2011/106** *Self Compacting Hybrid Fiber Reinforced Concrete Composites for Bridge Columns.* Pardeep Kumar, Gabriel Jen, William Trono, Marios Panagiotou, and Claudia Ostertag. September 2011.
- PEER 2011/105** *Stochastic Dynamic Analysis of Bridges Subjected to Spatially Varying Ground Motions.* Katerina Konakli and Armen Der Kiureghian. August 2011.
- PEER 2011/104** *Design and Instrumentation of the 2010 E-Defense Four-Story Reinforced Concrete and Post-Tensioned Concrete Buildings.* Takuya Nagae, Kenichi Tahara, Taizo Matsumori, Hitoshi Shiohara, Toshimi Kabeyasawa, Susumu Kono, Minehiro Nishiyama (Japanese Research Team) and John Wallace, Wassim Ghannoum, Jack Moehle, Richard Sause, Wesley Keller, Zeynep Tuna (U.S. Research Team). June 2011.
- PEER 2011/103** *In-Situ Monitoring of the Force Output of Fluid Dampers: Experimental Investigation.* Dimitrios Konstantinidis, James M. Kelly, and Nicos Makris. April 2011.
- PEER 2011/102** *Ground-motion prediction equations 1964 - 2010.* John Douglas. April 2011.
- PEER 2011/101** *Report of the Eighth Planning Meeting of NEES/E-Defense Collaborative Research on Earthquake Engineering.* Convened by the Hyogo Earthquake Engineering Research Center (NIED), NEES Consortium, Inc. February 2011.
- PEER 2010/111** *Modeling and Acceptance Criteria for Seismic Design and Analysis of Tall Buildings.* Task 7 Report for the Tall Buildings Initiative - Published jointly by the Applied Technology Council. October 2010.
- PEER 2010/110** *Seismic Performance Assessment and Probabilistic Repair Cost Analysis of Precast Concrete Cladding Systems for Multistory Buildings.* Jeffrey P. Hunt and Božidar Stojadinovic. November 2010.
- PEER 2010/109** *Report of the Seventh Joint Planning Meeting of NEES/E-Defense Collaboration on Earthquake Engineering. Held at the E-Defense, Miki, and Shin-Kobe, Japan, September 18–19, 2009.* August 2010.
- PEER 2010/108** *Probabilistic Tsunami Hazard in California.* Hong Kie Thio, Paul Somerville, and Jascha Polet, preparers. October 2010.
- PEER 2010/107** *Performance and Reliability of Exposed Column Base Plate Connections for Steel Moment-Resisting Frames.* Ady Aviram, Božidar Stojadinovic, and Armen Der Kiureghian. August 2010.
- PEER 2010/106** *Verification of Probabilistic Seismic Hazard Analysis Computer Programs.* Patricia Thomas, Ivan Wong, and Norman Abrahamson. May 2010.
- PEER 2010/105** *Structural Engineering Reconnaissance of the April 6, 2009, Abruzzo, Italy, Earthquake, and Lessons Learned.* M. Selim Günay and Khalid M. Mosalam. April 2010.
- PEER 2010/104** *Simulating the Inelastic Seismic Behavior of Steel Braced Frames, Including the Effects of Low-Cycle Fatigue.* Yuli Huang and Stephen A. Mahin. April 2010.
- PEER 2010/103** *Post-Earthquake Traffic Capacity of Modern Bridges in California.* Vesna Terzic and Božidar Stojadinović. March 2010.
- PEER 2010/102** *Analysis of Cumulative Absolute Velocity (CAV) and JMA Instrumental Seismic Intensity ( $I_{JMA}$ ) Using the PEER–NGA Strong Motion Database.* Kenneth W. Campbell and Yousef Bozorgnia. February 2010.
- PEER 2010/101** *Rocking Response of Bridges on Shallow Foundations.* Jose A. Ugalde, Bruce L. Kutter, and Boris Jeremic. April 2010.
- PEER 2009/109** *Simulation and Performance-Based Earthquake Engineering Assessment of Self-Centering Post-Tensioned Concrete Bridge Systems.* Won K. Lee and Sarah L. Billington. December 2009.
- PEER 2009/108** *PEER Lifelines Geotechnical Virtual Data Center.* J. Carl Stepp, Daniel J. Ponti, Loren L. Turner, Jennifer N. Swift, Sean Devlin, Yang Zhu, Jean Benoit, and John Bobbitt. September 2009.

- PEER 2009/107** *Experimental and Computational Evaluation of Current and Innovative In-Span Hinge Details in Reinforced Concrete Box-Girder Bridges: Part 2: Post-Test Analysis and Design Recommendations.* Matias A. Hube and Khalid M. Mosalam. December 2009.
- PEER 2009/106** *Shear Strength Models of Exterior Beam-Column Joints without Transverse Reinforcement.* Sangjoon Park and Khalid M. Mosalam. November 2009.
- PEER 2009/105** *Reduced Uncertainty of Ground Motion Prediction Equations through Bayesian Variance Analysis.* Robb Eric S. Moss. November 2009.
- PEER 2009/104** *Advanced Implementation of Hybrid Simulation.* Andreas H. Schellenberg, Stephen A. Mahin, Gregory L. Fenves. November 2009.
- PEER 2009/103** *Performance Evaluation of Innovative Steel Braced Frames.* T. Y. Yang, Jack P. Moehle, and Božidar Stojadinovic. August 2009.
- PEER 2009/102** *Reinvestigation of Liquefaction and Nonliquefaction Case Histories from the 1976 Tangshan Earthquake.* Robb Eric Moss, Robert E. Kayen, Liyuan Tong, Songyu Liu, Guojun Cai, and Jiaer Wu. August 2009.
- PEER 2009/101** *Report of the First Joint Planning Meeting for the Second Phase of NEES/E-Defense Collaborative Research on Earthquake Engineering.* Stephen A. Mahin et al. July 2009.
- PEER 2008/104** *Experimental and Analytical Study of the Seismic Performance of Retaining Structures.* Linda Al Atik and Nicholas Sitar. January 2009.
- PEER 2008/103** *Experimental and Computational Evaluation of Current and Innovative In-Span Hinge Details in Reinforced Concrete Box-Girder Bridges. Part 1: Experimental Findings and Pre-Test Analysis.* Matias A. Hube and Khalid M. Mosalam. January 2009.
- PEER 2008/102** *Modeling of Unreinforced Masonry Infill Walls Considering In-Plane and Out-of-Plane Interaction.* Stephen Kadysiewski and Khalid M. Mosalam. January 2009.
- PEER 2008/101** *Seismic Performance Objectives for Tall Buildings.* William T. Holmes, Charles Kircher, William Petak, and Nabih Youssef. August 2008.
- PEER 2007/101** *Generalized Hybrid Simulation Framework for Structural Systems Subjected to Seismic Loading.* Tarek Elkhoraibi and Khalid M. Mosalam. July 2007.
- PEER 2007/100** *Seismic Evaluation of Reinforced Concrete Buildings Including Effects of Masonry Infill Walls.* Alidad Hashemi and Khalid M. Mosalam. July 2007.

The Pacific Earthquake Engineering Research Center (PEER) is a multi-institutional research and education center with headquarters at the University of California, Berkeley. Investigators from over 20 universities, several consulting companies, and researchers at various state and federal government agencies contribute to research programs focused on performance-based earthquake engineering.

These research programs aim to identify and reduce the risks from major earthquakes to life safety and to the economy by including research in a wide variety of disciplines including structural and geotechnical engineering, geology/seismology, lifelines, transportation, architecture, economics, risk management, and public policy.

PEER is supported by federal, state, local, and regional agencies, together with industry partners.



PEER Core Institutions:  
University of California, Berkeley (Lead Institution)  
California Institute of Technology  
Oregon State University  
Stanford University  
University of California, Davis  
University of California, Irvine  
University of California, Los Angeles  
University of California, San Diego  
University of Southern California  
University of Washington

PEER reports can be ordered at [http://peer.berkeley.edu/publications/peer\\_reports.html](http://peer.berkeley.edu/publications/peer_reports.html) or by contacting

Pacific Earthquake Engineering Research Center  
University of California, Berkeley  
325 Davis Hall, mail code 1792  
Berkeley, CA 94720-1792  
Tel: 510-642-3437  
Fax: 510-642-1655  
Email: [peer\\_editor@berkeley.edu](mailto:peer_editor@berkeley.edu)

ISSN 1547-0587X